



# **Reactivation of T<sub>H</sub>1 cells in peripheral tissues**

Inaugural-Dissertation

zur

Erlangung des Doktorgrades

Dr. rer. nat.

der Mathematisch-Naturwissenschaftlichen Fakultät

der Universität zu Köln

vorgelegt von

Martha Kiljan

aus Kamp-Lintfort

03.06.2022, Köln

Die der vorliegenden Arbeit zugrundeliegenden Experimente wurden am Zentrum für Molekulare Medizin Köln des Universitätsklinikum Köln durchgeführt und an der Klinik und Poliklinik für Radioonkologie, Cyberknife- und Strahlentherapie.

1. Gutachter: PD Dr. rer.-nat. Thomas Wunderlich

2. Gutachter: Prof. Dr. rer.-nat. Björn Schumacher

Tag der mündlichen Prüfung: August 2022

## Table of Content

1.	Zusammenfassung.....	1
2.	Abstract.....	2
3.	Introduction .....	3
3.1	Adaptive immunity: T cell biology.....	3
3.2	Priming/TCR activation.....	5
3.3	CD4 <sup>+</sup> T cell subpopulations .....	7
3.4	Effector and memory T cell differentiation .....	10
3.5	Antigen-mediated T cell reactivation in peripheral tissues.....	12
3.6	CD4 <sup>+</sup> T cell-dependent disease model: Nephrotoxic nephritis (NTN) .....	14
3.7	CD4 <sup>+</sup> T cell-dependent disease model: experimental autoimmune encephalomyelitis (EAE) .....	17
3.8	Objective of this thesis.....	20
4.	Results .....	21
4.1	Kinetics of Nur77 and lead cytokines in activated naïve and reactivated T <sub>H1</sub> cells .....	21
4.2	Sorting of naïve, activated naïve, T <sub>H1</sub> and reactivated T <sub>H1</sub> cells.....	23
4.3	Transcriptome analysis revealed unique transcriptome for reactivated T <sub>H1</sub> cells .....	25
4.4	Characterization of CD4 <sup>+</sup> T cell subpopulations T <sub>H1</sub> , T <sub>H2</sub> , T <sub>H17</sub> and T <sub>reg</sub> cells via master transcription factor and lead cytokine expression upon antigen-specific reactivation .....	30
4.5	In-depth analysis of transcriptome data revealed significant upregulation of Clec4e, Clec7a, Siglec5, Pdzk1ip1, Edn1 and Lyz2 and significant downregulation of Ccr4, Soc2, Enah, Dach2 and Coro6 in antigen-stimulated T <sub>H1</sub> cells and identified similar expression patterns in other CD4 <sup>+</sup> T cell subpopulations.....	32
4.6	Lead cytokine expression and in-depth analysis of transcriptome data in CD4 <sup>+</sup> T cell subpopulations reactivated with PMA/Ionomycin showed similarities to antigen-stimulated CD4 <sup>+</sup> T cells .....	36

4.7	In vivo analysis of transcriptome data in NTN model confirmed significant upregulation of Clec4e on mRNA level and Siglec5 and Clec7a on protein level in inflamed kidneys.....	40
4.8	In vivo analysis of transcriptome data in EAE mode revealed significant upregulation of Clec7a on protein level and indicated differences in gene expression of selected genes on mRNA level in different tissues.....	44
4.9	In vitro analysis of identified genes in human TH1 cells confirmed significant upregulation of CLEC4e, PDZK1IP1 and EDN1, but also significant upregulation of GIPR, CCR4 and CORO6, which were significantly downregulated in murine TH1 cells .....	46
4.10	Proteome- and Phosphoproteomeanalysis.....	50
5.	Discussion.....	52
5.1	Identification and characterization of naïve, activated naïve, TH1, reactivated TH1 cells and other CD4 <sup>+</sup> T cell subpopulations .....	52
5.2	Commonly used activation marker .....	54
5.3	Reactivation-specific genes identified in transcriptome analysis .....	56
5.4	In vitro vs in vivo .....	59
5.6	Mouse vs human .....	60
5.7	Transcriptome and Proteome analysis .....	63
5.7	Outlook.....	65
6.	Materials and Methods.....	66
6.1	Materials.....	66
6.2	Mice.....	74
6.3	Genotyping .....	75
6.4	Cell culture .....	77
6.5	Flow cytometry .....	80
6.6	Molecular biological methods .....	81
6.7	Next-generation sequencing/RNA sequencing.....	83
6.8	Proteome- and Phosphoproteome analysis.....	84
6.9	In vivo experiments: Nephrotoxic nephritis (NTN) .....	85

6.10 In vivo experiments: Experimental autoimmune encephalomyelitis (EAE) ...	87
6.11 Statistical analysis .....	88
7. References.....	89
8. List of Abbreviation.....	112
9. List of Figures.....	115
10. List of Tables.....	116
Lebenslauf.....	117
Liste der Wissenschaftlichen Publikationen.....	118
Erklärung zur Dissertation.....	119

## 1. Zusammenfassung

CD4<sup>+</sup> T-Zellen spielen als Schlüsselakteur des adaptiven Immunsystems eine wichtige Rolle bei der Abwehr von Infektionen, Autoimmunität oder Krebs. Nur wenige Studien haben sich mit der Antigen-vermittelten Reaktivierung von T-Effektorzellen in peripheren Geweben befasst, im Gegensatz zu der gut untersuchten primären Aktivierung (Priming) in Lymphknoten. In dieser Arbeit untersuchte ich die transkriptomale Veränderung reaktivierter T<sub>H</sub>1 Effektorzellen, die unabhängig von den Veränderungen während des naiven T-Zell Primings und der T-Zell Differenzierung auftraten. Zur Untersuchung dieser Hypothese wurden OT-II/Nur77<sup>GFP</sup> Mäuse verwendet, die eine direkte Identifizierung von T-Zellrezeptor (TZR)-aktivierten Zellen ermöglichten. Die Transkriptomanalyse von *in vitro* kultivierten und sortierten naiven (CD62L<sup>+</sup>, CD44<sup>-</sup>, CD69<sup>-</sup>, Nur77<sup>GFP-</sup>), aktivierten naiven (CD62L<sup>int</sup>, CD44<sup>-</sup>, CD69<sup>+</sup>, Nur77<sup>GFP+</sup>), T<sub>H</sub>1 (CD62L<sup>+</sup>, CD44<sup>+</sup>, Nur77<sup>GFP-</sup>) und reaktivierten T<sub>H</sub>1 Zellen (CD62L<sup>+</sup>, CD44<sup>+</sup>, Nur77<sup>GFP+</sup>) zeigte 10736 differenziell exprimierte Gene der T<sub>H</sub>1 Reaktivierung. Davon wurden 3106 Gene überwiegend spezifisch in reaktivierten T<sub>H</sub>1 Zellen reguliert und 447 Gene wurden ausschließlich in reaktivierten T<sub>H</sub>1 Zellen reguliert. Die Expression einiger dieser reaktivierungs-spezifischer Gene wurde anschließend in T<sub>H</sub>1, T<sub>H</sub>2, T<sub>H</sub>17 und T<sub>reg</sub> Zellen verglichen. Während T<sub>H</sub>1 und T<sub>H</sub>17 Zellen ähnliche Genexpressionen aufwiesen, war der Unterschied in T<sub>H</sub>2 und T<sub>reg</sub> Zellen größer. Die ausgewählten Gene wurden in zwei CD4<sup>+</sup> T-Zell-abhängigen *in vivo* Modellen analysiert, der nephrotoxischen Nephritis (NTN) und der experimentellen autoimmunen Enzephalomyelitis (EAE), wobei Diskrepanzen zwischen *in vitro* und *in vivo* Experimenten sowie gewebespezifische Unterschiede aufgedeckt wurden. Schließlich wurden die ausgewählten Gene in menschlichen T<sub>H</sub>1 Zellen analysiert und Unterschiede zwischen menschlichen und murinen T<sub>H</sub>1 Zellen aufgezeigt. Ich berichte hier über eine einzigartige Signatur für die T<sub>H</sub>1 Zellreaktivierung und zeige, dass sich die Genexpression einiger reaktivierungs-spezifischer Gene zwischen verschiedenen CD4<sup>+</sup> T Zell Subpopulationen, reaktivierter CD4<sup>+</sup> T Zellen aus verschiedenen Geweben sowie in humanen T<sub>H</sub>1 Zellen unterscheidet. Diese Ergebnisse erweitern das Verständnis der peripheren T-Zell-Antwort als pathophysiologischer Prozess autoimmuner Erkrankungen und können zu neuen Angriffspunkten zukünftiger Therapien, insbesondere Immuntherapie, dienen.

## 2. Abstract

CD4<sup>+</sup> T cells play, as a key player of the adaptive immune system, a critical role in orchestrating an effective immune response during infections, autoimmunity or cancer. Few studies have addressed antigen-mediated reactivation of effector T cells in peripheral tissues, as opposed to the well-studied primary activation (priming) in lymph nodes. In this thesis, I investigated the transcriptional changes of reactivated T<sub>H</sub>1 cells that occur independent to changes during naïve T cell priming and T cell differentiation. OT-II/Nur77<sup>GFP</sup> mice were used which allowed direct identification of T cell receptor (TCR) activated T cells. Transcriptome analysis of *in vitro* cultured and sorted naïve (CD62L<sup>+</sup>, CD44<sup>-</sup>, CD69<sup>-</sup>, Nur77<sup>GFP-</sup>), activated naïve (CD62L<sup>int</sup>, CD44, CD69<sup>+</sup>, Nur77<sup>GFP+</sup>), T<sub>H</sub>1 (CD62L<sup>+</sup>, CD44<sup>+</sup>, Nur77<sup>GFP-</sup>) and reactivated T<sub>H</sub>1 cells (CD62L<sup>+</sup>, CD44<sup>+</sup>, Nur77<sup>GFP+</sup>) revealed 10736 differentially expressed genes of T<sub>H</sub>1 reactivation. Of these, 3106 genes were predominantly specifically regulated in reactivated T<sub>H</sub>1 cells and 447 genes were solely regulated in reactivated T<sub>H</sub>1 cells and did not appear in the other comparisons. Furthermore, I compared the expression of some identified genes in different CD4<sup>+</sup> T cell subpopulations: T<sub>H</sub>1, T<sub>H</sub>2, T<sub>H</sub>17 and T<sub>reg</sub> cells. Gene expression was similar in T<sub>H</sub>1 and T<sub>H</sub>17 cells, while the difference in T<sub>H</sub>2 and T<sub>reg</sub> cells was greater. Subsequently, selected genes were analyzed in two CD4<sup>+</sup> T cell-dependent *in vivo* models, the Nephrotoxic Nephritis (NTN) and the experimental autoimmune encephalomyelitis (EAE), revealing discrepancies between *in vitro* and *in vivo* experiments as well as tissue-specific differences. Finally, selected genes were analyzed in human T<sub>H</sub>1 cells, polarized from peripheral blood of healthy donors, showing differences in gene expression of selected genes in reactivated human T<sub>H</sub>1 cells compared to reactivated murine T<sub>H</sub>1 cells. Here, I report a unique signature to T<sub>H</sub>1 cell reactivation that goes beyond lineage alterations. I showed that gene expression of some reactivation-specific genes differed between different reactivated CD4<sup>+</sup> T cell subpopulations *in vitro* and reactivated CD4<sup>+</sup> T cells from different tissues *in vivo* as well as in reactivated human T<sub>H</sub>1 cells *in vitro*. These findings increase the understanding of the peripheral T cell response as a pathophysiological process in autoimmune diseases and could serve as new targets for future therapies, especially immunotherapy.

### 3. Introduction

#### **3.1 Adaptive immunity: T cell biology**

The immune system is categorized into two defense mechanisms, innate and adaptive immunity. The innate immune system is the first line of defense against pathogens and consists among other cells of dendritic cells (DCs), monocytes, macrophages, neutrophils, granulocytes, eosinophils, mast cells, basophils and natural killer (NK) cells. These cells provide a rapid immune response by identifying conserved structures, named pathogen-associated molecular patterns (PAMPs), by pattern recognition receptors (PRRs). The second line of defense, the adaptive immune system, reacts specifically to defined protein stimuli, termed “antigens”, for targeted effector responses, which are carried out by B and T cells. In contrast to immune cells from the innate immune system, these cells are able to generate an immunological memory and thus respond more rapidly and effectively to pathogens encountered previously (Marshall et al., 2018; Parkin & Cohen, 2001).

The focus of this thesis is on T cells. T cell precursors develop in the bone marrow and mature in the thymus, where they differentiate into either CD8<sup>+</sup> T cells or CD4<sup>+</sup> T cells and are selected not to recognize self-antigens to prevent autoimmunity (Germain, 2002). These CD8<sup>+</sup> and CD4<sup>+</sup> T cells migrate from the thymic medulla to peripheral lymphoid sites (Weinreich & Hogquist, 2008). Classically, DCs take up and process antigen at the site of inflammation and emigrate into secondary lymphoid organs to present antigen to naïve T cells (L. Chen & Flies, 2013). During this process called priming, naïve T cells interact with DCs, undergo expansion and differentiate into effector T cells upon encountering their specific antigen. CD4<sup>+</sup> T cells are one of the main subgroups of lymphocytes and key players in adaptive immunity. They play a critical role in generating and orchestrating an effective immune response during bacterial and viral infections, autoimmunity or cancer. CD4<sup>+</sup> T cells may differentiate into different subsets: T helper type 1 (T<sub>H1</sub>), T<sub>H2</sub>, T<sub>H9</sub>, T<sub>H17</sub>, T<sub>H22</sub>, regulatory T (T<sub>reg</sub>) and follicular helper T (T<sub>fh</sub>) cells, which are characterized by different cytokine profiles and functions (Jiang & Dong, 2013). Differentiated effector T cells, especially T<sub>fh</sub> cells, can mediate antibody production by B cells in secondary lymphoid structures. Furthermore, effector T cells circulate through the blood and transmigrate from the

vasculature to the side of inflammation, where they can act directly on cellular immunity, such as in viral infections or recognize and kill cancer cells (Figure 1). Effector T cells are recruited into the inflamed tissue in a comparatively non-specific manner (David et al., 2009; Herter et al., 2015; Kawakami et al., 2005), whereas antigen recognition in the tissue drives effector functions (McLachlan, Catron, Moon, & Jenkins, 2009). When CD4<sup>+</sup> effector T cells encounter their specific antigen, they primarily act as a helper by releasing inflammatory mediators/cytokines such as interferon gamma (IFN $\gamma$ ) in the case of TH1 cells. CD8<sup>+</sup> T cells, also called cytotoxic T cells, recognize infected or degenerated cells via their specific antigen and eliminate them directly. However, in recent years several studies identified CD4<sup>+</sup> T cell subpopulations that also express key molecules associated with cytolytic granules such as granzymes (GZM) and perforin (PRF1) and have cytotoxic characteristics that

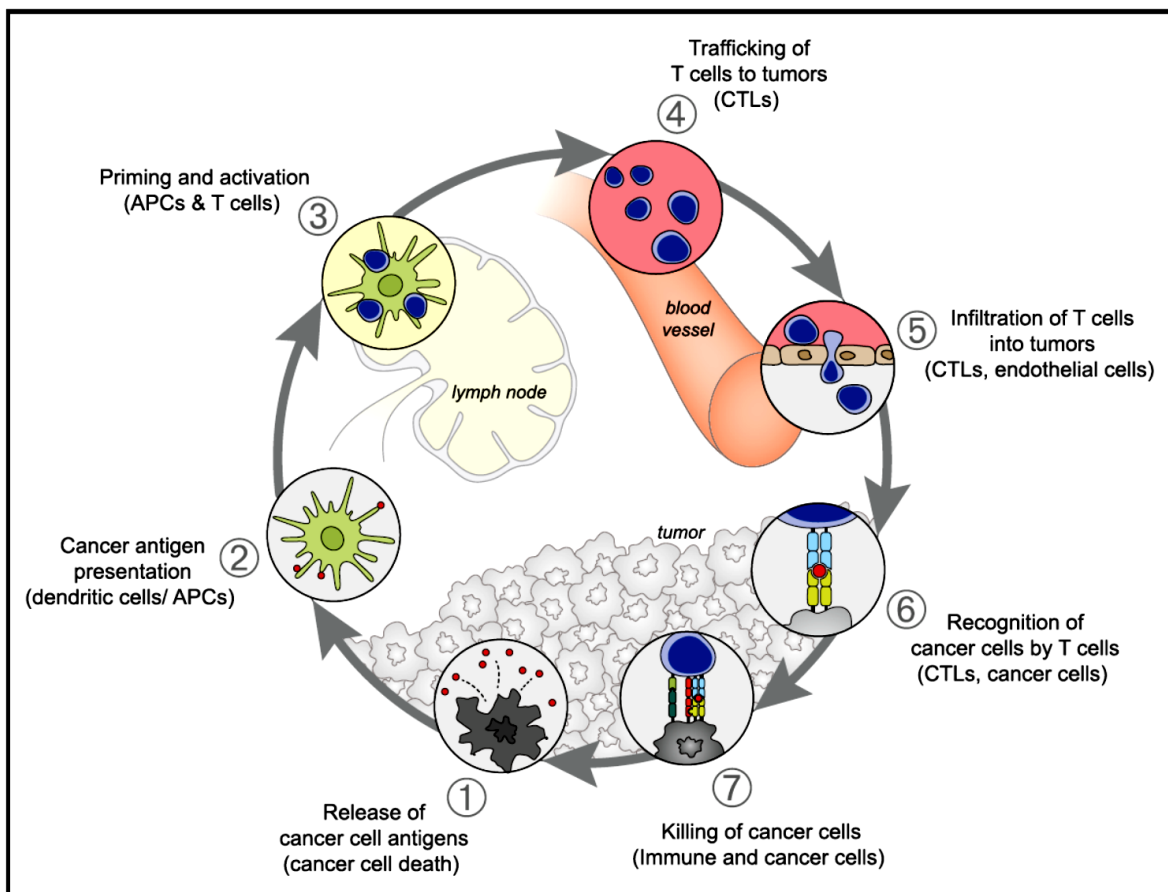


**Figure 1: The cancer-immunity cycle (Chen et al., *Immunity*, 2013)**

DCs take up antigen from the tumor, or in general from inflamed tissues, and migrate to secondary lymphoid organs to present antigen to naïve T cells, which then get activated, proliferate and differentiate into effector T cells. These effector T cells then circulate through the blood, transmigrate through the vasculature to the side of inflammation where they get reactivated and carry out their effector function.

underlie both pathogenic and protective immunity, and have therefore been named cytotoxic CD4<sup>+</sup> T cells (D. Y. Oh & Fong, 2021).

### **3.2 Priming/TCR activation**

Primary T cell activation, or priming, in the lymph nodes is mediated by mature DCs. DCs are professional antigen-presenting cells (APCs), which collect antigens in peripheral tissues and migrate to lymph nodes through lymphatic vessels, where they activate naïve T cells. T cell/DC interactions in lymph nodes during lymphocyte priming are sustained and can last for hours (Rothoef et al., 2006). Using intravital microscopy, it was shown that priming occurs in three distinct phases: Within the first 8 hours, T cells undergo multiple short encounters with DCs and upregulate early activation markers like CD25, CD44 and CD69. During the next 12 hours, T cells form long-lasting stable conjugates with DCs, which remain stable for more than an hour, and secrete cytokines such as interleukin-2 (IL-2) and IFN $\gamma$ . After 24 hours, T cells resume their rapid migration and short DC contacts and undergo massive proliferation and clonal expansion (Mempel et al., 2004).

T cell activation is mediated by the interaction between the T cell receptor (TCR), a membrane-bound protein complex on the surface of T cells, and the antigen presented on major histocompatibility complex (MHC) molecules on APCs. The TCR is a heterodimer and forms a complex with the subunits of the CD3 complex, which is involved in the transmission of the signal after the binding of the antigen. It belongs to the immunoglobulin superfamily and consists of a constant region ( $\gamma/\delta/\epsilon/\zeta$ ) mediating effector functions and a variable region ( $\alpha/\beta$ ) carrying the antigen-specificity. The interaction between TCR and the antigen presented on MHC proteins is reinforced either by the binding of the CD4 co-receptor on helper T cells with MHC class II molecules or the CD8 co-receptor on cytotoxic T cells with MHC class I molecules. In addition, these interactions are stabilized by additional adhesion molecules forming an immunological synapse (Bhattacharyya & Feng, 2020). The TCR signaling pathway is illustrated in figure 2. In detail, TCR activation results in the phosphorylation of Immunoreceptor Tyrosine based Activation Motifs (ITAMs), which serve as binding sites for the zeta chain of T cell receptor Associated Protein kinase 70 (Zap70).

Activated Zap70 is released from the ITAM binding site and further phosphorylates signaling scaffold adaptor proteins, like the Linker for Activated T cells (LAT) leading to the initiation of Phosphatidylinositol 3-Kinases (PI3K), which results in the AKT-dependent activation of Mechanistic Target of Rapamycin (mTOR) and the nuclear translocation of Nuclear Factor Kappa-light-chain-enhancer of activated B cells (NF- $\kappa$ B). Furthermore, phosphorylation of LAT leads to activation of ITK and subsequent phosphorylation of the lipase Phospholipase C gamma (PLC- $\gamma$ ), which results in the downstream release of calcium ions ( $\text{Ca}^{2+}$ ) from the endoplasmic reticulum (ER) and nuclear translocation of Nuclear Factor of Activated T cells (NFAT). NFAT was initially identified in activated T cells but some members of the NFAT family are also regulated in other cell types. T cells mainly express calcium- and calcineurin-regulated NFAT1, NFAT2 and NFAT4. In addition, phosphorylation of PLC- $\gamma$  leads to the activation of the Mitogen Activated Protein Kinase (MAPK)/Extracellular signal Regulated Kinase (ERK) and NF- $\kappa$ B pathways. Activation of the MAPK/ERK signaling cascade leads to the nuclear translocation and transcriptional activity of Adaptor-related Protein complex 1

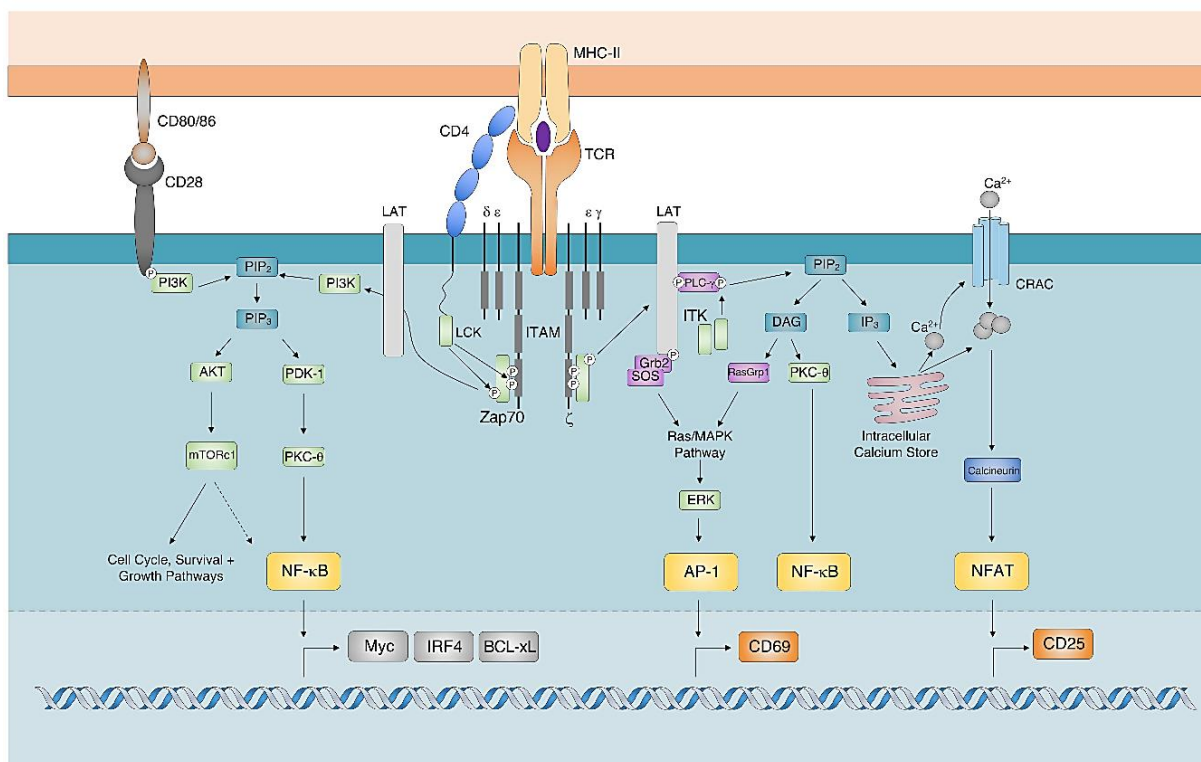


**Figure 2: TCR signaling cascade (Bhattacharyya, Front. Immunol., 2020)**

*T cell activation is mediated by the interaction between the TCR on the surface of T cells and the antigen presented on MHC molecules on APC. The binding of co-receptors on T cells reinforces this interaction. The signaling cascade activates NF- $\kappa$ B, AP-1 and NFAT, which translocate into the nucleus and orchestrate T cell activation.*

(AP-1), which orchestrates T cell activation and function together with NFAT and NF- $\kappa$ B. NF- $\kappa$ B is mainly responsible for the induction of genes for survival, proliferation and cytokine production (Jutz et al., 2016). AP-1 is a dimer of FOS and JUN, which can form a complex with NFAT. NFAT-AP-1 complex initiates a specific set of genes including functional activation of T cells such as IL-2. In the absence of AP-1, caused by the absence of co-stimulation during TCR activation, different set of genes is activated, which leads to T cell exhaustion (Macian, 2005; Martinez et al., 2015). Exhausted T cells have reduced effector functions, express inhibitory receptors, like programmed death-1 (PD-1) and have distinct metabolic and transcriptional profiles (Wherry et al., 2007).

### **3.3 CD4<sup>+</sup> T cell subpopulations**

CD4<sup>+</sup> T cells, as well as CD8<sup>+</sup> T cells (St Paul & Ohashi, 2020), can differentiate into distinct subpopulations with different functions. In this simplified model, each subpopulation has specialized functions to control immune responses like the clearance of pathogens, control of autoimmunity, immune homeostasis, and immune responses against tumors (Figure 3). Due to the dynamic nature of cytokine and cell marker characteristics, categorization of different T cell subpopulations is complex. In 1986, for the first time, two distinct CD4<sup>+</sup> T cell subpopulations (T<sub>H1</sub> and T<sub>H2</sub> cells) were identified according to the cytokines they secrete (Mosmann et al., 1986). T<sub>H1</sub> cells are characterized as CD4<sup>+</sup> T cells producing primarily IFN $\gamma$ , but also IL-2, granulocyte-macrophage colony-stimulating factor (GM-CSF) as well as IL-3. T<sub>H2</sub> cells secrete IL-3, BSF1, a mast cell growth factor and a T cell growth factor in response to T cell activation. Nowadays, T<sub>H2</sub> cells are identified mainly by the secretion of IL-4. Studies showed that T<sub>H1</sub> cells play a role in the immunity against intracellular pathogens, in autoimmunity and inflammation while T<sub>H2</sub> cells play a role mainly in the immunity of extracellular pathogens, in allergy and asthma. In 1995, another subpopulation was identified which was named T<sub>reg</sub> cells (Rudensky, 2011; Sakaguchi et al., 1995). These cells expressing CD25 mediate immunological self-tolerance. In contrast to most of the other CD4<sup>+</sup> T cell subpopulations, T<sub>reg</sub> cells have suppressive rather than activating functions. Follicular helper (T<sub>fh</sub>) cells stimulating antigen-specific naïve or memory B-cell activation and triggering germinal center (GC) formation were

characterized in 2000 (Breitfeld et al., 2000; Schaerli et al., 2000). In 2005, the IL-17 producing  $T_H17$  cells were discovered, which play a role in the immunity against extracellular pathogens, autoimmunity and inflammation (Harrington et al., 2005; Park et al., 2005). In 2008 and 2009, two more  $CD4^+$  T cell subsets were characterized, namely IL-9 producing  $T_H9$  cells (Dardalhon et al., 2008; Veldhoen et al., 2008) and IL-22 secreting  $T_H22$  cells (Duhon et al., 2009; Eyerich et al., 2009; Trifari et al., 2009). In recent years, another highly interesting  $CD4^+$  T cell subpopulation was identified: It was found that  $CD26^{\text{high}}$  T cells, which were often characterized as  $T_H17$  cells, are transcriptionally and epigenetically different, elicit potent immunity against solid tumors and have a rather cytotoxic phenotype (Nelson et al., 2020).

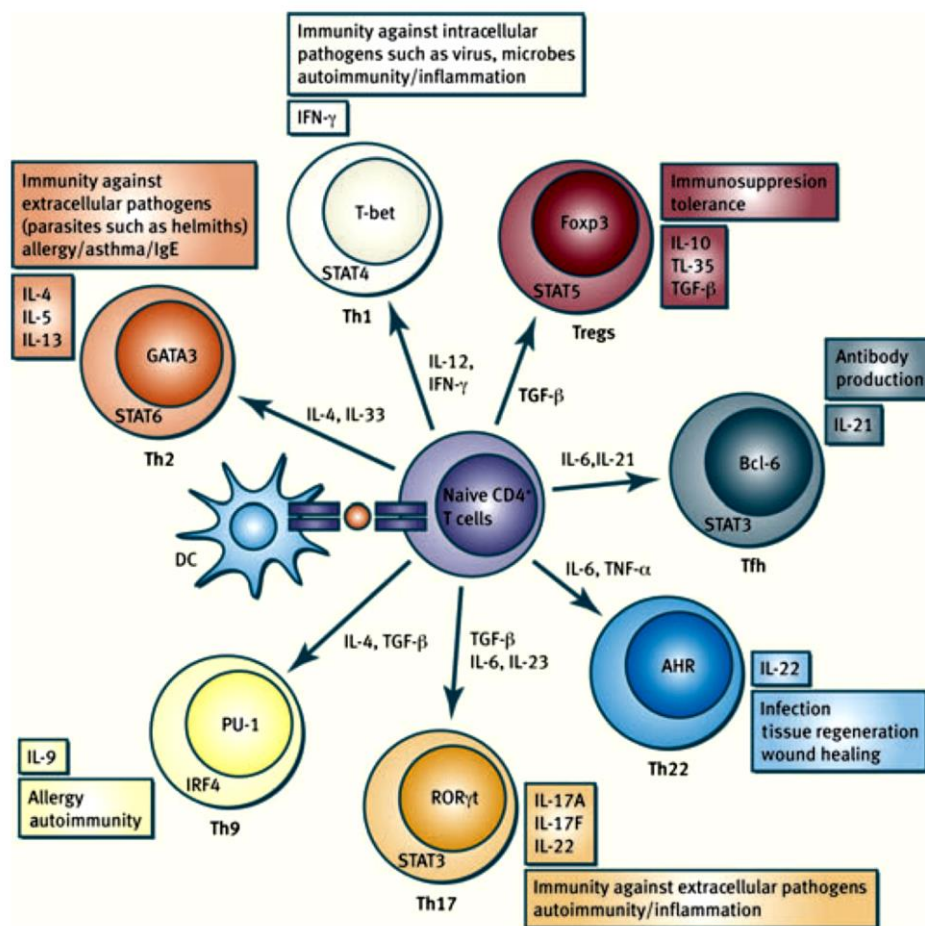


**Figure 3:  $CD4^+$  T cell subpopulations (Jiang, Immunol Rev, 2013)**

Naïve T cells differentiate into different effector T cell subpopulation under the influence of polarizing cytokines. Each subpopulation has specialized functions, set of master regulators/transcription factors and secrete lead cytokines to control immune responses like the clearance of pathogens, control of autoimmunity, immune homeostasis, and immune responses against tumors.

During the years, many factors involved in the control of CD4<sup>+</sup> T cell differentiation were identified (Jiang & Dong, 2013). First, the strength of the TCR signaling influences T<sub>H</sub> cell polarization. While weak signaling favors T<sub>H2</sub> differentiation, stronger signaling leads to T<sub>H1</sub> differentiation (van Panhuys, Klauschen, & Germain, 2014). Furthermore, naïve CD4<sup>+</sup> T cells receiving weak TCR signals fail to differentiate into T<sub>H17</sub> cells but instead express Forkhead Box P3 (FOXP3), a transcription factor (TF) associated with T<sub>reg</sub> cells, even though they were exposed to T<sub>H17</sub>-inducing cytokines (Vahedi et al., 2013; Yamane & Paul, 2013). Second, which is the most important factor, the cytokine milieu during T cell activation has a significant impact on the decision of differentiation. Thus, by adding specific cytokines into the culture, naïve T cells can be polarized to a specific subpopulation *in vitro*. For instance, T<sub>H1</sub> cells can be generated by neutralizing IL-4 and adding IL2 and IL-12 to the cell culture, while the presence of both IL-2 and IL-4 is necessary to generate T<sub>H2</sub> cells (Zhu et al., 2010). T<sub>H17</sub> cell differentiation requires transforming growth factor beta (TGF-β), IL-6, IL-21, and IL-23, while Treg differentiation requires TGF-β and IL-2 (Zhou et al., 2009). Third, TCR signaling and cytokine milieu activate certain master TF and signaling transducer and activator of transcription (STAT) proteins, which are essential for T<sub>H</sub> cell differentiation and cytokine production: T-Box transcription factor (T-Bet) and STAT4 for T<sub>H1</sub> cells, GATA Binding Protein 3 (GATA3) and STAT6 for T<sub>H2</sub> cells, RAR-related orphan receptor gamma (RORγt) and STAT3 for T<sub>H17</sub> cell and FoxP3 and STAT5 for T<sub>reg</sub> cells (Vahedi et al., 2013). Fourth, NF-κB family members are involved in subset differentiation and function. Different NF-κB subunits and the interaction of the NF-κB pathway with other signaling pathways influence transcriptional programs that allow for the differentiation into the various CD4<sup>+</sup> T cell subsets (H. Oh & Ghosh, 2013). Last, metabolic processes influence T cell differentiation. Due to an increase in cell size, high division and protein synthesis rate upon T cell activation, the metabolic signature changes from oxidative phosphorylation to anaerobic metabolism, called glycolysis (Pearce, 2010). For example, the kinase mTOR, which plays a central role in the regulation of metabolism, also regulates the differentiation of helper T cells. While T<sub>H1</sub> and T<sub>H17</sub> differentiation require mTORC1 signaling, T<sub>H2</sub> differentiation requires mTORC2 signaling (Delgoffe et al., 2011).

Furthermore, a recent study indicates that T-T cell antigen cross-presentation might influence T cell differentiation as well. CD4<sup>+</sup> T cells can act as antigen-presenting cells, take up and cross-present MHC-II from APCs in a process called trogocytosis. These antigen-presenting cells predominantly differentiate into T<sub>reg</sub> cells. T cells that have been subsequently stimulated by these antigen-presenting T<sub>reg</sub> cells predominantly differentiate into T<sub>H17</sub> cells (Boccasavia et al., 2021).

It was initially suggested that T cell differentiation was irreversible (Murphy et al., 1996), but accumulating evidence suggests that this process is more flexible than previously thought (Zhou et al., 2009). For instance, T<sub>H17</sub>/T<sub>reg</sub>-like cells were found to be both FOXP3<sup>+</sup> and express IL-17a (Huang & Fu, 2011; Kryczek et al., 2011; Yang et al., 2011). Furthermore, T<sub>H17</sub> cells can transdifferentiate into T<sub>H1</sub> cells and vice versa (Y. K. Lee et al., 2009; H. P. Liu et al., 2015).

### ***3.4 Effector and memory T cell differentiation***

Immunological memory, characterized by a faster and stronger response to repeated stimulation by a previously encountered antigen, is the hallmark of adaptive immunity. After differentiation and clearance of the pathogen, most effector T cells undergo apoptosis during the first two weeks, while some cells become long-lived antigen-experienced memory T cells. These memory T cells have a lower activation threshold and less co-stimulation dependency (Raphael et al., 2020).

So far, at least four distinct subsets of memory T lymphocytes have been described: central memory T cells (T<sub>CM</sub> cells), effector memory T cells (T<sub>EM</sub> cells), tissue-resident memory T cells (T<sub>RM</sub> cells), and stem cell-like memory T cells (T<sub>SCM</sub> cells) (Chang et al., 2014). In 1999, two functionally distinct memory T cell subsets (T<sub>CM</sub> and T<sub>EM</sub> cells) were identified by the expression of CCR7, a chemokine receptor that controls homing to secondary lymphoid organs (Sallusto et al., 1999). T<sub>CM</sub> cells are present in secondary lymphoid organs like lymph nodes and the white pulp (WP) of the spleen and express lymph-node homing receptors like CD62L and CCR7. These cells are characterized by rapid proliferation upon antigen stimulation. They lack immediate effector functions, but efficiently stimulate B cells and differentiate into CCR7<sup>-</sup> effector T cells upon secondary stimulation (Hengel et al., 2003; MacLeod et

al., 2011).  $T_{EM}$  cells lack these lymph-node homing receptors but express receptors for migration to inflamed tissues. They circulate between blood, spleen and peripheral tissues and they are characterized by rapid execution of effector functions (Sallusto et al., 2014). Another memory T cell subpopulation are the  $T_{RM}$  cells, which constitute a memory lineage remaining in peripheral tissues without the ability to recirculate into peripheral blood or lymph nodes (Schenkel & Masopust, 2014). Recently a new memory T cell subpopulation was identified and called  $T_{SCM}$  cells. These cells express  $CD95^+$ ,  $CD122^+$ ,  $CXCR3^+$ ,  $CD11a^+$  markers and are characterized by their self-renewal capacity and ability to generate both  $T_{CM}$  cells and  $T_{EM}$  cells (Gattinoni et al., 2011).

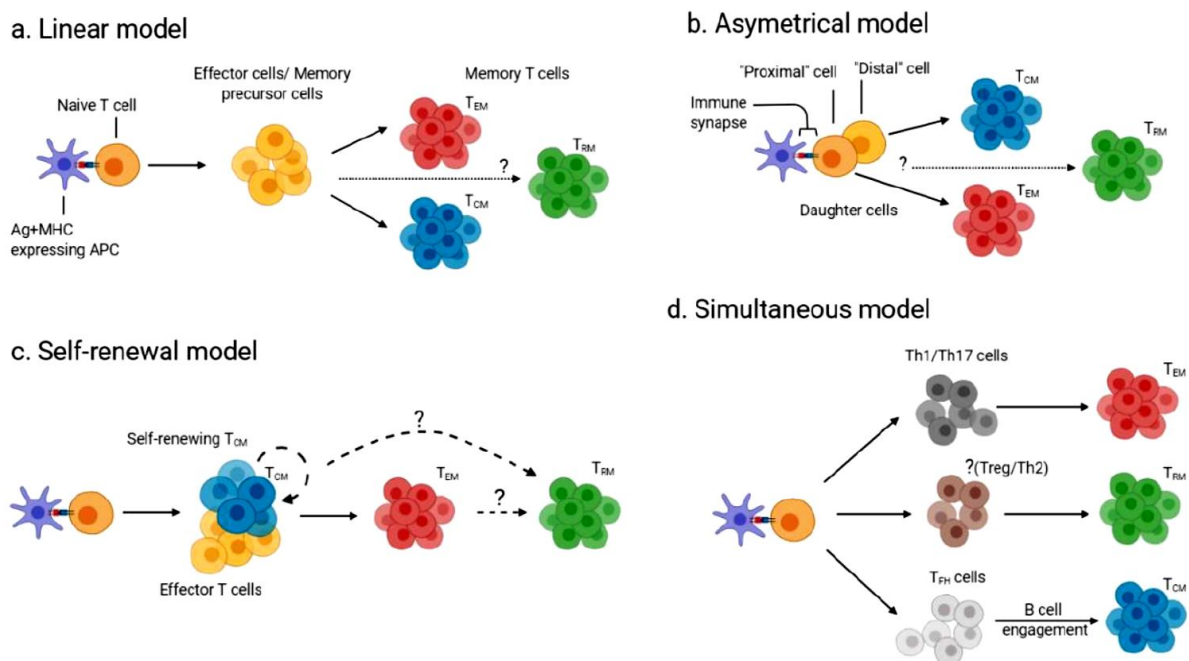


**Figure 4: Suggested models for memory T cell development (Raphael et al., Cells, 2020)**

In the linear model naïve T cells differentiate into precursor cells which further give rise to memory T cells. The asymmetrical model suggests that two daughter cells of the same clone can undergo different fates: one cell proximal to the immunological synapse can give rise to  $T_{EM}$  cells, while the distal daughter cell gives rise to  $T_{CM}$  cells. In the self-renewal model naïve T cells first differentiate to either self-renewing  $T_{CM}$  or effector T cells, which further differentiate to  $T_{EM}$  cells, which finally give rise to  $T_{RM}$  cells. The simultaneous model suggests that the effector T cell subset determines the fate of the generated memory T cell subset.

T cell differentiation and effector function are comparably well studied. However, the development of immunological memory in T cells, especially  $CD4^+$  T cells, is still merely understood. Different models for the development of memory T cell subsets were proposed (Figure 4), yet these models remain subject of debate (Raphael et al., 2020). In the linear model, naïve T cells differentiate into effector T cells/memory

precursor cells, which further give rise to  $T_{EM}$  or  $T_{CM}$  or possibly  $T_{RM}$  cells. The asymmetrical model suggests that two daughter cells of the same clone can undergo different fates: the cell proximal to the immunological synapse can give rise to  $T_{EM}$  cells, while the distal daughter cell gives rise to  $T_{CM}$  cells. In the self-renewal model, naïve T cells first differentiate to either self-renewing  $T_{CM}$  or effector T cells, then those can further differentiate to  $T_{EM}$  cells, which finally can give rise to  $T_{RM}$  cells. The simultaneous model suggests that the effector T cell subset determines the fate of the generated memory T cell subset. For example,  $T_{H1}$  cell or  $T_{H17}$  cell subsets can generate  $T_{EM}$  cells, whereas  $T_{FH}$  cells can generate  $T_{CM}$  with the help of B cells. Different studies support each model, but the heterogeneity of memory T cell phenotypes might rather be explained by a combination of these models.

While mTORC1 and mTORC2 play an essential role in  $CD4^+$  T cell subset differentiation, a recent study indicates that mTORC2 also plays a vital role in maintaining T cell memory, not only in  $CD8^+$  T cells (Pollizzi et al., 2015), but also in  $CD4^+$  T cells (Y. Wang et al., 2021). However, further studies are needed to clarify the molecular mechanisms of T cell memory.

### ***3.5 Antigen-mediated T cell reactivation in peripheral tissues***

So far, very few studies have addressed antigen-mediated reactivation of effector T cells in peripheral tissues as opposed to the well-studied priming and differentiation in the lymph nodes. As mentioned before, effector T cells are recruited rather unspecifically to inflamed tissue independent of their antigen-specificity. While recruited, non-specific T cells that fail to be activated *in situ* are shown to exit inflamed tissue via afferent lymphatics or may undergo apoptosis, little is known about the fate of antigen-specific T cells in the tissue (Debes et al., 2005). Using intravital microscopy, studies showed that the mechanisms involved in reactivation in the tissue are distinctly different from those involved in primary activation in lymph nodes. While T cell/DC interactions in lymph nodes during lymphocyte priming are sustained and can last for hours, T cells in peripheral tissues require a series of brief interactions with APCs, indicating that signal integration between contacts is necessary to achieve activation (Lodygin et al., 2013; Marangoni et al., 2013). Besides this difference in activation

kinetics, there is indication that numerous APCs are able to reactivate effector T cells in the tissue (Low et al., 2020). It is not known which APCs specifically activate effector T cells in the tissue, but there is indication that tissue-specific cells can act as these APCs. For instance, there is a variety of tissue-resident macrophages with various functions, which are still not completely understood (Blériot et al., 2020). Studies found that macrophages can highly express MHC-II, like monocytes migrating into the intestine and differentiating into macrophages to become MHC-II<sup>+</sup> (Desalegn & Pabst, 2019; Shaw et al., 2018). Furthermore, macrophages and T cells can affect each other by the secretion of different cytokines (Guerriero, 2019; Roberts et al., 2015). Nevertheless, it is not known if macrophages initiate effector T cells reactivation in tissues. Furthermore, evidence shows that podocytes in the kidney may constitute APCs responsible for T cell reactivation in the tissue (Goldwich et al., 2013). In the example of the brain and central nervous system (CNS), there is indication that microglia may play a role in boosting CD4<sup>+</sup> T cell reactivation (Juedes & Ruddle, 2001; Odoardi et al., 2007; Wlodarczyk et al., 2014). However, the plasticity of DCs, macrophages and microglia in the CNS is still debated. Furthermore, it was merely a decade ago that Marc Jenkins' group demonstrated that antigen presentation in the tissue is in fact necessary to elicit effector T cell functions and they characterized the APCs mediating reactivation in the skin: the skin-specific Langerin<sup>+</sup> cells (McLachlan et al., 2009). In addition, a recent study showed that CXCL10<sup>+</sup> perivascular clusters enriched for CD11c<sup>+</sup> MHC-II<sup>+</sup> monocyte-derived DCs serve as an entry spot and early peripheral activation for T<sub>H</sub>1 cells into the inflamed skin (Prizant et al., 2021). However, the phenotypic distinction of the individual APC populations is still challenging and studies addressing the question of which cells are mediating reactivation in other organs like the lung or central nervous system are largely missing.

As opposed to stimulation in lymph nodes, there are no specific markers for reactivated effector T cells in the tissue. However, there is frequent misconception, mainly due to the lack of distinction between primary T cell activation in the lymph nodes and secondary T cell reactivation in the tissue. Many surface markers are used to define phenotypically distinct populations of antigen-specific T cells like CD45RO, CD45RA, CD62L, CD28, CD27, CD7, CD57, CD127, and CCR7 (Harari et al., 2006). These markers rather identify T cell populations at different stages of differentiation

than the current activation state of a T cell. In addition, the definition of activation markers can also be misleading. For instance, it is thought that CD69 upregulation is a marker of early T cell activation, thereby not a specific marker for reactivation. However, CD69 is also upregulated in T<sub>RM</sub> cells, even if there is no evidence of recent T<sub>RM</sub> cell activation (Raphael et al., 2020). Furthermore, CD69 upregulation can be induced by inflammatory stimuli, so it is not a specific marker for TCR stimulation (Cibrián & Sánchez-Madrid, 2017). Therefore, CD69 is a marker for memory cells rather than effector activation (Schreiner & King, 2018).

Commonly a cytokine secretion assay is used to examine T cell reactivation. T cells recovered from the site of inflammation are stimulated by using the phorbol ester PMA, which activates protein kinase C, in combination with the calcium ionophore ionomycin, or by co-culture with antigen-loaded APCs to elicit effector cytokine production. However, the observed cytokine or proliferative response *ex vivo* does not mean that these T cells were previously reactivated *in vivo*. Whether these T cells were recruited unspecifically due to an inflammatory reaction or are actually active in the tissue (in the sense of a directed immune defense) cannot be determined by this method. Overall, a proper measurement of the physiological functionality *in vivo* is currently not possible.

### **3.6 CD4<sup>+</sup> T cell-dependent disease model: Nephrotoxic nephritis (NTN)**

There are just a few CD4<sup>+</sup> dependent T cell disease models available to study CD4<sup>+</sup> T cell functions in the tissue *in vivo*. One of the established CD4<sup>+</sup> T cell-dependent disease models is a polyclonal kidney inflammation model, the nephrotoxic nephritis (NTN) (Brähler et al., 2018; Herter et al., 2015; Nishi et al., 2017; Nosko et al., 2017). NTN is an immune complex-mediated inflammation of the kidney that corresponds to that of human glomerulonephritis. So far, there are hardly any targeted therapy options for patients with this disease. The main function of the kidney is to cleanse the blood of final products of metabolism and to regulate the water, electrolyte and acid-base balance. Under normal conditions, the kidneys filter primary urine, which is further reabsorbed into secondary urine in the tubular system. The decisive structure for filtration is within the renal cortex and medullary region and consists of ~1 million filter

units per kidney, called glomeruli. These glomeruli consist of a capillary convolute and a capsule (Bowman's capsule, Figure 5). The actual filtration barrier is formed by the endothelial cells of the capillaries and highly specialized epithelial cells (podocytes), as well as the basement membrane in between (Pavenstädt et al., 2003). In glomerulonephritis, this filter unit is destroyed by an autoimmune inflammation. The causes of glomerulonephritis are many and varied, but the resulting inflammation of the kidney has dramatic consequences for the patients: Blood (hematuria) and proteins (proteinuria) leak into the urine. This situation sometimes leads to massive edema, both subcutaneously and in the lungs (pulmonary edema, with associated shortness of breath), an increase in blood lipids (hyperlipoproteinemia) and a lack of essential serum proteins. The lack of serum proteins also leads to blood clotting disorders and susceptibility to infection. At the same time, blood pressure increases due to kidney deficiency, which might increase the risk for cardiovascular diseases (Hutton et al., 2017). This clinical outcome, mainly presented by proteinuria, is called nephrotic syndrome, unlike nephritic syndrome, which is mainly associated with hematuria. As the inflammation progresses, the kidney filter is completely destroyed, scarred with life-threatening loss of kidney function and i.e. necessity for renal replacement function (Kurts et al., 2013).

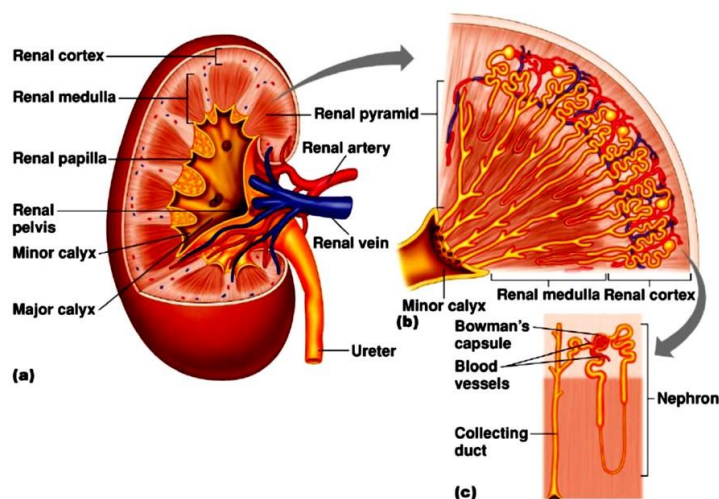


**Figure 5: Anatomy of the kidney**

*(Principles of Human Physiology, Third Edition, Figure 18.2, The Urinary System: Renal Function @ 2008 Pearson Education, Inc. Benjamin Cummings, Co.)*

NTN in mice is triggered by a serum, which is directed against glomeruli obtained from immunized sheep. Sheep are usually immunized with purified glomeruli from rat or rabbit or cell extracts, so that antibodies against glomerular structures are formed. The antiserum is administered to mice by a single injection of serum via the tail vein or intraperitoneal injection. The antibodies from the sheep serum bind to the glomerular basement

membrane and, analogous to the clinical picture in humans, lead to the formation of complexes of complement and anti-sheep antibodies in mice (immune complex), which in turn activate host immune cells (Kurts et al., 2013).

So far, it is proposed that cells of the innate immune system like neutrophils, mast cells and  $\gamma\delta$  T cells, which link innate and adaptive immunity (Papadopoulou et al., 2020), trigger the first kidney damage after antibody injection. The injected antibodies form immune complexes and activate complement components, which lead to the recruitment of innate immune cells. In parallel, DCs activate T cells in lymphatic tissues by presenting heterologous nephrotoxic antibody epitopes. These T cells mainly differentiate into  $T_H1$  and  $T_H17$  cells and subsequently infiltrate the inflamed kidney. The first wave of pro-inflammatory T cells consists of pathogenic  $T_H17$  cells. This infiltration is counter-regulated by  $T_{reg}$  cells that produce the anti-inflammatory cytokine IL-10. Eventually, mature DCs recruit  $T_H1$  cells, which secrete IFN $\gamma$ . These

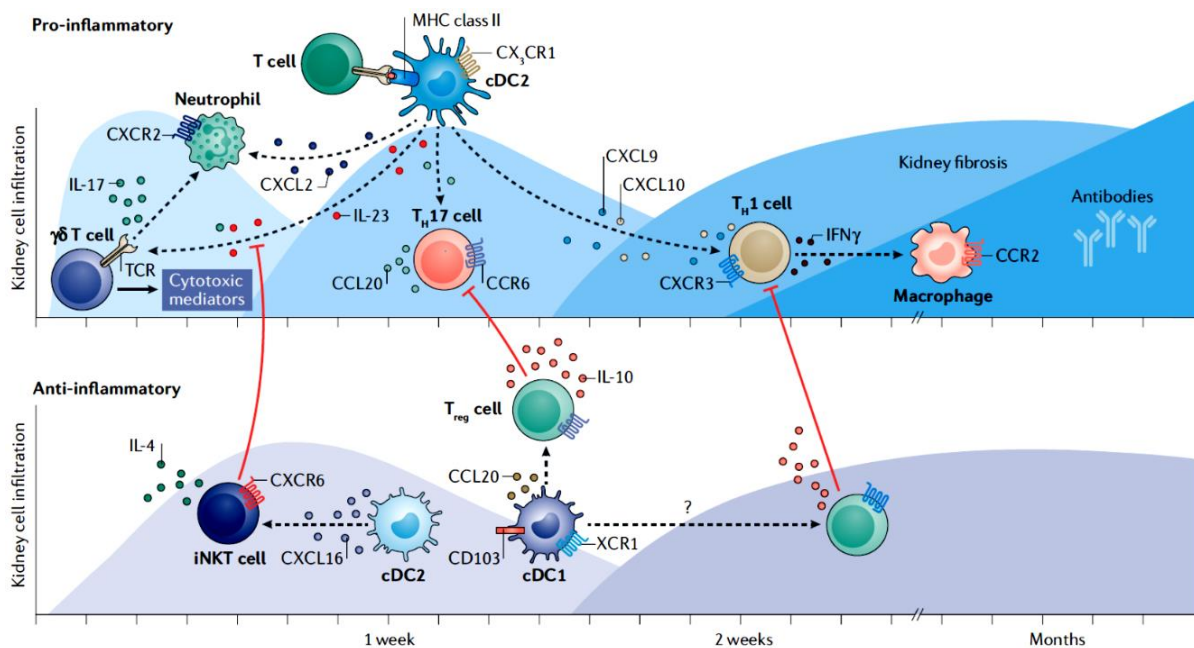


**Figure 6: Course of nephrotoxic nephritis model. Illustration of the four stages of immune activation in NTN (Kurts, Ginhoux, & Panzer, 2020).**

*Pro-inflammatory:* NTN is induced by injection of a heterologous serum against glomeruli. Within hours, DCs recruit neutrophils and stimulate  $\gamma\delta$  T cells. In parallel DCs activate naïve T cells in secondary lymphatic organs, which differentiate into  $T_H17$  cells and migrate to the kidney. During the third stage  $T_H1$  cells are recruited to the kidney which further stimulate macrophages. In the fourth stage, most antibodies form immune complexes in the kidney, which further damages the kidney.

*Anti-inflammatory:* During the second and third stage of immune activation first regulatory invariant natural killer cells (iNKT) then also  $T_{regs}$  are recruited to the kidney, which protect the inflamed tissue by partly inhibiting  $T_H17$  and  $T_H1$  cells.

T<sub>H</sub>1 cells recruit then pro-inflammatory cells, including monocytes and macrophages, which produce pro-inflammatory factors such as nitric oxide (NO) and tumor necrosis factor-alpha (TNF $\alpha$ ) (Figure 6). Overall, this process ultimately leads to kidney scarring and thus the loss of function of the glomerulus (Disteldorf et al., 2015; Hoppe & Vielhauer, 2014; Riedel et al., 2012; Turner et al., 2012).

Recent studies indicate that in certain cases, CD4<sup>+</sup> effector T cells can also act very early in inflammatory response. So far, this has mainly been investigated in a murine model of acute kidney damage (ischemia, reperfusion damage). It was shown that the activation of T<sub>H</sub>1 cells (as well as other CD4<sup>+</sup> subpopulations such as the anti-inflammatory CD4<sup>+</sup> T<sub>reg</sub> cells) in the kidney and particularly the local release of IFN $\gamma$  have critical functions for the subsequent immune response of the innate immune system. Mice without T cells are protected from the development of reperfusion damage. The administration of monoclonal T cells specific for an antigen that is not present in the body, like ovalbumin, does not change this. Therefore, reperfusion damage only develops if polyclonal T cells, in other words, T cells including those for the presented antigens, are present in the kidney (Satpute et al., 2009). It is certain that antigen presentation takes place in the kidney. However, it is still unclear how this happens and which cells present antigens to reactivate effector T cells in the tissue.

### ***3.7 CD4<sup>+</sup> T cell-dependent disease model: experimental autoimmune encephalomyelitis (EAE)***

Another established CD4<sup>+</sup> T cell-dependent disease model is the experimental autoimmune encephalomyelitis (EAE), which corresponds to human multiple sclerosis. Multiple sclerosis is a neurological disease, mainly manifested by demyelination of the CNS, inflammation of the CNS and axonal damage or loss and gliosis (astrocytic reaction to CNS damage) (Constantinescu et al., 2011). Symptoms include visual disturbances, muscle weakness, trouble with coordination and balance, sensations such as numbness, prickling and others, as well as thinking and memory problems. The specific mechanism leading to this neurological autoimmune disease is largely unknown.

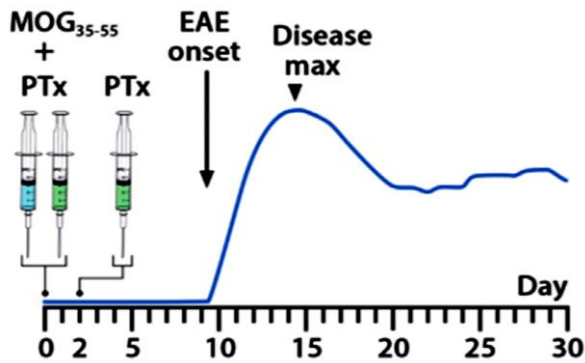


**Figure 7: Experimental setup and disease progression of EAE (Huntemann et al., 2022)**

*MOG<sub>35-55</sub> peptide emulsified in CFA is injected s.c. at day 0. On Day 0 and 2 PTX is injected i.p. Mice develop disease indicated by tail paralysis and hind limb paresis between day 9 and 14.*

Especially MOG<sub>35-55</sub> peptide injection leads to EAE progression indicating that this peptide plays a pathogenic role in this disease (Mendel et al., 1995). Adjuvants are used to increase antigen-specific immune responses and activate autoimmune mechanisms in this model, especially in CD4<sup>+</sup> T cells ('t Hart et al., 2011). DCs take up the peptide at the injection site and activate T cells in peripheral lymph nodes. Studies showed that T<sub>H</sub>1 and T<sub>H</sub>17 cells play a predominant role in the development of EAE (Bettelli et al., 2004; Fletcher et al., 2010; Komiyama et al., 2006). In addition, mice are administered with PTX intraperitoneally (i.p.) on day 0 and 2. PTX is commonly administered to promote efficient induction of EAE (Huntemann et al., 2022). The exact mechanism is not fully understood, but it is assumed that PTX may increase the permeability of the blood-brain barrier, inhibit G-protein signaling and activate TLR4 signaling (Hasselmann et al., 2017; Ronchi et al., 2016). However, it is clear that PTX significantly enhances leukocyte response in lymphoid organs and consequently enhances disease development and progression in the CNS (Hasselmann et al., 2017). Disease onset is indicated by hind tail paralysis and hind limb paresis around day 14. Furthermore, during this disease peak CD4<sup>+</sup> T cell infiltration into the CNS is highest (Dusi et al., 2019; Leuenberger et al., 2013).

There are different EAE models available, but in this thesis, the chronic EAE model was used, in which mice were treated with complete Freund's adjuvant (CFA) mixed with myelin oligodendrocyte glycopeptide (MOG<sub>35-55</sub>) and Bordetella pertussis toxin (PTX) (Figure 7). MOG peptides are expressed on the outermost lamella of the myelin sheath and on oligodendrocytes.

The proposed mechanism of T cell priming, migration, CNS infiltration and reactivation in the EAE model is depicted in Figure 8 (Goverman, 2009). Most EAE studies investigate the adhesion and transmigration mechanisms of CD4<sup>+</sup> T cells into the CNS (Azcutia et al., 2017; Gerwien et al., 2016; Kawakami et al., 2005; X. Zhang et al., 2020), especially with the focus on the interaction of T cells with the endothelial basement membrane (C. Wu et al., 2009; X. Zhang et al., 2020). Furthermore, there are publications available investigating T cell migratory activity of CD4<sup>+</sup> T cells in the CNS (Flügel et al., 2001; Lodygin et al., 2013). However, in these studies only commonly known activation markers were analyzed, which are not reactivation-specific markers.

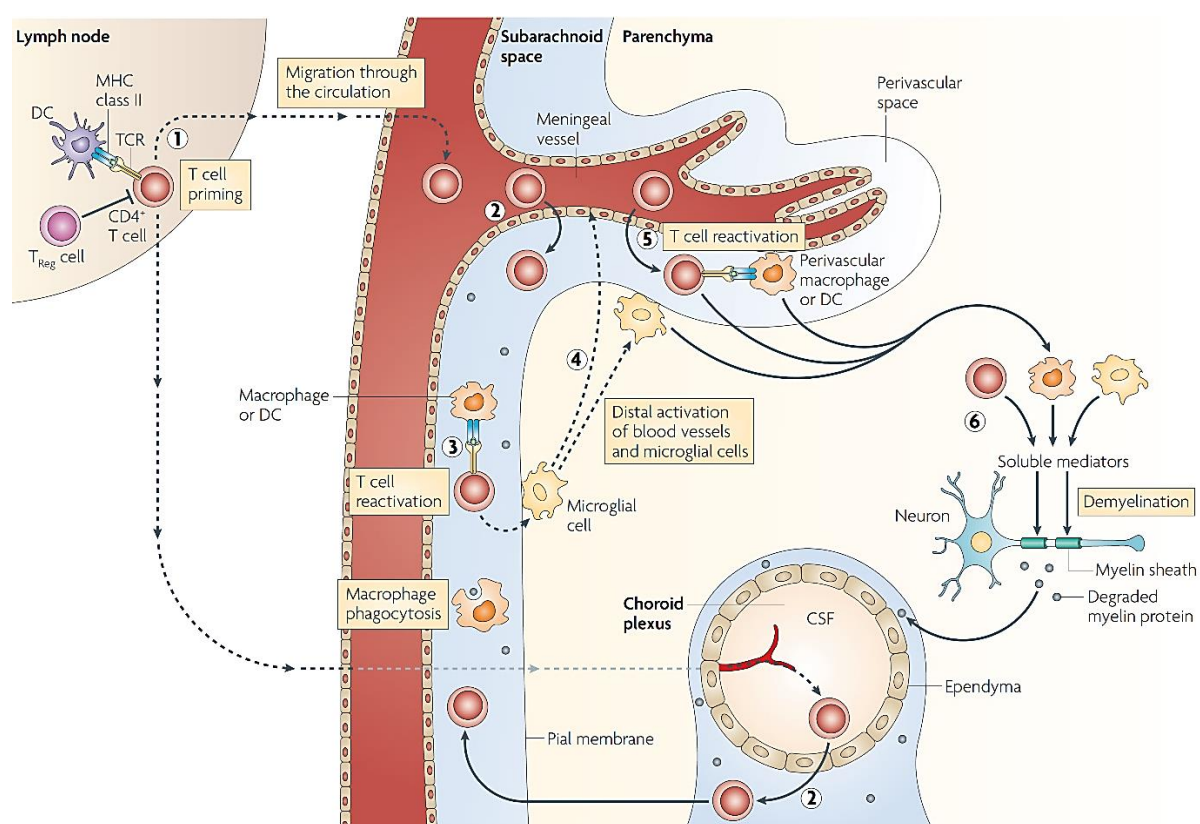


**Figure 8: The role of CD4<sup>+</sup> T cells in EAE (Goverman, 2009)**

CD4<sup>+</sup> T cells are primed in peripheral lymph nodes by DCs presenting myelin epitopes (1). CD4<sup>+</sup> effector T cells enter the subarachnoid space by crossing the blood–brain barrier (2); CD4<sup>+</sup> effector T cells are reactivated within the subarachnoid space by MHC-II expressing APCs presenting myelin epitopes (3). These reactivated T cells activate microglial cells, triggering activation of distal microglial cells and blood vessels (4). Reactivated CD4<sup>+</sup> T cells adhere to and cross the activated blood–brain barrier, enter the perivascular space and are reactivated again by APCs (5). T cells enter the parenchyma and, together with activated macrophages and microglial cells, secrete soluble mediators that trigger demyelination (6).

### **3.8 Objective of this thesis**

Surprisingly, only few studies have addressed antigen-mediated reactivation of effector T cells in peripheral tissues, as opposed to the well-studied primary activation or “priming” in the lymph nodes. While T cell/DC interaction in lymph nodes during lymphocyte priming can last for hours, T cells in peripheral tissues require a series of brief interactions, indicating that signal integration between contacts is necessary to achieve activation. Molecular characterization of the reactivation process is virtually non-existent, i.e. limited to the aforementioned description of the spatiotemporal movement of T cells in tumors and the brain (Lodygin and others 2013; Marangoni and others 2013) and two studies describing the upregulation of CD25 and Ox40 (TNF Receptor Superfamily Member 4) on reactivated T cells (Flügel and others 2001; Kawakami and others 2005). The functional state of T cells is of great clinical interest, especially in the context of autoimmunity and immunotherapy. Despite the importance of effector T cell function for inflammation, autoimmunity and cancer immunity, characterization of this process is elusive. The central aim of this thesis was to perform an in-depth characterization of the transcriptome of reactivated CD4<sup>+</sup> effector T cells in order to improve our understanding of this process, identify novel targets to influence this process and at the same time identify pathways and targets for future studies. I focused on T<sub>H</sub>1 cells, which are primarily responsible for activating and regulating the development and persistence of cytotoxic T cells, for the immunity of intracellular pathogens and activation of APCs, which take up infected cells or tumor cells.

Differential gene expression analysis of *in vitro* cultured naïve, activated naïve, T<sub>H</sub>1 and reactivated T<sub>H</sub>1 cells revealed that T<sub>H</sub>1 reactivation is a process transcriptionally different to naïve T cell activation and differentiation. Furthermore, some identified genes were analyzed in other CD4<sup>+</sup> T cell subpopulations *in vitro* and in two clinically relevant disease models: the NTN and the EAE model. Two different *in vivo* disease models were used to investigate the question if reactivation mechanisms are different in different tissues. Lastly, the identified genes were analyzed in human T<sub>H</sub>1 cells to translate the findings into the human setting. Taken together this is the first thorough examination of effector T cell reactivation in peripheral tissues - a process that is undoubtedly of immense significance well beyond the scope of the kidney injury and neurodegenerative disease examined here.

## 4. Results

### 4.1 Kinetics of Nur77 and lead cytokines in activated naïve and reactivated $T_H1$ cells

Aim of this thesis was the identification of genes, which were specifically regulated during effector T cell reactivation, with the focus on  $T_H1$  cells. To this end, I characterized naïve, activated naïve, differentiated  $T_H1$  and reactivated  $T_H1$  cells. These four populations were needed to identify genes specific for initial TCR activation, T cell differentiation and finally effector T cell reactivation. Naïve T cells were isolated from the spleen of OT-II/Nur77<sup>GFP</sup> mice and differentiated for 5 days to  $T_H1$  cells *in vitro*.  $T_H1$  cells were reactivated by co-culture with Ova<sub>323-339</sub> peptide-pulsed bone marrow derived macrophages (Figure 9). Kinetics of endogenous Nur77, IL-2 and Nur77<sup>GFP</sup> reporter expression in activated naïve T cells has been performed via qRT-PCR and flow cytometry to assess transcriptional and protein changes over time and to identify the right time point for transcriptome analysis of activated naïve T cells. Nur77 is a gene upregulated early during TCR signaling and IL-2 is one important

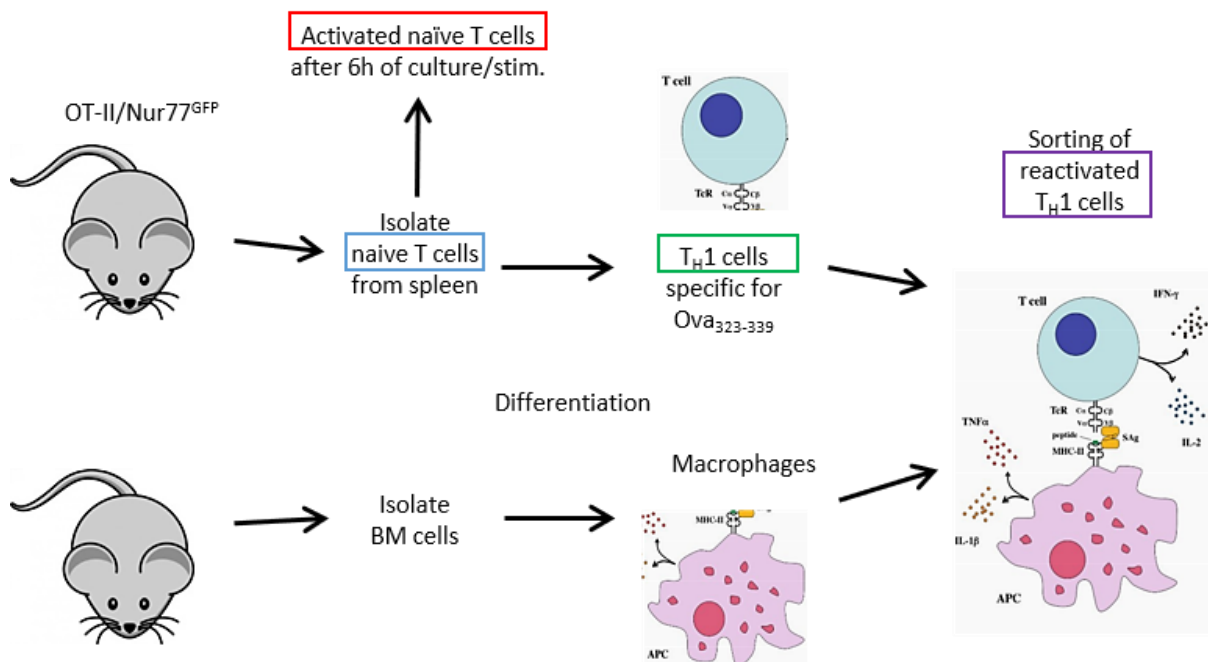


**Figure 9: Schematic experimental design**

Isolation, differentiation and stimulation of naïve, active naïve,  $T_H1$  and reactivated  $T_H1$  cells. Naïve T cells were isolated from spleens of OT-II/Nur77<sup>GFP</sup> mice and differentiated for 5 days to  $T_H1$  cells. In parallel bone marrow cells were isolated and differentiated for 7 days to macrophages. These macrophages were pulsed with 10  $\mu\text{g/ml}$  Ova<sub>323-339</sub> peptide for 1 hour and  $T_H1$  cells were reactivated by co-culture with these Ova<sub>323-339</sub>-peptide-pulsed macrophages for six hours

cytokine upregulated during primary, naïve TCR activation. qRT-PCR has shown a rapid upregulation of endogenous Nur77 within the first two hours of activation which already declined after six hours of activation while IL-2 gene expression slowly increased within the first hours up to 24 hours (Figure 10, A). On protein level, expression of Nur77<sup>GFP</sup> reporter rapidly increased within the first two hours, reaching a plateau after around six hours. It was stably expressed for 24 hours while IL-2 protein expression was first detectable after 24 hours of activation (Figure 10, B). The relatively late upregulation of IL-2 is in line with other publications (Hwang, Hong, & Glimcher, 2005; Sojka, Bruniquel, Schwartz, & Singh, 2004).

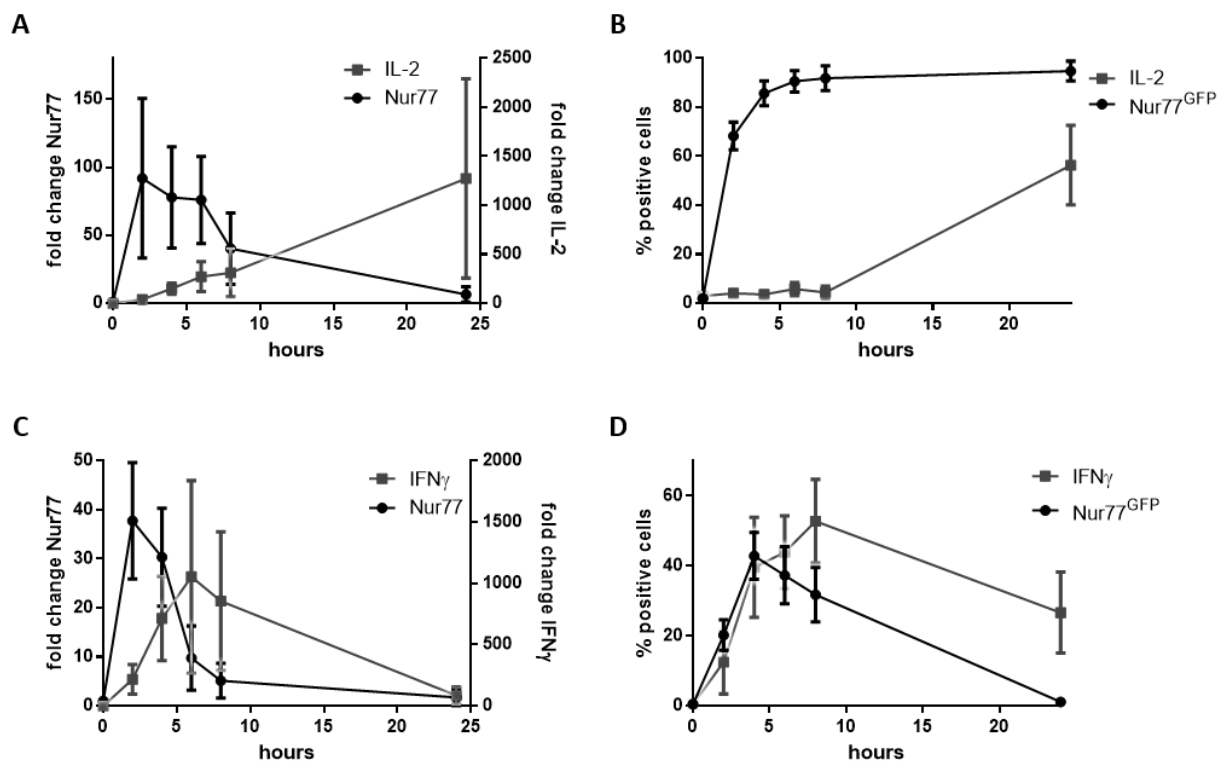


**Figure 10: Kinetics of activated naïve T cells and reactivated TH1 cells**

*A: Kinetics of IL-2 and endogenous Nur77 via qRT-PCR in naïve T cells isolated from the spleen of OT-II-Nur77<sup>GFP</sup> mice. B: Kinetics of IL-2 and Nur77<sup>GFP</sup> via flow cytometry in naïve T cells isolated from the spleen of OT-II-Nur77<sup>GFP</sup> mice. C: qRT-PCR of IFN $\gamma$  and endogenous Nur77 in TH1 cells differentiated from OT-II-Nur77<sup>GFP</sup> mice; D: Kinetics of IFN $\gamma$  and Nur77<sup>GFP</sup> via flow cytometry in TH1 cells OT-II-Nur77<sup>GFP</sup> mice; mean with SD (n=6)*

Furthermore, kinetics of endogenous Nur77, IFN $\gamma$  and Nur77<sup>GFP</sup> in reactivated TH1 cells has been performed via qRT-PCR and flow cytometry to identify the right time point for transcriptome analysis of reactivated effector T cells. IFN $\gamma$  expression was analyzed, because it is the lead cytokine of TH1 cells (Reinhardt, Liang, & Locksley, 2009). The analysis showed that endogenous Nur77 mRNA expression rapidly increased within the first two hours and decreased after four hours while IFN $\gamma$  gene

expression increased slowly and reached a maximum after six hours of co-culture (Figure 10, C). On protein level, Nur77<sup>GFP</sup> reached a peak after four hours of co-culture while the maximum of IFN $\gamma$  expression was reached after 8 hours of co-culture (Figure 10, D).

It is worth noting that endogenous Nur77 gene expression was overall higher in activated naïve CD4<sup>+</sup> T cells (up to 90 fold change) than in reactivated T<sub>H1</sub> cells (up to 40 fold change). Moreover, over 90% of activated naïve T cells expressed Nur77<sup>GFP</sup> compared to 40% Nur77<sup>GFP+</sup> reactivated T<sub>H1</sub> cells indicating that even in a transgenic model not all ovalbumin-specific T<sub>H1</sub> cells get reactivated by antigen stimulation. This goes in line with previous studies (Ashouri & Weiss, 2017; Flügel et al., 2001; Moran et al., 2011; Westhorpe et al., 2018). Based on the results showing that most naïve T cells were Nur77<sup>GFP+</sup> and IL-2 mRNA could be detected after six hours of stimulation, this time point was determined as the optimal time point for the analysis of activated naïve T cells. Furthermore, a similar stimulation time point was applied during T<sub>H1</sub> cell reactivation as IFN $\gamma$  mRNA level reached a peak and Nur77<sup>GFP</sup> signal remained persisted after six hours of stimulation. However, similar time points for TCR signaling in activated naïve as well as in reactivated T<sub>H1</sub> cells make these groups more comparable.

#### **4.2 Sorting of naïve, activated naïve, T<sub>H1</sub> and reactivated T<sub>H1</sub> cells**

Naïve CD4<sup>+</sup>, activated naïve CD4<sup>+</sup>, T<sub>H1</sub> and reactivated T<sub>H1</sub> cells from OT-II/Nur77<sup>GFP</sup> mice were sorted via fluorescence activated cell sorting (FACS) for bulk transcriptome analysis. To obtain good quality of RNA, each population was identified only by the expression of Nur77<sup>GFP</sup> and cell membrane markers as intracellular staining interferes both quantity and quality of the sorted samples. Based on previous studies, the expression of CD62L and CD44 were used to identify naïve and effector CD4<sup>+</sup> T cells (Gerberick, Cruse, Miller, Sikorski, & Ridder, 1997). Activated and reactivated CD4<sup>+</sup> T cells were identified by the expression of Nur77<sup>GFP</sup>. Figure 11 shows the gating strategy for the sorting of each population: naïve T cells were identified as CD62L<sup>+</sup>, CD44<sup>-</sup> and Nur77<sup>GFP-</sup> while activated naïve T cells were CD62L<sup>int</sup>, CD44<sup>-</sup>, CD69<sup>+</sup> and Nur77<sup>GFP+</sup>. T<sub>H1</sub> cells showed a T<sub>CM</sub> cell phenotype and were identified as CD62L<sup>+</sup>, CD44<sup>+</sup> and Nur77<sup>GFP-</sup> while reactivated T<sub>H1</sub> cells were CD62L<sup>int</sup>, CD44<sup>+</sup> and Nur77<sup>GFP+</sup>.

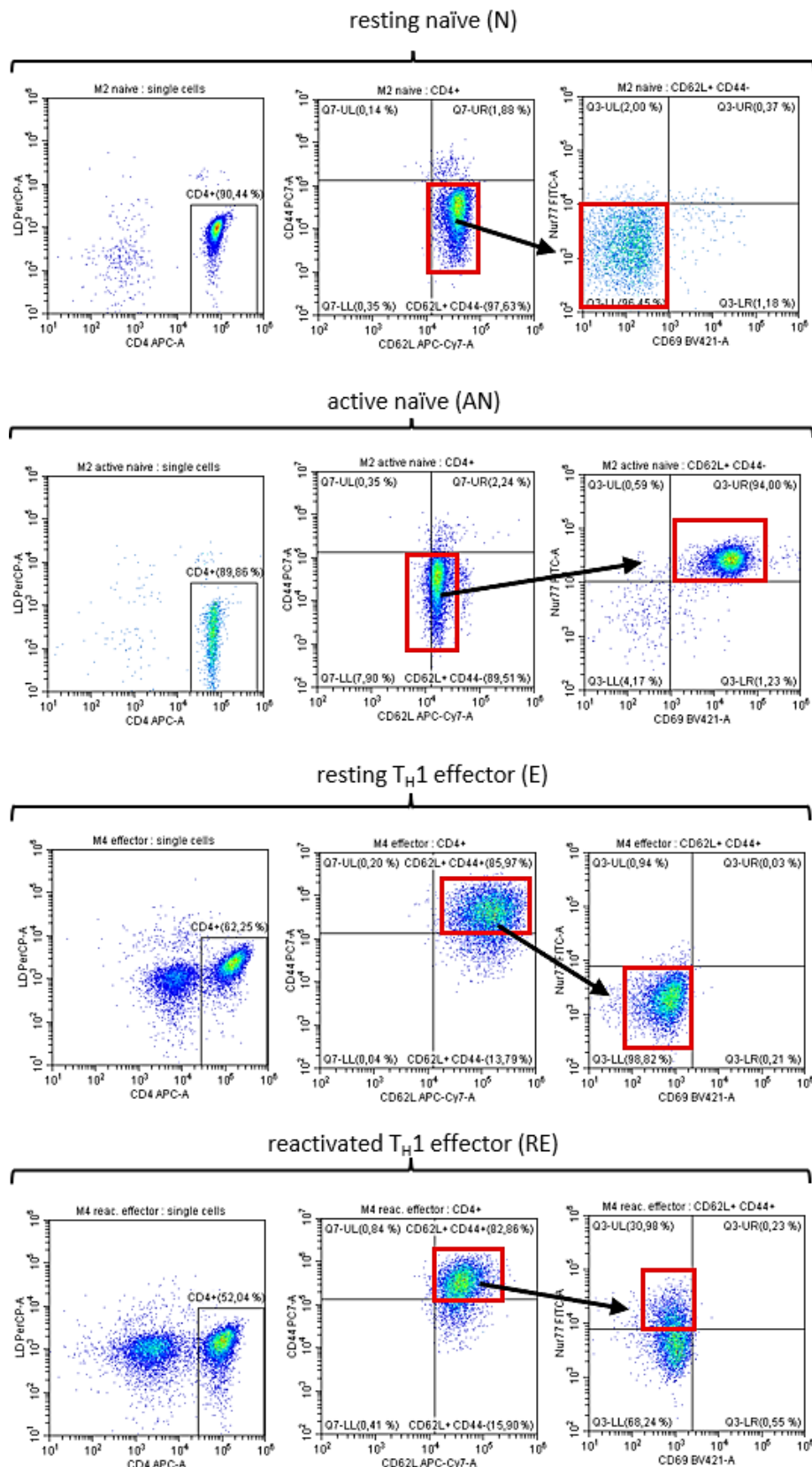


**Figure 11: Gating strategy**

Sorting of naïve (N; CD62L<sup>+</sup>, CD44<sup>-</sup>, CD69<sup>-</sup>, Nur77<sup>GFP+</sup>), activated naïve (AN; CD62L<sup>int</sup>, CD44<sup>-</sup>, CD69<sup>+</sup> Nur77<sup>GFP+</sup>), T<sub>H</sub>1 (E; CD62L<sup>+</sup>, CD44<sup>+</sup>, Nur77<sup>GFP-</sup>) and reactivated T<sub>H</sub>1 cells (RE; CD62L<sup>+</sup>, CD44<sup>+</sup>, Nur77<sup>GFP+</sup>) cells

For confirmation purposes, CD4<sup>+</sup> T cells were stained for the expression of the master transcription factor T-Bet. Naïve T cells did not express T-Bet after six hours of T cell stimulation and therefore were still naïve T cells (Figure 12, A). Furthermore, these activated naïve T cells were also negative for other master transcription factors like Gata3, ROR $\gamma$  or FoxP3, which identify other CD4<sup>+</sup> T cell subsets (Figure 16). In contrast, almost all CD4<sup>+</sup> effector T cells expressed T-bet (over 97%) confirming a T<sub>H</sub>1 cell-like phenotype and importantly all Nur77<sup>GFP+</sup> T<sub>H</sub>1 cells expressed IFN $\gamma$  showing that these cells were functionally reactivated (Figure 12, B).

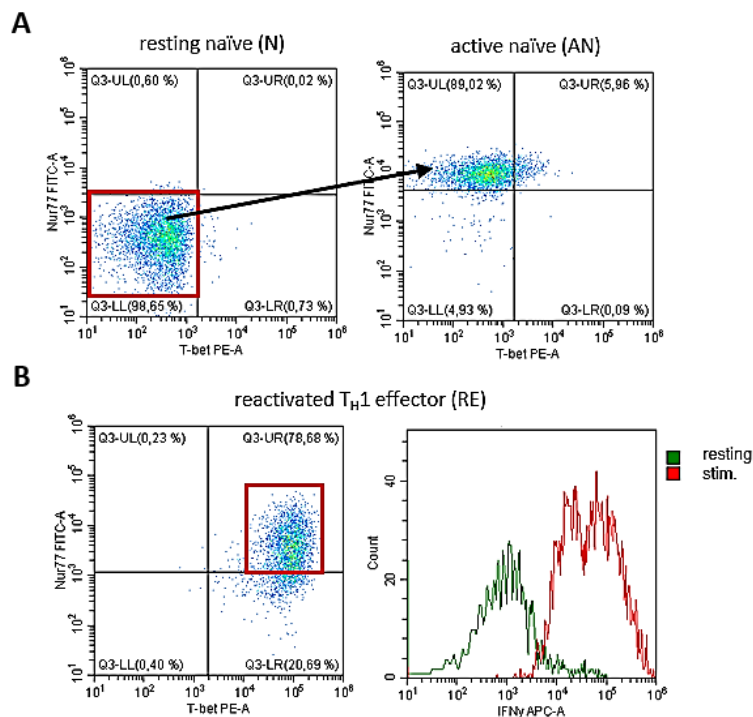


**Figure 12: Expression of T-Bet and IFN $\gamma$  during naïve T cell activation and T<sub>H</sub>1 reactivation**

*A: Naïve and activated naïve T cells do not express T-Bet confirmed by flow cytometry. B: Almost all T<sub>H</sub>1 cells express T-Bet and nearly all of reactivated Nur77<sup>GFP+</sup> T<sub>H</sub>1 cells are IFN $\gamma$ <sup>+</sup> confirmed by flow cytometry*

### **4.3 Transcriptome analysis revealed unique transcriptome for reactivated T<sub>H</sub>1 cells**

Following cell sorting of naïve CD4<sup>+</sup>, activated naïve CD4<sup>+</sup>, T<sub>H</sub>1 and reactivated T<sub>H</sub>1 cells, I proceeded with transcriptome analysis of these cells. RNA was isolated from sorted cells and sequenced in cooperation with the Cologne Center for Genomics (CCG) NGS platform (Cologne). I applied principal component analysis (PCA), which

is a statistical method used to reduce the dimensions of a data set allowing the projection of large data set information onto a 2D plane. Similarities between data sets were correlated to the distances in the 2D plane. PCA of this transcriptome analysis showed clustering of each sample with a high degree of similarity in designated T cell populations (Figure 13, A). Furthermore, the individual groups were separated far away from each other depicting significant transcriptional differences between the four groups. The heat map shows the most differentially expressed genes between the four groups (Figure 13, B). Most interesting were *Ccl3*, *Ccl1*, *Il3*, *Pdzk1ip1*, *Siglec5* and *Ccl9*, which were just differentially expressed in reactivated  $T_H1$  cells but not in any of the other three groups.

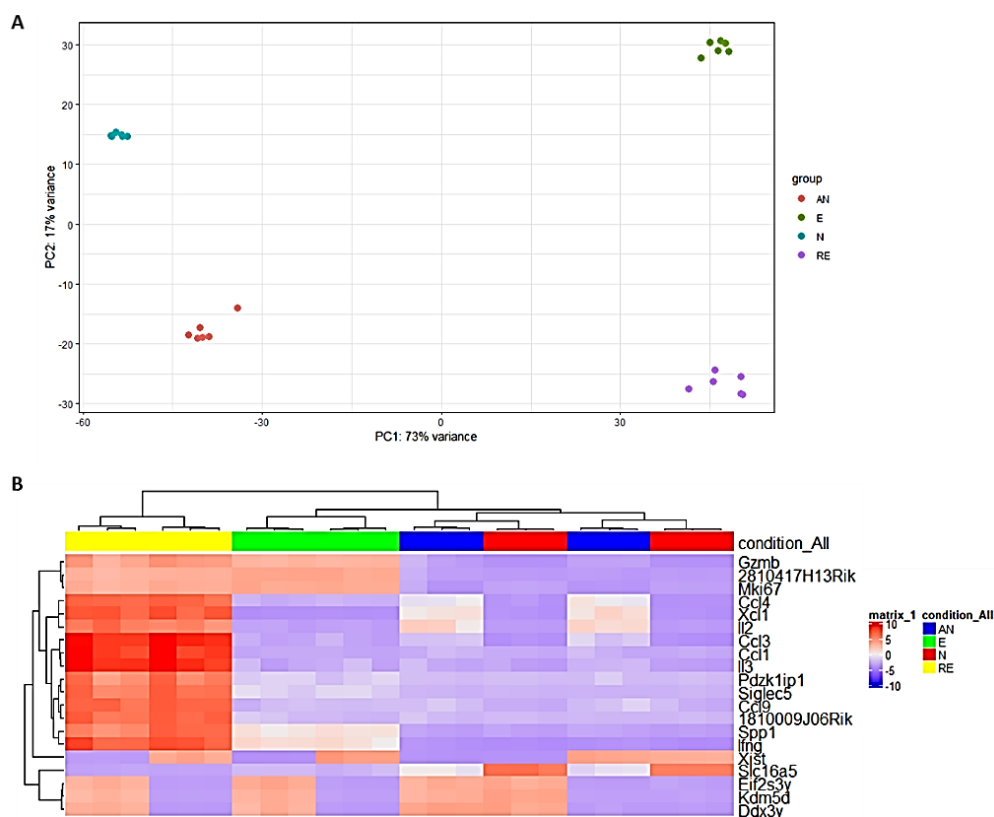


**Figure 13: Transcriptome analysis**

A: Principal component analysis (PCA) of all four groups; B: heat map of the most differentially expressed genes; (N= naïve, AN= activated naïve, E=  $T_H1$  cells, RE= reactivated  $T_H1$  cells)

Furthermore, I analyzed the expression of commonly used activation markers expressed in reactivated  $T_H1$  cells by comparing resting and reactivated  $T_H1$  cells. CD69 (Log<sub>2</sub>Foldchange of 0.44), Ox40 (Log<sub>2</sub>Foldchange of 1.08) or Ki67 (Log<sub>2</sub>Foldchange of -0.25) showed minor regulation in reactivated  $T_H1$  cells. While Nr4a1 (Nur77) was slightly upregulated (Log<sub>2</sub>Foldchange of 1.35), the other members

of the family like Nr4a2 and especially Nr4a3 showed higher upregulation (Log<sub>2</sub>Foldchange of 1.91 and 5.1). Moreover, the expression of the T<sub>H</sub>1 lead cytokine IFN $\gamma$  showed a Log<sub>2</sub>Foldchange of 5.97 confirming functional reactivation. Furthermore, Nfatc2 expression was upregulated (Log<sub>2</sub>Foldchange of 2.01), while Jun and Fos were downregulated (Log<sub>2</sub>Foldchange of -1.52 and -1.03). In addition, PD-1 was upregulated (Log<sub>2</sub>Foldchange of 3.81) indicating T cell anergy (Table 1).

gene	Log2foldchange	counts RE
CD25	-1,3	42786
CD44	1,51	10656
CD62L	-2,86	2648
CD69	0,44	3471
Ctla4	-2,75	2364
Fos	-1,03	227
Fosl1	3,95	592
Fosl2	-1,86	1682
Gzmb	1,35	58993
Icos	-1,54	4009
IFN $\gamma$	5,97	330644
Jun	-1,52	1298
Ki67	-0,25	11484
Lfa1	0,11	27706
Nfatc1	1,55	8179
Nfatc2	2,01	1623
Nfkb1	0,97	24592
Nfkb2	1,7	17033
Nr4a1	1,35	20155
Nr4a2	1,91	5080
Nr4a3	5,1	5090
Ox40	1,08	13814
PD1	3,81	3463
PD-L1	1,56	5247
PD-L2	1,54	1287

**Table 1: Commonly used activation marker**

Log<sub>2</sub>Foldchange expression from pairwise comparison of resting and reactivated T<sub>H</sub>1 cells and counts for each gene after DESeq2 analysis

Pairwise comparison between each group identified 10840 significantly differentially expressed genes of naïve T cell activation (N vs AN; naïve vs active naïve), 11583 genes of T<sub>H</sub>1 differentiation (N vs E; naïve vs effector), 10736 genes of T<sub>H</sub>1 reactivation (E vs RE; effector vs reactivated effector) and 11899 genes of overall T cell differentiation and activation (N vs RE; naïve vs reactivated effector) (Figure 14 and Figure 15). These results indicated comparably complex transcriptional alterations in each comparison.

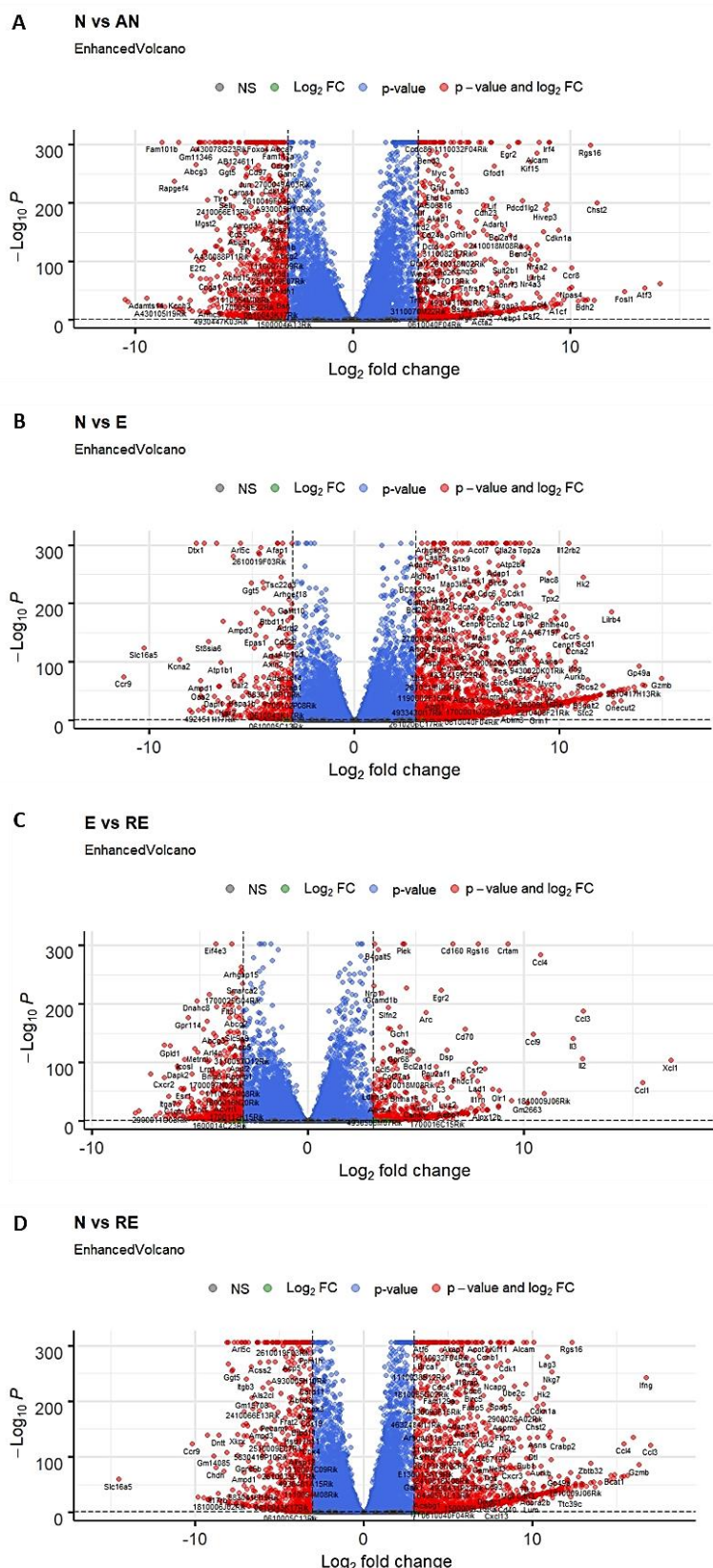


**Figure 14: Volcano blots of pairwise comparisons between the four groups**

A: Analysis of generic TCR activation signature (N vs AN= naïve vs activated naïve T cells), B: T cell differentiation signature (N vs E= naïve vs  $T_H1$  cells), C: T cell reactivation signature (E vs RE=  $T_H1$  vs reactivated  $T_H1$  cells), and overall T cell signature (N vs RE= naïve vs reactivated  $T_H1$  cells)

Next, I compared differentially expressed genes from each comparison with each other (naïve vs activated naïve, naïve vs effector, effector vs reactivated effector) as depicted in following Venn diagrams (Figure 15). The analysis showed that 3106 (1193 up-regulated and 1913 down-regulated) genes were specifically regulated in reactivated T<sub>H</sub>1 cells and not in the other groups. Interestingly, almost one in three genes transcribed in reactivated T<sub>H</sub>1 cells was unique to this process. Furthermore, this set of genes was merely three times as big as the set of genes unique to naïve T cell activation (1109 genes). Among these differentially expressed genes in reactivated T<sub>H</sub>1 cells, 447 genes were solely regulated in reactivated T<sub>H</sub>1 cells and did not appear in the other comparisons at all. The number of genes uniquely expressed was similar to the number of genes unique to activation of naïve cells (488 genes). Interestingly, the group of genes attributable to T<sub>H</sub>1 differentiation over naïve T cells (922 genes) was merely twice as big as the genes unique to reactivation. In summary, the results showed that T<sub>H</sub>1 cell reactivation was transcriptionally significantly distinct from naïve T cell activation and differentiation.

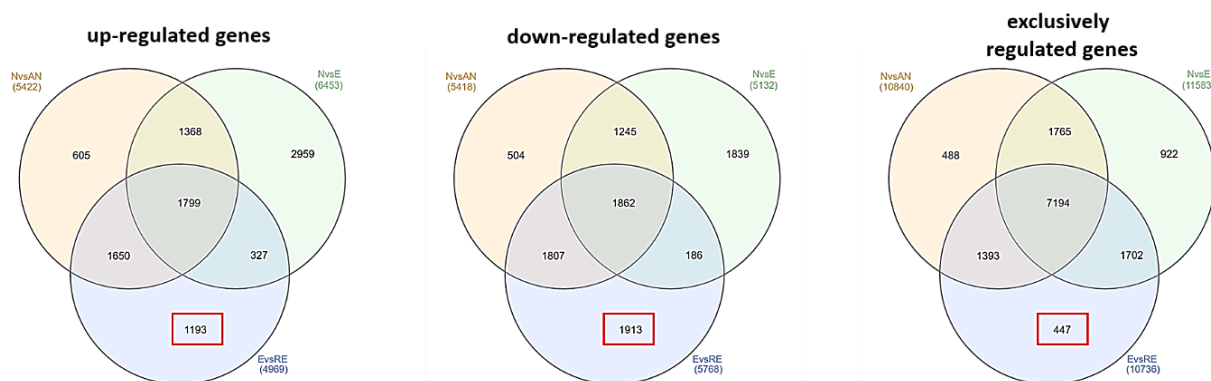


**Figure 15: Venn diagrams of upregulated, downregulated and exclusively regulated genes identified via transcriptome analysis of reactivated T<sub>H</sub>1 cells**

*NvsAN=naïve vs activated naïve T cells, NvsE=naïve vs T<sub>H</sub>1 cells, EvsRE=T<sub>H</sub>1 vs reactivated T<sub>H</sub>1 cells*

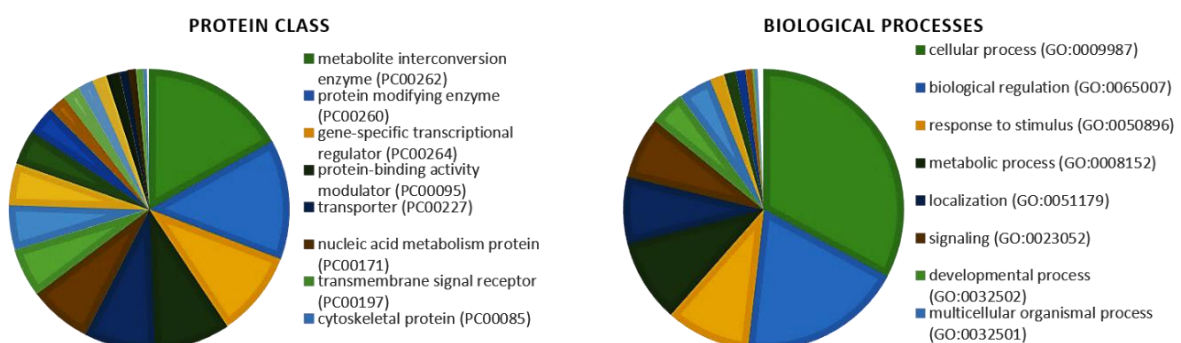


**Figure 16: Gene ontology analysis via PANTHER of differentially expressed genes identified via transcriptome analysis specific for reactivated T<sub>H</sub>1 cells**

Subsequently, gene Ontology Analysis via PANTHER was performed to understand if particular pathways or processes during  $T_H1$  reactivation were influenced. The analysis showed that most genes specific for  $T_H1$  reactivation were involved in cellular and metabolic processes (Figure 16). That was expected, because it is already known that T cell activation and differentiation lead to metabolic changes (Buck, O'Sullivan, & Pearce, 2015).

For a more robust transcriptome analysis, Kallisto/Sleuth pipeline was performed in addition to HTSeq/DESeq2 pipeline, which revealed 4581 genes uniquely regulated in reactivated  $T_H1$  cells of which 1796 were present in both pipelines.

#### ***4.4 Characterization of CD4<sup>+</sup> T cell subpopulations $T_H1$ , $T_H2$ , $T_H17$ and $T_{reg}$ cells via master transcription factor and lead cytokine expression upon antigen-specific reactivation***

For verification of transcriptome data, I performed further analysis in  $T_H1$  cells and in other CD4<sup>+</sup> T cell subpopulations. Different  $T_H$  subpopulations were analyzed for the expression of selected genes found in the high throughput analysis to analyze whether the reactivation-specific genes were  $T_H1$  specific or if they could also be found in other CD4<sup>+</sup> T cell subpopulations. For this thesis, I chose the most commonly known subpopulations:  $T_H2$ ,  $T_H17$  and  $T_{reg}$  cells. Commonly used master transcription factors were used to identify each subpopulation: T-Bet for  $T_H1$  cells, Gata3 for  $T_H2$  cells, ROR $\gamma$ t for  $T_H17$  cell and FoxP3 for  $T_{reg}$  cells (Vahedi et al., 2013). qRT-PCR analysis showed that  $T_H1$  cells expressed the master transcription factor T-Bet, which was also slightly upregulated in  $T_{reg}$  cells (Figure 17, A).  $T_H2$  cells highly expressed the master transcription factor Gata3. Interestingly,  $T_{reg}$  cells also slightly expressed Gata3 (Figure 17, B). Furthermore, ROR $\gamma$ t was solely expressed by  $T_H17$  cells and FoxP3 was solely expressed by  $T_{reg}$  cells (Figure 17, C and D). Flow cytometric analysis demonstrated that over 40% of differentiated  $T_{reg}$  cells expressed FoxP3 (Figure 17, E).

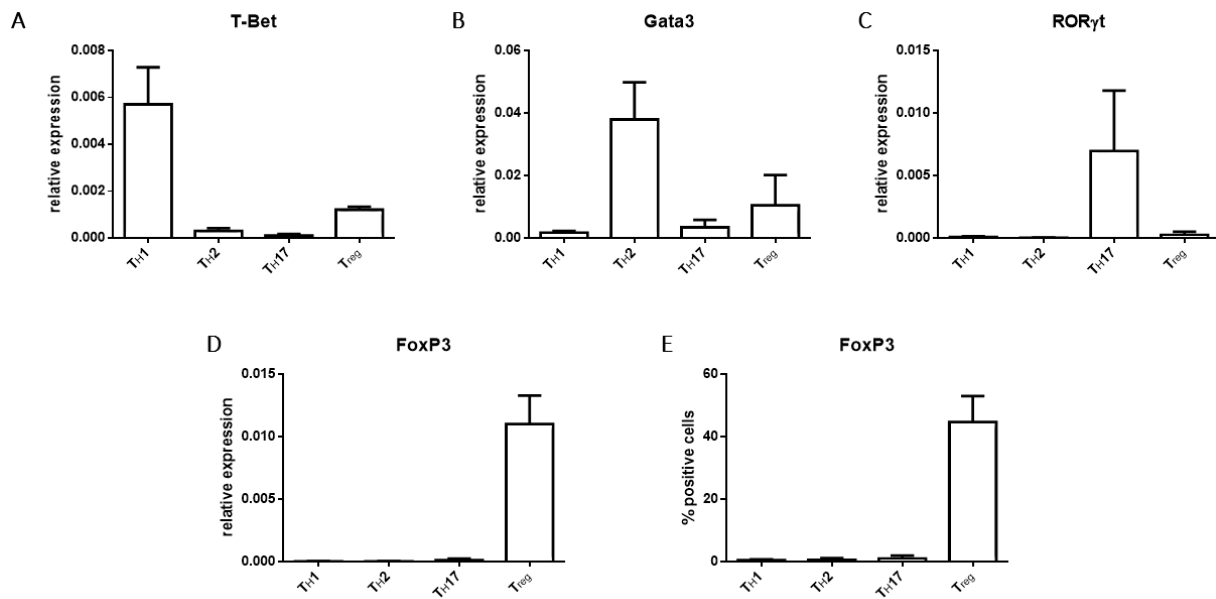


**Figure 17: Transcription factor/master regulator expression of CD4<sup>+</sup> T cell subpopulations**

*T-Bet* (A), *Gata3* (B), *RORγt* (C) and *FoxP3* (D) expression via qRT-PCR and *FoxP3* expression via flow cytometry (E) of *in vitro* differentiated TH1, TH2, TH17 and Treg cells 5 days after differentiation; mean with SD (n=5)

Following the analysis of master transcription factors, I analyzed the secretion of each lead cytokine upon reactivation to investigate the reactivation potential of each CD4<sup>+</sup> T cell subpopulation. Each CD4<sup>+</sup> T cell subpopulation was reactivated with Ova<sub>323-339</sub> peptide-pulsed macrophages for six hours. On average ~40% of TH1, 10% of TH2, 48% of TH17 and 65% of Treg cells were Nur77<sup>GFP+</sup> after reactivation (data not shown). Upon reactivation, TH1 cells upregulated the expression of IFNγ (~35%), TH2 cells expressed IL-4 (~30%) and TH17 cells expressed IL-17a (~10%) verified via flow cytometry (Figure 18, A-C). Around 20% of differentiated Treg cells secreted IFNγ upon stimulation, but not IL-4 or IL-17a, indicating a mixed population of Treg and TH1 cells (Figure 18, A-C). Furthermore, resting and reactivated effector T cells from each subpopulation were sorted according to their Nur77<sup>GFP</sup> expression to verify these results. qRT-PCR analysis was in line with flow cytometric data showing the expression of the corresponding lead cytokines in each sorted CD4<sup>+</sup> T cell population (Figure 18, D-H). TH1 cells only upregulated IFNγ, TH2 cells just upregulated IL-4 and TH17 cells only upregulated IL-17a. Treg cells also slightly upregulated IFNγ. Moreover, all subpopulations upregulated TGFβ upon reactivation while IL-10 was mainly upregulated by TH2 cells (Figure 18, G-H).

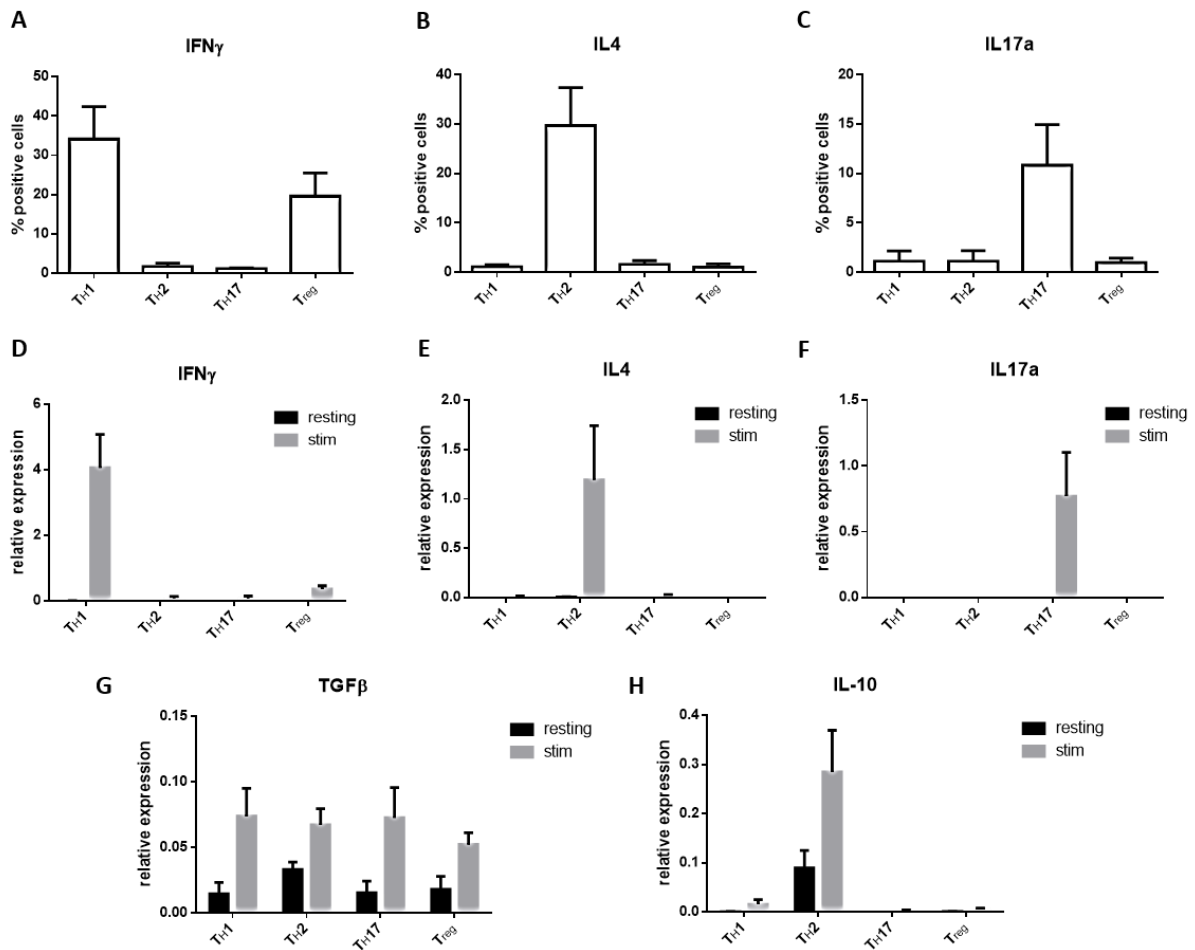


**Figure 18: Lead cytokine expression in CD4<sup>+</sup> T cell subpopulations**

$T_H1$ ,  $T_H2$ ,  $T_H17$  and  $T_{reg}$  cells were stimulated via Ova<sub>323-339</sub> pulsed-macrophages for six hours. Lead cytokine expression was analyzed via flow cytometry for IFN $\gamma$  (A), IL4 (B) and IL17a (C). Further cytokine expression of Nur77<sup>GFP+</sup> sorted reactivated effector T cells was analyzed via qRT-PCR for IFN $\gamma$  (D), IL4 (E), IL17a (F), TGF $\beta$  (G) and IL-10 (H);. mean with SD (n=5)

#### **4.5 In-depth analysis of transcriptome data revealed significant upregulation of Clec4e, Clec7a, Siglec5, Pdzk1ip1, Edn1 and Lyz2 and significant downregulation of Ccr4, Soc2, Enah, Dach2 and Coro6 in antigen—stimulated TH1 cells and identified similar expression patterns in other CD4<sup>+</sup> T cell subpopulations**

For further analysis, 12 uniquely regulated genes that were differentially expressed in both HTSeq/DESeq2 and Kallisto/Sleuth pipelines, and had a Log2Fold-change > 2 and at least a count > 10 in HTSeq/DESeq2 analysis were chosen. Clec4e (also called Mincle) and Clec7a (also called Dectin1) are C-type lectin receptors, which are mainly characterized as co-stimulatory receptors on myeloid cells (Daley et al., 2017;

Drummond et al., 2016; Kalia, Singh, & Kaur, 2021; Ni et al., 2010; Patin, Orr, & Schaible, 2017). Siglec5 is a glycan binding protein expressed on many immune cells, mainly characterized on eosinophils (Feng & Mao, 2012; Gonzalez-Gil & Schnaar, 2021; M. Zhang et al., 2007). Pdzk1ip1 (also called Map17) plays a role in ROS signaling and is overexpressed in some cancer types (F. Dong et al., 2021; Rivero et al., 2018). Edn1 (endothelin 1) is a peptide hormone and vasoconstrictor mainly found in endothelial cells (Sutton, Pugh, & Dhaun, 2019). Lysozymes, like Lyz2, play a role in bacterial immune defense (Ragland & Criss, 2017). Ccr4 is a CC chemokine receptor predominantly expressed on T<sub>H</sub>2 cells, but also on T<sub>H</sub>17 and T<sub>reg</sub> cells (Baatar et al., 2007; Bonecchi et al., 1998; Iellem et al., 2001; Lim, Lee, Hillsamer, & Kim, 2008; Yamamoto et al., 2000). Furthermore, it is a skin-homing molecule expressed mainly on T<sub>CM</sub> cells (Casciano et al., 2020), but it has not been described as a reactivation marker. Socs2 (suppressor of cytokine signals 2) is a transcription factor described as a negative regulator of T<sub>H</sub>2 cell, NK cell differentiation and DC activation (W. S. Kim et al., 2017; Knosp et al., 2011; Posselt, Schwarz, Duschl, & Horejs-Hoeck, 2011). Enah (enabled homolog), which is a member of the enabled (Ena)/vasodilator-stimulated phosphoprotein (VASP) family, plays a role in actin-based motility and adhesion and correlates with tumor progression (D. Chen et al., 2018; D. D. Wang et al., 2017). Dach2 (dachshund 2) is a transcription factor predominantly expressed in innervated muscle and can be used as a prognostic marker for bladder and ovarian cancer (He et al., 2015; Macpherson, Farshi, & Goldman, 2015; Nodin, Fridberg, Uhlén, & Jirström, 2012; Tang & Goldman, 2006). Coro6 (Coronin 6) plays a role in actin dynamics and can be used as a prognostic marker for some cancer types (Qiao et al., 2020; X. Wang, Xiao, Li, Yan, & Luo, 2021; Y. Wu et al., 2021). Most analyzed genes were not characterized in T cells, especially not specifically in reactivated effector T cells.

Above-mentioned genes were analyzed via qRT-PCR in Nur77<sup>GFP</sup> sorted resting and reactivated T<sub>H</sub>1 cells as well as in T<sub>H</sub>2, T<sub>H</sub>17 and T<sub>reg</sub> cells. qRT-PCR analysis of these chosen genes confirmed transcriptome analysis data. Clec4e, Clec7a, Siglec5, Pdzk1ip1, Edn1 and Lyz2 were significantly upregulated in T<sub>H</sub>1 cells as well as in T<sub>H</sub>2 cells (Figure 19). Except Clec7a, all genes were also upregulated in T<sub>H</sub>17 cells. T<sub>H</sub>1 and T<sub>H</sub>17 cells showed similar expression strength in the selected genes, especially in the expression of Clec4e, Pdzk1ip1 and Lyz2, while T<sub>H</sub>2 cells showed the highest expression of Edn1. Furthermore, all selected upregulated genes

were significantly upregulated in  $T_{reg}$  cells, but overall  $T_{reg}$  cells showed lower expression of all genes compared to the other subpopulations.

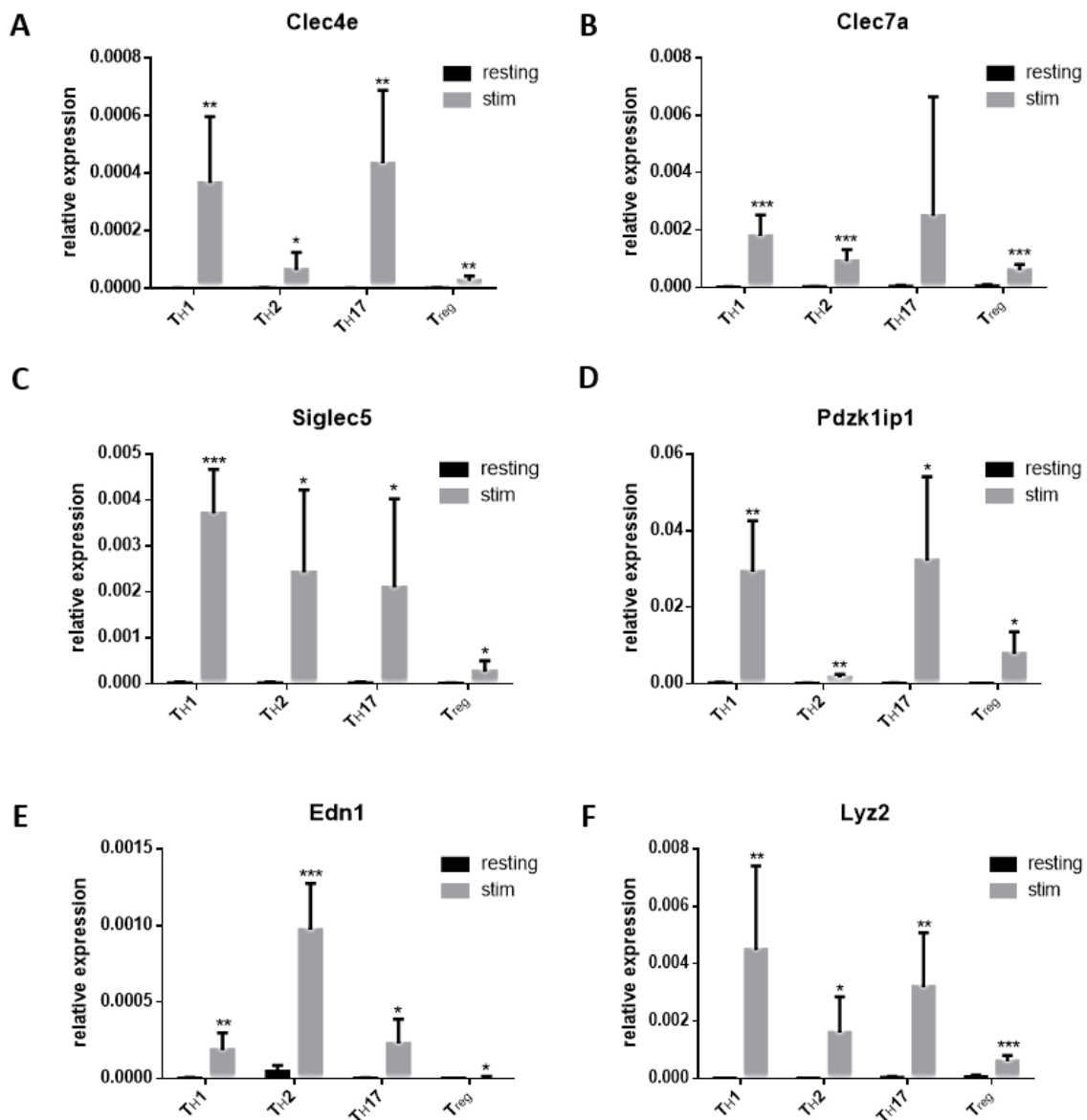


**Figure 19: Upregulated genes identified via reactivated  $T_{H1}$  transcriptome analysis in  $CD4^+$  T cell subpopulations stimulated with antigen-pulsed macrophages**

Gene expression analysis of sorted effector T cells of *Clec4e* (A), *Clec7a* (B), *Siglec5* (C), *Pdzk1ip1* (D), *Edn1* (E) and *Lyz2* (F) via qRT-PCR; mean with SD ( $n=5$ )

All selected downregulated genes from the transcriptome analysis, i.e. *Ccr4*, *Socs2*, *Enah*, *Dach2* and *Coro6*, were significantly downregulated in  $T_{H1}$  cells, except *Gipr* (Figure 20). However, results showed a tendency towards *Gipr* downregulation upon reactivation. Furthermore, most of those genes were significantly downregulated in  $T_{H2}$  cells, except *Gipr* and *Enah*, but results showed a tendency towards downregulation of both genes (Figure 20). In comparison to the other  $CD4^+$  T cell

subpopulations, *Gipr* and *Ccr4* were highly expressed under the resting condition in  $T_H2$  cells. Furthermore, only *Socs2* and *Coro6* were significantly downregulated in  $T_H17$  cells, but *Ccr4* and *Dach2* showed a tendency towards downregulation. Finally, most of these genes were differentially expressed in  $T_{reg}$  cells, except *Gipr* and *Ccr4*.  $T_{reg}$  cells showed overall low gene expression in most downregulated genes.  $T_H17$  and

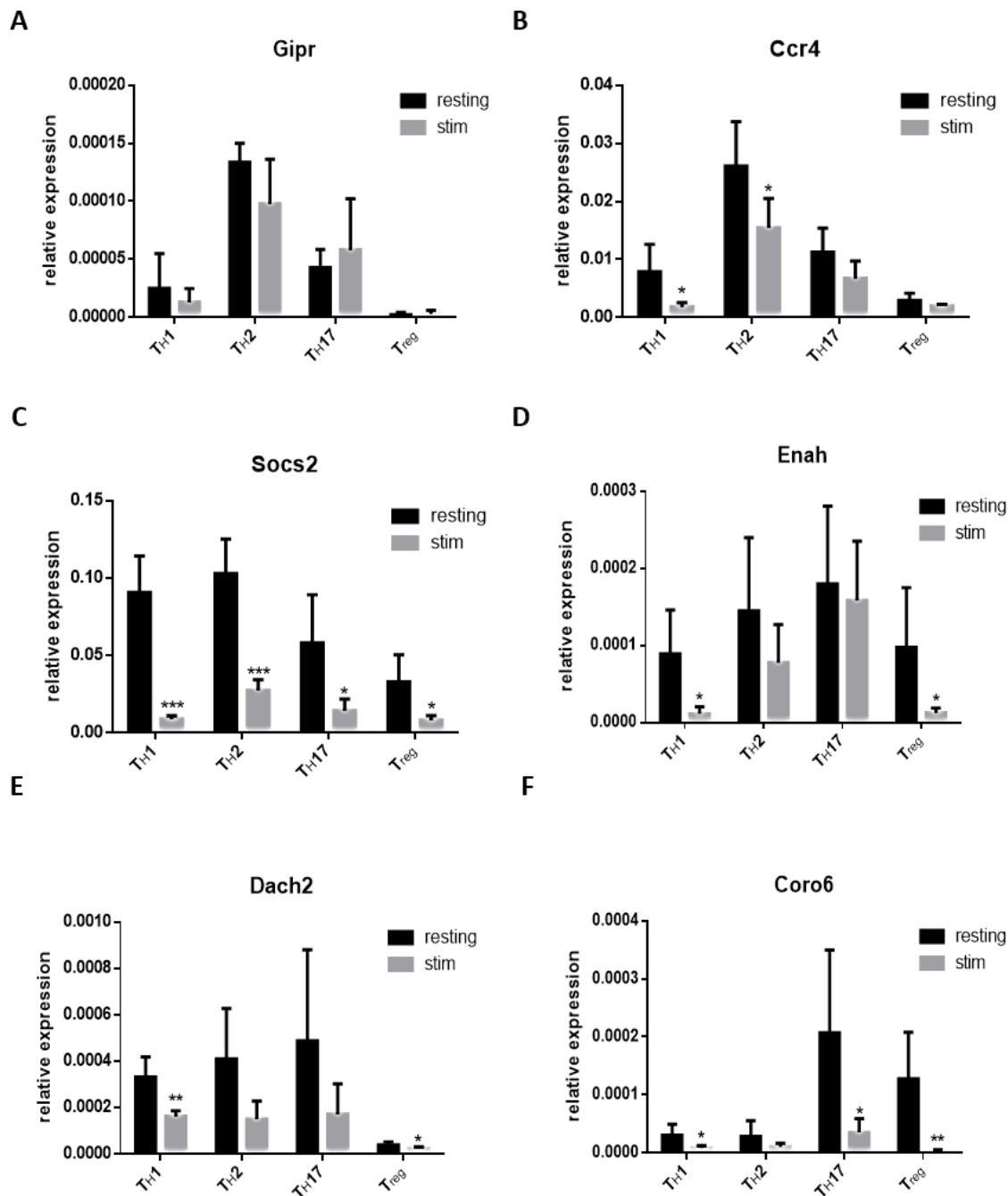


**Figure 20: Downregulated genes identified via reactivated  $T_H1$  transcriptome analysis in  $CD4^+$   $T$  cell subpopulations stimulated with antigen-pulsed macrophages**

Gene expression analysis of sorted effector  $T$  cells of *Gipr* (A), *Ccr4* (B), *Socs2* (C), *Enah* (D), *Dach2* (E) and *Coro6* (F) via qRT-PCR; mean with SD ( $n=5$ )

T<sub>reg</sub> cells showed higher Coro6 gene expression, which was downregulated upon reactivation, while T<sub>H1</sub> and T<sub>H2</sub> cells already had extremely low Coro6 expression in resting T cells. Altogether, the expression of the selected genes was more similar between T<sub>H1</sub> and T<sub>H17</sub> cells, whereas there was quite a difference in the expression of some genes in T<sub>H2</sub> and T<sub>reg</sub> cells.

#### ***4.6 Lead cytokine expression and in-depth analysis of transcriptome data in CD4<sup>+</sup> T cell subpopulations reactivated with PMA/Ionomycin showed similarities to antigen-stimulated CD4<sup>+</sup> T cells***

In addition to antigen-stimulation by macrophages, all four CD4<sup>+</sup> T cell subpopulations were also stimulated with PMA/Ionomycin, which is a commonly used method to reactivate T cells in many publications. The aim was to investigate if the chosen reactivation method had an impact on CD4<sup>+</sup> T cell reactivation-specific gene expression. The results showed that upon PMA/Ionomycin stimulation, on average ~30% of T<sub>H1</sub>, 35% of T<sub>H2</sub>, 80% of T<sub>H17</sub> and 80% of T<sub>reg</sub> cells were Nur77<sup>GFP+</sup> (data not shown). Compared to antigen-stimulated T cells, less T<sub>H1</sub> cells, but more T<sub>H2</sub>, T<sub>H17</sub> and T<sub>reg</sub> cells expressed Nur77<sup>GFP</sup> and therefore got activated with PMA/Ionomycin. Furthermore, PMA/Ionomycin stimulated T cells showed less lead cytokine expression on protein level in T<sub>H1</sub> and T<sub>H2</sub> cells (Figure 21, A-C). On mRNA level, T<sub>H1</sub> and T<sub>H17</sub> cells showed higher lead cytokine expression while T<sub>H2</sub> cells showed decreased lead cytokine expression compared to antigen-stimulated T<sub>H2</sub> cells (Figure 21, D-F). However, similar to antigen-stimulated T cells, IFN $\gamma$  was mainly expressed by T<sub>H1</sub> and to a lesser extent by T<sub>reg</sub> cells, IL-4 was specifically expressed by T<sub>H2</sub> cells and IL-17a was specifically expressed by T<sub>H17</sub> cells, both on protein and mRNA level. All subpopulations upregulated TGF $\beta$  upon reactivation similar to antigen-stimulated cells (Figure 21, G). The most significant difference compared to antigen-stimulated cells was the expression of IL-10. During antigen-stimulation only T<sub>H2</sub> cells expressed IL-

10, however, upon PMA/Ionomycin stimulation,  $T_H1$ ,  $T_H2$  and  $T_{reg}$  cells expressed IL-10 (Figure 21, H).

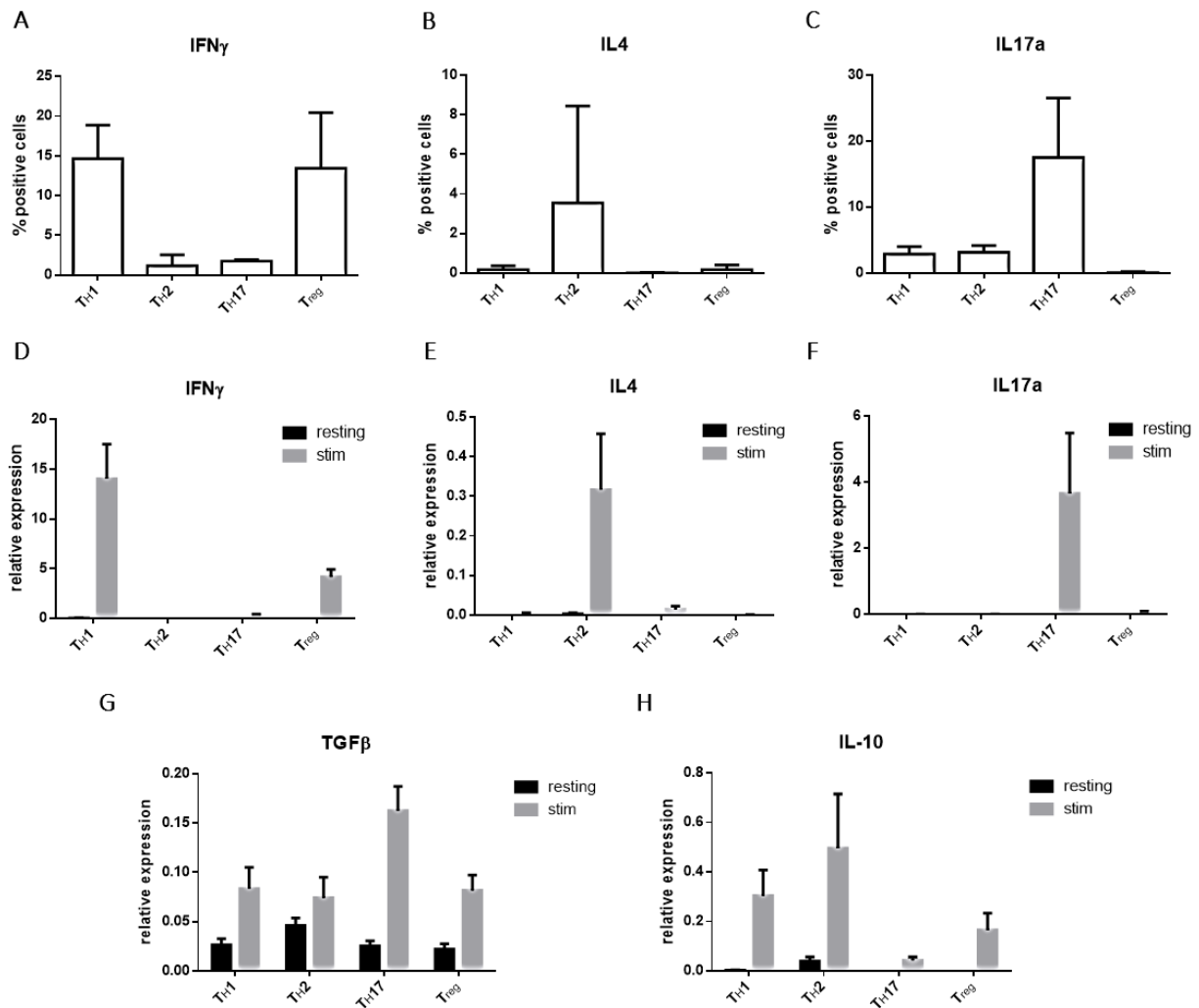


**Figure 21: Lead cytokine expression in  $CD4^+$  T cell subpopulations stimulated with PMA/Ionomycin**

$T_H1$ ,  $T_H2$ ,  $T_H17$  and  $T_{reg}$  cells were stimulated with PMA/Ionomycin for four hours. Lead cytokine expression was analyzed via flow cytometry for IFN $\gamma$  (A), IL4 (B) and IL17a (C). Further cytokine expression was analyzed via qRT-PCR for IFN $\gamma$  (D), IL4 (E), IL17a (F), TGF $\beta$  (G) and IL-10 (H);. mean with SD (n=5)

Next, the expression of selected genes from transcriptome analysis was also analyzed in PMA/Ionomycin stimulated T cells. Clec4e, Clec7a, Siglec5, Pdzk1p1, Edn1 and Lyz2 were all significantly upregulated in reactivated  $T_H1$  cells (Figure 22).  $T_H2$  cells significantly upregulated most of the genes except Clec4e, which was significantly upregulated in antigen-stimulated  $T_H2$  cells. However, results indicated a tendency towards upregulation. Moreover,  $T_H17$  and  $T_{reg}$  cells significantly upregulated

all genes except *Lyz2*, which was also significantly upregulated in antigen-stimulated T cells.

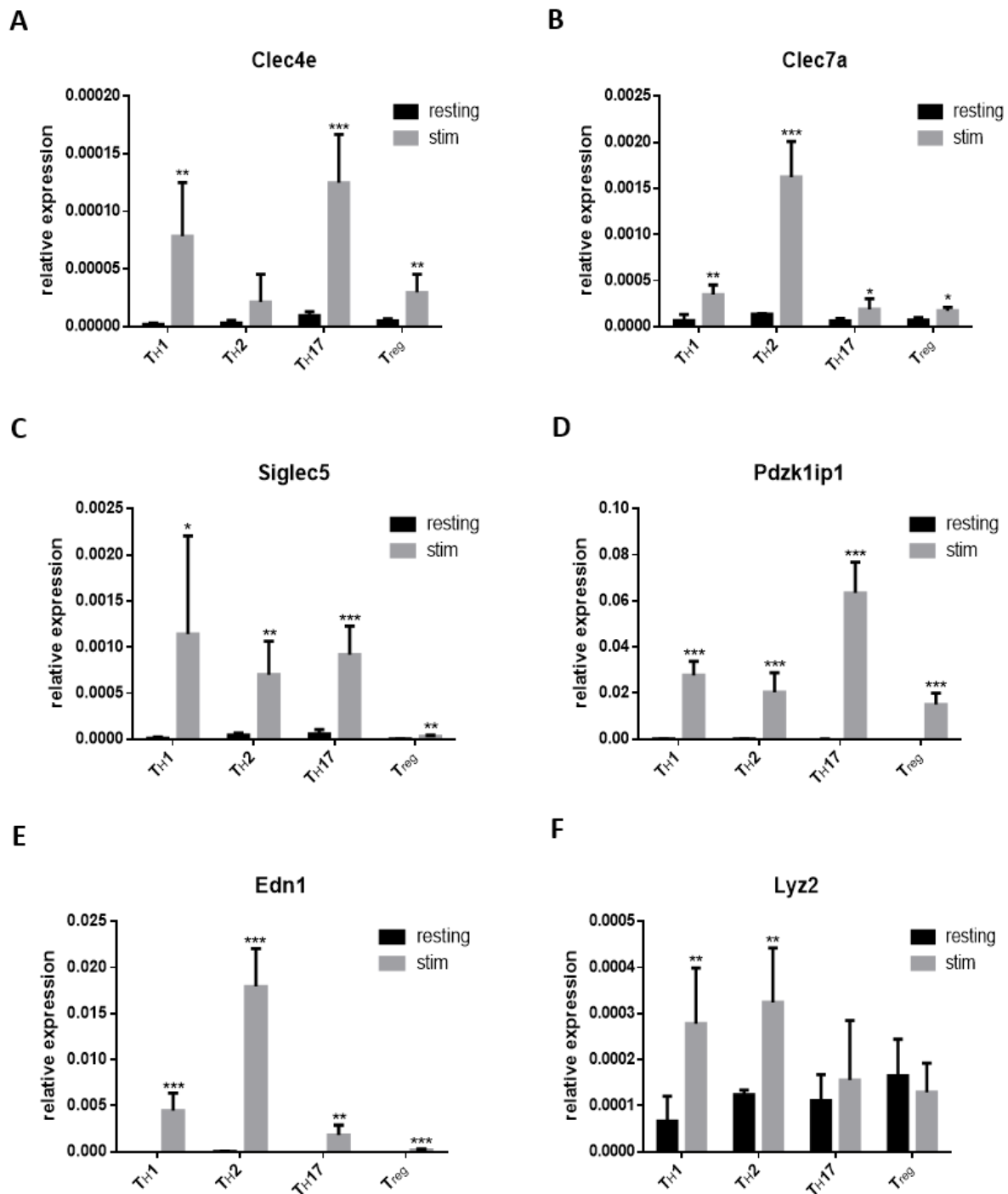


**Figure 22: Upregulated genes identified via reactivated  $T_H1$  transcriptome analysis in  $CD4^+$  T cell subpopulations stimulated with PMA/Ionomycin**

Gene expression analysis of effector T cells stimulated with PMA/Ionomycin: *Clec4e* (A), *Clec7a* (B), *Siglec5* (C), *Pdzk1ip1* (D), *Edn1* (E) and *Lyz2* (F) via qRT-PCR; mean with SD (n=5)

PMA/Ionomycin stimulated  $T_H1$  as well as  $T_H17$  cells significantly downregulated *Ccr4*, *Socs2* and *Coro6*, but not *Gipr*, *Enah* and *Dach2* (Figure 23).  $T_H2$  cells were the only T cell subpopulation, which significantly upregulated *Gipr*. *Enah*, *Ccr4* and *Socs2* were significantly downregulated, while *Dach2* and *Coro6* were not regulated in  $T_H2$  cells. In comparison to antigen-stimulated  $T_{reg}$  cells, PMA/Ionomycin stimulated  $T_{reg}$  cells did

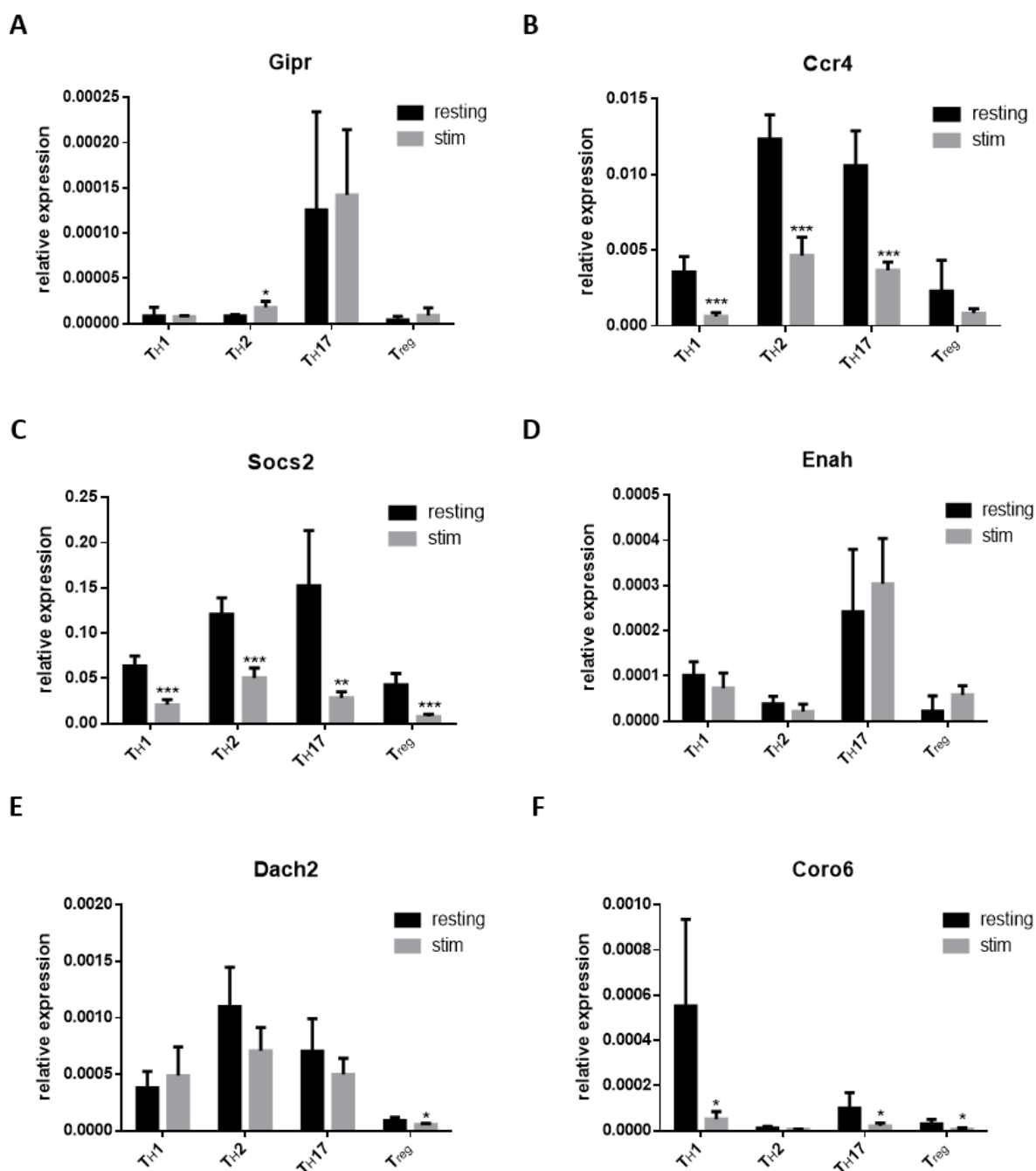


**Figure 23: Downregulated genes identified via reactivated  $T_H1$  transcriptome analysis in  $CD4^+$  T cell subpopulations stimulated with PMA/Ionomycin**

Gene expression analysis of effector T cells stimulated with PMA/Ionomycin: *Gipr* (A), *Ccr4* (B), *Socs2* (C), *Enah* (D), *Dach2* (E) and *Coro6* (F) via qRT-PCR; mean with SD (n=5)

not significantly downregulate *Enah*. However, *Socs2*, *Dach2* and *Coro6*, were significantly downregulated although the expression during resting state was already quite low. Altogether, the results showed that the expression of *Nur77<sup>GFP</sup>* and the lead cytokines of the four subpopulations differed between antigen- and PMA/Ionomycin stimulation. However, there were slight differences in the expression of the selected genes stimulated with both methods. Furthermore, upon resting condition, the expression of some genes differed between antigen- and PMA/Ionomycin stimulation experiments indicating that there are minor fluctuations in gene expression in resting effector T cells.

#### ***4.7 In vivo analysis of transcriptome data in NTN model confirmed significant upregulation of *Clec4e* on mRNA level and *Siglec5* and *Clec7a* on protein level in inflamed kidneys***

To address whether the identified genes were regulated physiologically by CD4<sup>+</sup> effector T cells in the tissue, the NTN kidney disease mouse model was used as a CD4<sup>+</sup> T cell-dependent disease model for *in vivo* experiments. *Nur77<sup>GFP</sup>* mice were injected with a heterologous serum from sheep that have been immunized against rabbit glomeruli. This model leads to acute kidney damage quantified by urinary protein excretion level during NTN induction. After NTN induction, total albumin levels increased rapidly during the first five days and decreased gradually after 10 days (Figure 24, A and B). Furthermore, the number of leukocytes and CD4<sup>+</sup> T cells rapidly increased 10 days after NTN induction due to inflammatory processes in the damaged kidney (Figure 24, C and D).

As mentioned in the introduction, T<sub>H</sub>1 cells predominantly infiltrate the inflamed kidney in a second wave. Therefore, CD4<sup>+</sup> T cells were isolated 10 days after NTN induction and reactivated *Nur77<sup>GFP+</sup>* CD4<sup>+</sup> T cells were sorted (Kurts et al., 2020). In addition, CD4<sup>+</sup> T cells from healthy *Nur77<sup>GFP</sup>* reporter mice were isolated from the kidney. On average around 8% of the CD4<sup>+</sup> T cells in NTN induced mice were *Nur77<sup>GFP+</sup>*. The low percentage of reactivated T cells is due to the nature of this polyclonal T cell model.

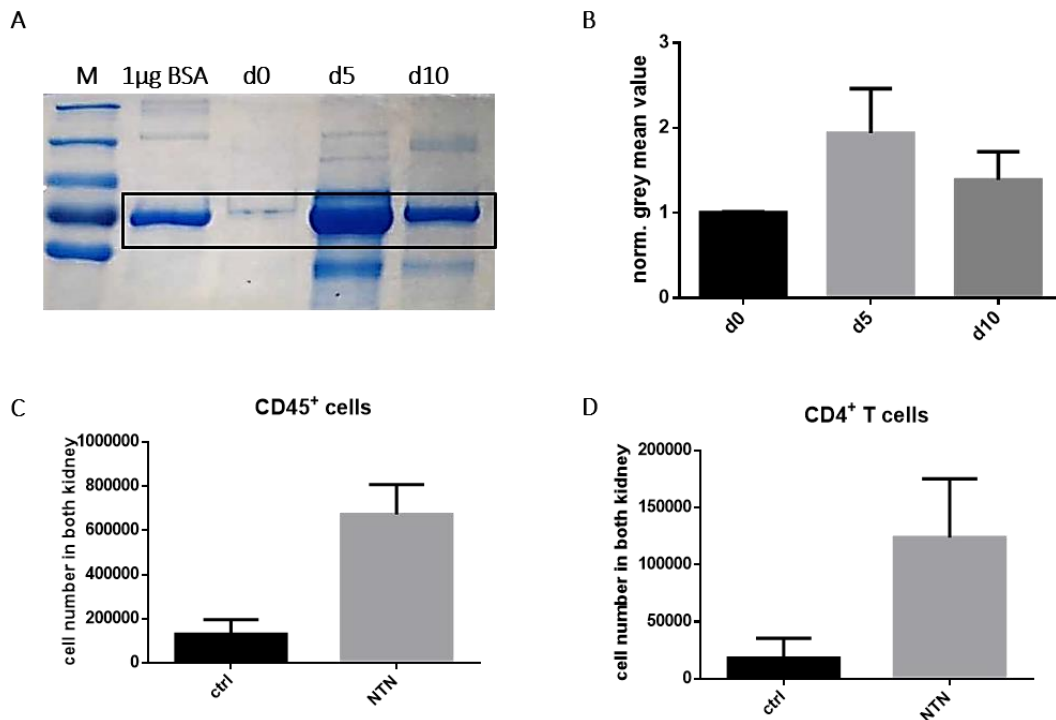


**Figure 24: NTN model**

*A: Colloid Coomassie gel; 1 $\mu$ l urine of NTN induced mice was mixed with 9 $\mu$ l H<sub>2</sub>O and loaded onto an SDS Gel. Indicated bands show proteinuria of NTN induced mice; B: Densitometry of colloid coomassie gels, grey mean value normalized to background; C: Flow cytometric analysis of immune cell infiltration into both kidney of healthy and NTN mice 10 days after induction; mean with SD (n=4); D: CD4<sup>+</sup> T cell number in both kidneys analyzed via flow cytometry; mean with SD (n=4)*

To understand if the selected genes were differentially regulated *in vivo*, qRT-PCR was performed on the 12 selected genes on sorted cells. The results showed that *Clec4e* was significantly upregulated, whereas *Pdzk1ip1* was significantly downregulated in NTN induced mice. However, *Clec7a*, *Siglec5* and *Lyz2* were not significantly upregulated, but showed tendency towards upregulation while *Edn1* showed tendency towards downregulation (Figure 25). Surprisingly, none of the identified downregulated genes from the transcriptome analysis was significantly regulated in the NTN model (Figure 26), although *Ccr4* and *Dach2* showed a tendency towards upregulation in some mice. Furthermore, no expression of *Gipr*, *Socs2* or *Coro6* could be identified in the NTN model.

In addition to qRT-PCR analysis, I also performed flow cytometric analysis for *Siglec5* and *Clec7a*. The expression of both *Siglec5* and *Clec7a* was significantly upregulated in CD4<sup>+</sup> T cells isolated from NTN induced kidneys compared to untreated controls (Figure 27).

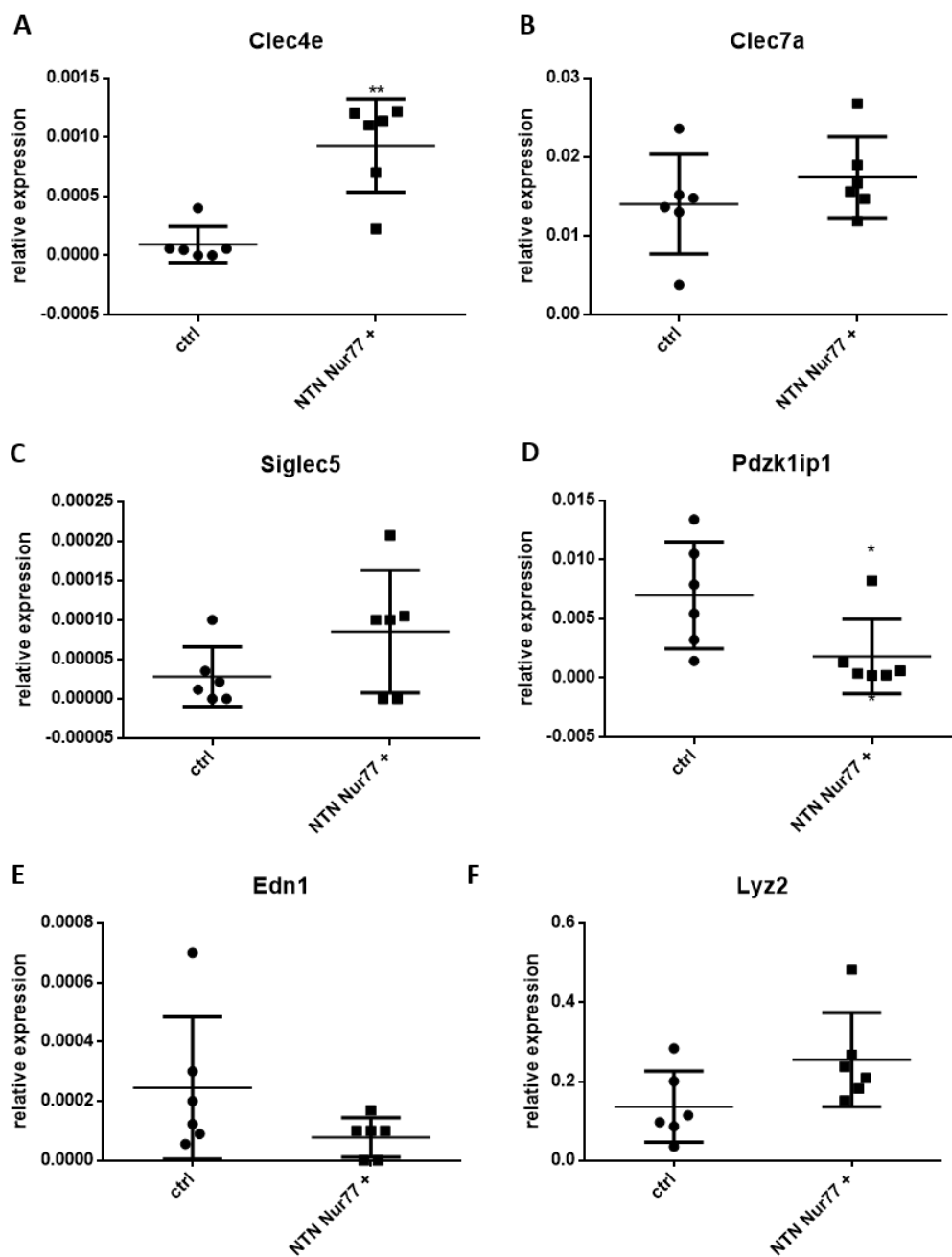


**Figure 25: Gene expression analysis of upregulated genes from transcriptome analysis in CD4<sup>+</sup> T cells isolated from NTN induced kidneys**

Gene expression analysis of sorted CD4<sup>+</sup> T cells from the kidney of Clec4e (A), Clec7a (B), Siglec5 (C), Pdzk1ip1 (D), Edn1 (E) and Lyz2 (F) via qRT-PCR; mean with SD (n=6)

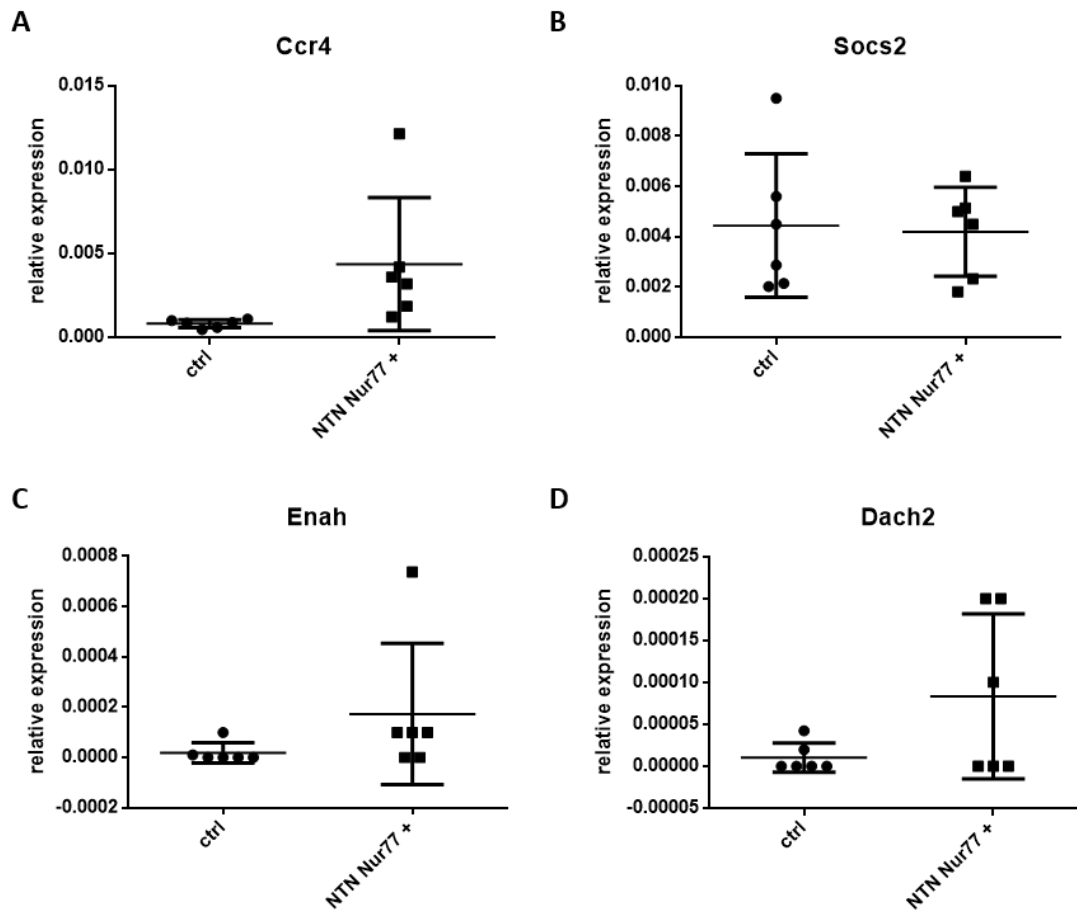


**Figure 26: Gene expression analysis of downregulated genes from transcriptome analysis in CD4<sup>+</sup> T cells isolated from NTN induced kidneys**

Gene expression analysis of sorted CD4<sup>+</sup> T cells of *Ccr4* (A), *Socs2* (B), *Enah* (C), *Dach2* (D) via qRT-PCR; no expression of *Gipr*, *Socs2* and *Coro6* was detected; mean with SD (n=6)

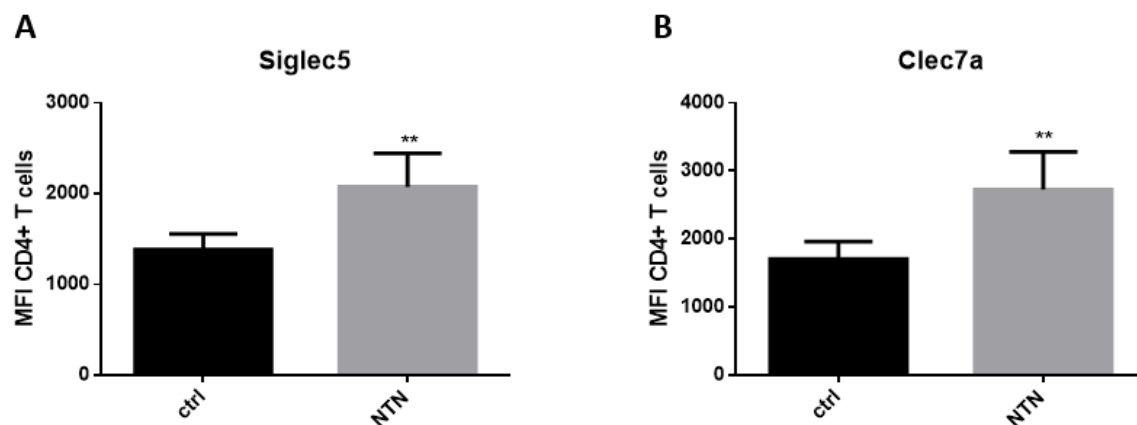


**Figure 27: Flow cytometric analysis of Siglec5 (A) and Clec7a (B) expression on CD4<sup>+</sup> T cells in the kidney of ctrl and NTN induced mice**

**4.8 *In vivo* analysis of transcriptome data in EAE mice revealed significant upregulation of *Clec7a* on protein level and indicated differences in gene expression of selected genes on mRNA level in different tissues**

To address whether the selected genes were similarly regulated by CD4<sup>+</sup> effector T cells in other tissues, the EAE disease mouse model was used additionally as another CD4<sup>+</sup> T cell-dependent *in vivo* model. As mentioned in the introduction, EAE disease onset characterized by tail paralysis and hind limb paresis started around day 14. Furthermore, EAE onset was indicated by high infiltration of CD45<sup>+</sup> cells and CD4<sup>+</sup> T cells into the CNS. Since there are no T cells in the healthy CNS, reactivated Nur77<sup>GFP+</sup> cells and resting Nur77<sup>GFP-</sup> CD4<sup>+</sup> T cells were isolated from the inflamed spine and brain and sorted for qRT-PCR of EAE induced mice at day 14.

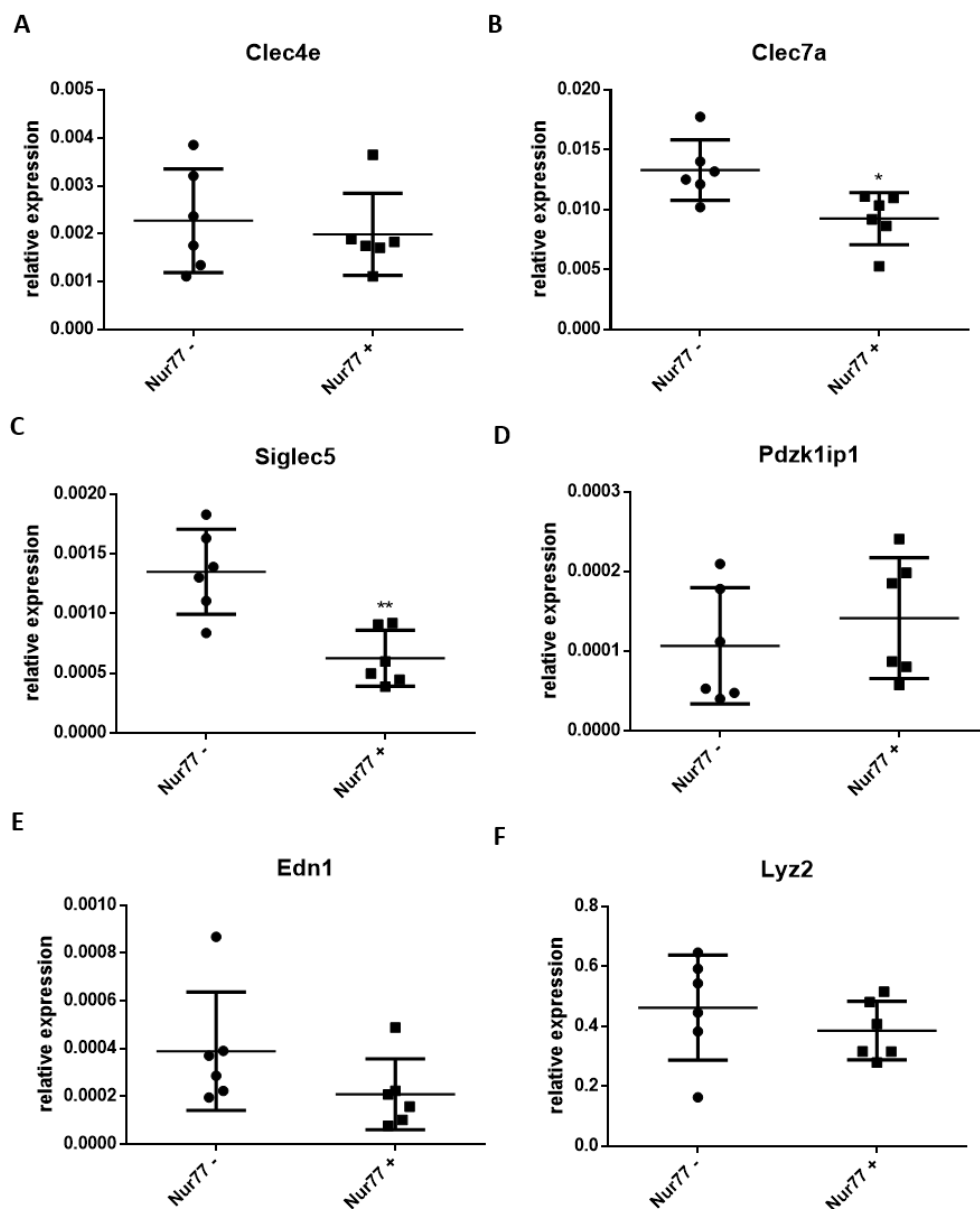


**Figure 28: Gene expression analysis of upregulated genes from transcriptome analysis in CD4<sup>+</sup> T cells isolated from EAE induced CNS**

Gene expression analysis of sorted Nur77<sup>GFP-</sup> and Nur77<sup>GFP+</sup> CD4<sup>+</sup> T cells from the spine and brain of EAE induced mice. Expression of Clec4e (A), Clec7a (B), Siglec5 (C), Pdzk1ip1 (D), Edn1 (E) and Lyz2 (F) via qRT-PCR; mean with SD (n=6)

qRT-PCR analysis of selected genes revealed no changes in expression of Clec4e, Pdzk1ip, Edn1 and Lyz2 and showed significant downregulation of Clec7a and Siglec5 in Nur77<sup>GFP+</sup> CD4<sup>+</sup> T cells (Figure 28). Furthermore, Gpr, Enah and Dach2 were not detected and Coro6 was not differentially expressed. In addition, Ccr4 and Socs2 were significantly upregulated in Nur77<sup>GFP+</sup> CD4<sup>+</sup> T cells (Figure 29). While there were no changes in Siglec5 protein expression, Clec7a protein expression was significantly upregulated on Nur77<sup>GFP+</sup> CD4<sup>+</sup> T cells (Figure 30). Overall, the expression of the selected genes was different in the inflamed kidney compared to the inflamed CNS.

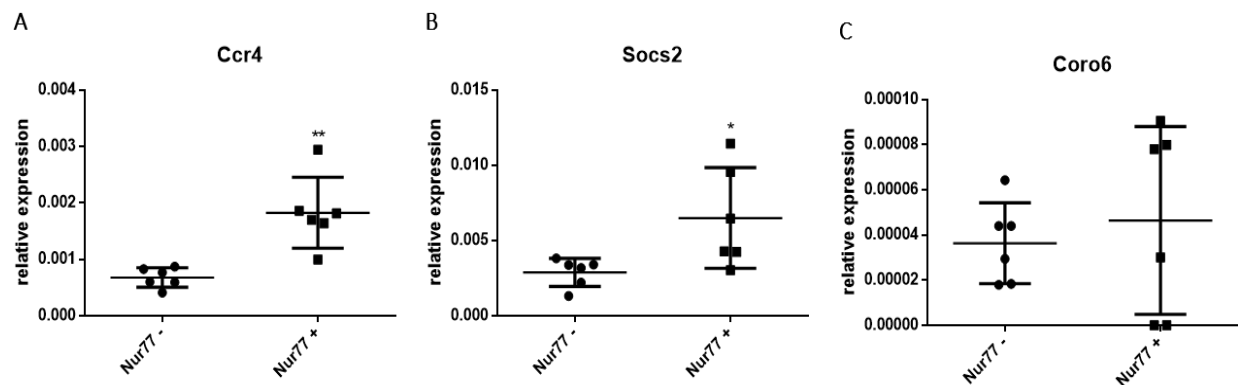


**Figure 29: Gene expression analysis of downregulated genes from transcriptome analysis in CD4<sup>+</sup> T cells isolated from EAE induced CNS**

Gene expression analysis of sorted Nur77<sup>GFP-</sup> and Nur77<sup>GFP+</sup> CD4<sup>+</sup> T cells from the spine and brain of EAE induced mice. Expression of Ccr4 (A), Socs2 (B) and Coro6 (C) via qRT-PCR; mean with SD (n=6)

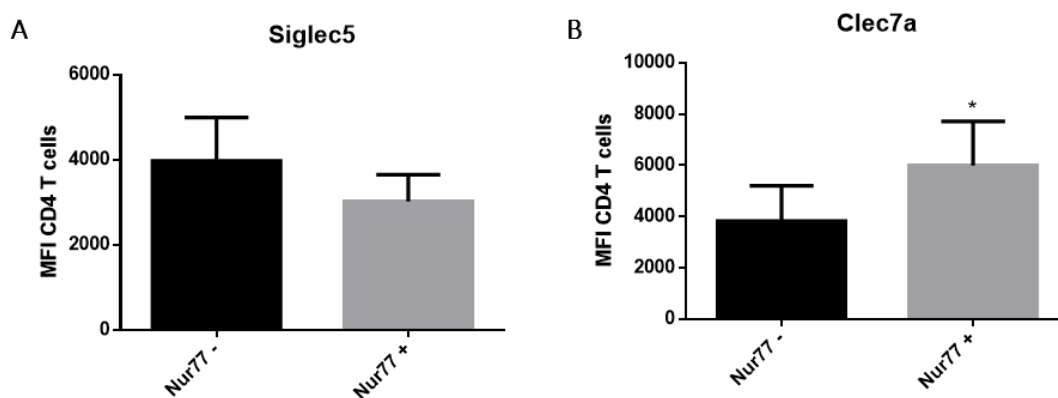


**Figure 30: Flow cytometric analysis of Siglec5 and Clec7a expression on sorted Nur77<sup>GFP-</sup> and Nur77<sup>GFP+</sup> CD4<sup>+</sup> T cells isolated from EAE induced CNS (n=6)**

However, Clec7a expression on protein level was upregulated on reactivated CD4<sup>+</sup> T cells in the NTN as well as in the EAE model.

#### **4.9 In vitro analysis of identified genes in human T<sub>H</sub>1 cells confirmed significant upregulation of CLEC4e, PDZK1IP1 and EDN1, but also significant upregulation of GIPR, CCR4 and CORO6, which were significantly downregulated in murine T<sub>H</sub>1 cells**

Finally, I investigated whether the selected genes were regulated in human CD4<sup>+</sup> T cells as well. Therefore, human naïve CD4<sup>+</sup> T cells were isolated from peripheral blood mononuclear cells (PBMCs) of healthy donors and differentiated to T<sub>H</sub>1 cells. qRT-PCR analysis showed that human T<sub>H</sub>1 cells upregulated T-Bet upon differentiation and around 80% of these cells secreted IFN $\gamma$  upon reactivation with PMA/Ionomycin for four hours (Figure 31).

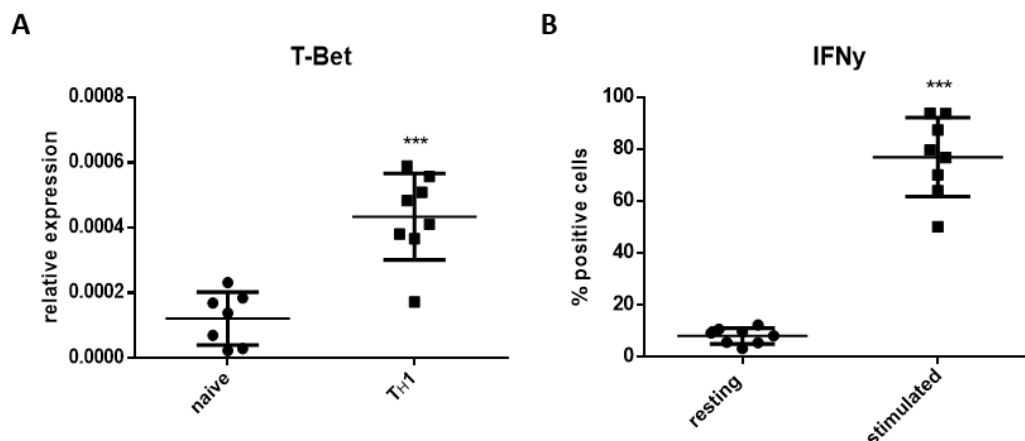


**Figure 31: T<sub>H</sub>1 differentiation of human CD4<sup>+</sup> T cells isolated from peripheral blood**

A: T-Bet expression in T<sub>H</sub>1 polarized CD4<sup>+</sup> T cells via qRT-PCR; B: IFN $\gamma$  expression after four hours of PMA/Ionomycin stimulation in human T<sub>H</sub>1 cells; mean with SD (n=8)

Human T<sub>H</sub>1 cells were reactivated for four hours with PMA/Ionomycin and analyzed for the expression of the human ortholog of the before analyzed murine genes. CLEC4e, PDZK1ip1 and EDN1 were also significantly upregulated in human T<sub>H</sub>1 cells upon reactivation (Figure 32). CLEC7a showed a trend towards upregulation while LYZ2 was not regulated during reactivation. Orthologue SIGLEC5 and paralogue SIGLEC8 to murine Siglec5 were not detected in resting or reactivated human T<sub>H</sub>1 cells. In contrast to murine gene expression, GIPR, CCR4 and CORO6 were

significantly upregulated in human T<sub>H</sub>1 cells (Figure 33). Furthermore, SOCS2 showed a trend towards downregulation, while DACH2 and ENAH were not regulated during reactivation.

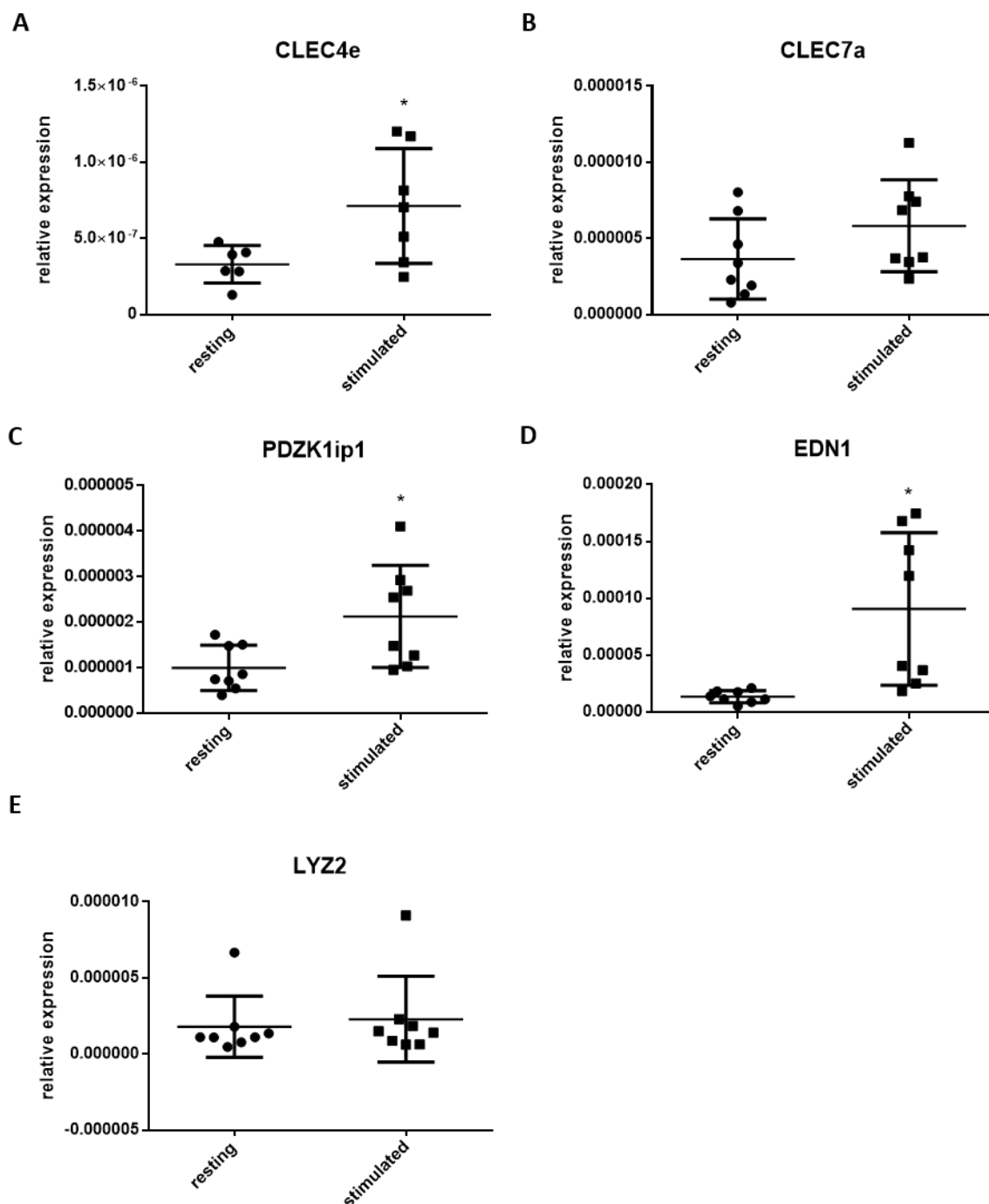


**Figure 32: Gene expression analysis of upregulated genes from transcriptome analysis in human T<sub>H</sub>1 cells restimulated with PMA/Ionomycin**

Gene expression of CLEC4e (A), CLEC7a (B), PDZK1ip1 (C), EDN1 (C) and LYZ2 (E) via qRT-PCR; no expression of SIGLEC5 and SIGLEC8 detected; mean with SD (n=8)

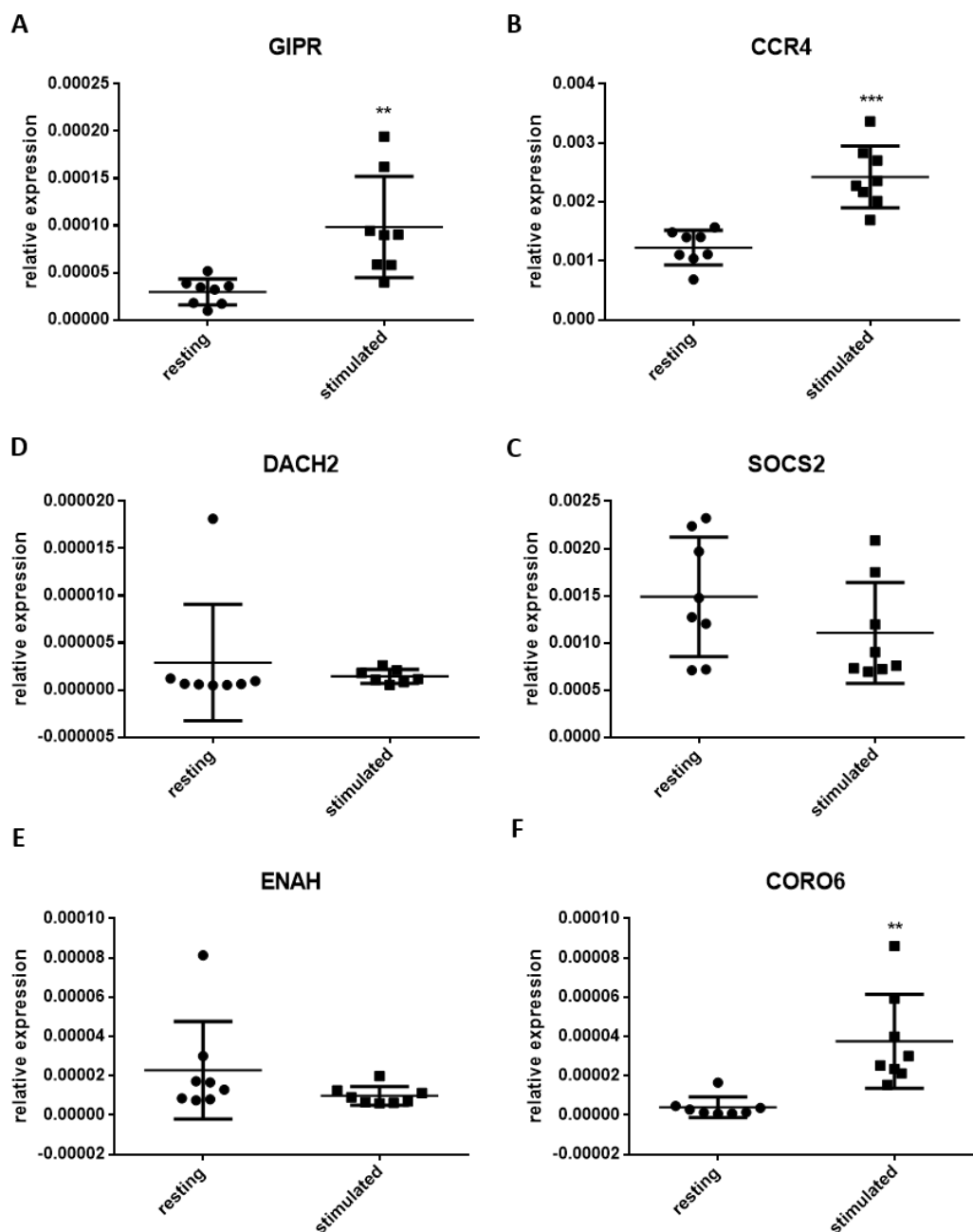


**Figure 33: Gene expression analysis of downregulated genes from transcriptome analysis in human  $T_H1$  cells restimulated with PMA/Ionomycin**

Gene expression analysis of GIPR (A), CCR4 (B), SOCS2 (C), DACH2 (D), ENAH (D), CORO6 (F) via qRT-PCR; mean with SD ( $n=8$ )

Following table gives an overview of each analyzed gene according to differential expression from transcriptome analysis in reactivated murine CD4<sup>+</sup> T<sub>H1</sub> cells, NTN model, EAE model and human CD4<sup>+</sup> T cells (Table 2):

	<b>Function</b>	<b>RNAseq</b>	<b>Murine T<sub>H</sub>1 cells</b>	<b>in vivo NTN model</b>	<b>in vivo EAE model</b>	<b>human T<sub>H</sub>1 cells</b>
Clec4e/ Mincle	calcium dependent lectin, cell adhesion, innate immune receptor on myeloid cells	↑	↑	↑	=	↑
Clec7a/ Dectin1	calcium dependent lectin, cell adhesion, macrophages, neutrophils and DCs	↑	↑	= (protein up)	↓ (protein up)	=
Siglec5	Sialic acid-binding Ig-like lectin, cell adhesion, monocytic/myeloid lineage cells	↑	↑	↑ (protein up)	↓	no expression
Siglec8	Human paralogue of mouse siglec5					no expression
Pdzk1ip1/ Map17	membrane protein in plasma membrane and Golgi apparatus, predictive marker for ROS, overexpressed in tumors, function not clear	↑	↑	↓	=	↑
Edn1	Endothelin, potent vasoconstrictor	↑	↑	↓	=	↑
Lyz2	Lysozyme, bacteriolytic function, associated with monocyte-macrophage system	↑	↑	↑	=	=
Gipr	glucose-dependent insulinotropic polypeptide, insulin signaling	↓	=	no expression	no expression	↑
Ccr4	chemokine receptor, G-protein coupled receptor	↓	↓	↑	↑	↑
Socs2	Suppressor of cytokine signaling (JAK/STAT pathway)	↓	↓	↓	↑	=

Enah	involved in actin-based motility, involved in translocation of Zap-70	↓	↓	no expression	no expression	=
Dach2	transcription factor in regulation of organogenesis	↓	↓	↑	no expression	=
Coro6	belongs to coronin family, actin binding protein	↓	↓	no expression	=	↑

**Table 2: Overview of each analyzed gene according to differential expression from transcriptome analysis, *in vitro* reactivated murine CD4<sup>+</sup> T<sub>H</sub>1 cells, NTN model, EAE model and human CD4<sup>+</sup> T cells**

#### **4.10 Proteome- and Phosphoproteomeanalysis**

To identify more potential molecular targets, I performed proteomics and phosphoproteomics on *in vitro* differentiated murine T<sub>H</sub>1 cells. Principal component analysis (PCA) showed distinct differences between resting and reactivated T<sub>H</sub>1 cells (Figure 34, A and B). Pairwise comparison revealed 305 differentially expressed proteins and 2565 differentially expressed phosphoproteins (different isoforms not included). To identify proteins, which are reactivation-specific, I compared proteome with transcriptome data and found 35 genes overlapping in both data sets (Figure 34, D). Despite the low number of overlapping genes, most of the identified proteins play a role in metabolic processes (Figure 34, E), similar to the genes which were identified as reactivation-specific genes during transcriptome analysis. One of the identified gene in proteome analysis that was differentially expressed was Enah, which was also found in transcriptome analysis. These 35 reactivation-specific proteins identified during proteome analysis will be investigated in detail in future experiments in addition to the reactivation-specific genes identified during transcriptome analysis.

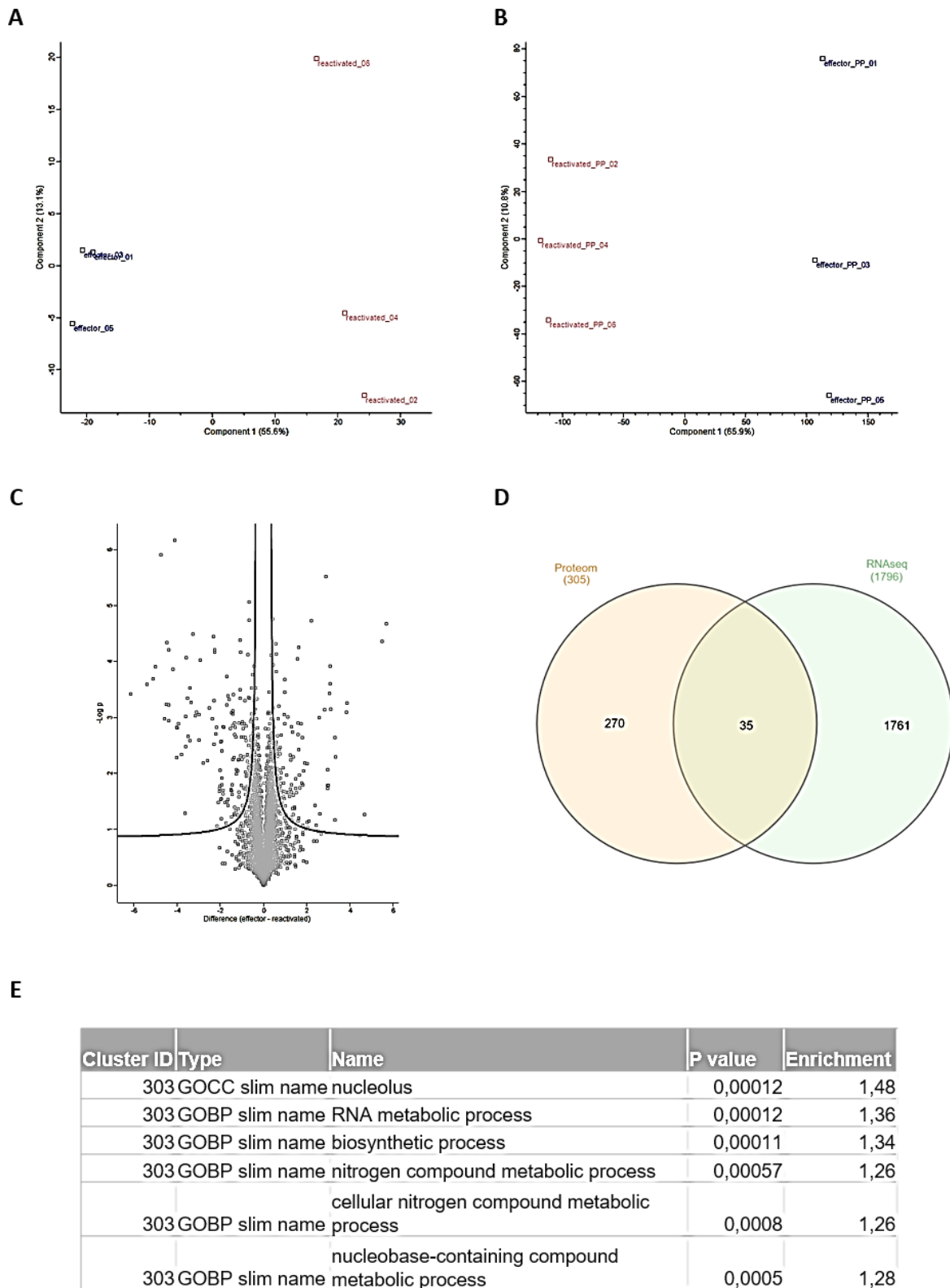


**Figure 34: Proteome and phosphoproteome analysis of resting and reactivated TH1 cells stimulated for 6 hours with anti-CD3 and anti-CD28**

A: PCA proteome; B: PCA phosphoproteome; C: Volcano blot proteome of resting vs stimulated TH1 cells; D: Venn diagram comparison Proteome vs RNAseq data; E: Table of enriched proteome signaling pathways (n=3)

## 5. Discussion

### **5.1 Identification and characterization of naïve, activated naïve, T<sub>H</sub>1, reactivated T<sub>H</sub>1 cells and other CD4<sup>+</sup> T cell subpopulations**

CD4<sup>+</sup> T cells play an important role in immune responses during infection, autoimmunity or tumor development. The identification of genes, which are specific for reactivated effector T cells in the tissue is of great interest clinically. Especially in the context of autoimmune diseases and immunotherapy, specific genes and proteins unique for reactivation might constitute attractive therapeutic targets. Therefore, I characterized naïve, activated naïve, T<sub>H</sub>1 and reactivated T<sub>H</sub>1 cells, performed kinetics of endogenous Nur77, Nur77<sup>GFP</sup> reporter, IL-2, IFN $\gamma$  and performed bulk transcriptome analysis to identify genes specific for primary T cell activation, T cell differentiation and especially effector T cell reactivation. RNA isolation from fixed cells causes certain purity and quantity limitations for transcriptome analysis, although techniques have been improved in recent years (Channathodiyil & Houseley, 2021; L. Liu et al., 2017; Phan et al., 2021). Therefore, I used the Nur77<sup>GFP</sup> reporter mouse model to directly identify TCR activated T cells without the need of any fixation and intracellular staining that might cause variability in results due to the technique (Figure 10 and 11). Nur77 is a gene, which is upregulated early during T cell receptor activation and whose expression correlates with the activation strength of the TCR (Au-Yeung et al., 2014; Moran et al., 2011). While TCR activation is a prerequisite for the functional activation of the T cell, it is not proof as the stimulation of the TCR alone is not sufficient for a functional stimulation. Functional stimulation requires stimulation strength to exceed a certain threshold. Therefore, I performed kinetics of IFN $\gamma$  expression in reactivated OT-II/Nur77<sup>GFP+</sup> T<sub>H</sub>1 cells to confirm functional activation. Overall, the advantage of this reporter system is that it can be used for all reactivated T cell subpopulations, unlike, for example, the IFN $\gamma$ <sup>YFP</sup> reporter mouse model, which is specific for IFN $\gamma$  secreting cells, like T<sub>H</sub>1 and CD8<sup>+</sup> effector T cells. Beside the Nur77<sup>GFP</sup> reporter, there is another Nr4a reporter available: the Nr4a3-Timer of cell kinetics and activity (Tocky) mouse model (Bending et al., 2018). Using this model, Jennings *et al.* found that Nr4a3, unlike Nr4a1 (Nur77), is dependent on the calcineurin/NFAT pathway. Furthermore, Nur77 has a two- to three-fold higher sensitivity to TCR signaling and can be detected early during TCR signaling compared to Nr4a3 (E. Jennings et al., 2020; E. Jennings et al.,

2021). The latter finding was confirmed by my transcriptome analysis. While Nur77 was slightly upregulated (Log<sub>2</sub>Foldchange of 1,35), the other members of the family like Nr4a2 and especially Nr4a3 showed higher upregulation after six hours of stimulation (Log<sub>2</sub>Foldchange of 1,91 and 5,1). Overall, including the control staining for IFN $\gamma$  and the staining of surface markers for each population, the Nur77<sup>GFP</sup> reporter mouse model proved to be a suitable model to identify and sort recently functionally activated naïve and effector T cells.

In this thesis, commonly used markers for the identification of each CD4<sup>+</sup> T cell subpopulation were used (Figure 16, 17 and 20). Based on the literature, T<sub>H</sub>1 cell can be characterized by T-Bet and IFN $\gamma$  expression, T<sub>H</sub>2 cells can be characterized by the expression of Gata3 and IL-4, T<sub>H</sub>17 cells can be characterized by the expression of ROR $\gamma$ t and IL-17a and T<sub>reg</sub> cells can be characterized by the expression of FoxP3 and IL-10 or TGF $\beta$  (Hoepli et al., 2015; Nelson et al., 2020). However, my results showed that T<sub>reg</sub> cells also expressed Gata3 and T-Bet. Many studies showed, that these markers can be dynamic, especially within the T<sub>reg</sub> cell population (Duhon et al., 2012; Y. Wang et al., 2011; Wohlfert et al., 2011; Yu et al., 2015). Surprisingly, there are no publications available, that analyzed the expression of master transcription factors and lead cytokines in all CD4<sup>+</sup> T cell subpopulations simultaneously. There are rather collections of publications, which analyzed each CD4<sup>+</sup> subpopulation individually. In summary, the identification of T cell subpopulations is rather difficult due to the high degree of heterogeneity and plasticity within and in between CD4<sup>+</sup> T cell subpopulations (Becattini et al., 2015). Nonetheless, the results showed that each CD4<sup>+</sup> subpopulation can be identified by the expression of specific master transcription factors. However, I did not only analyze the expression of transcription factors, but I also analyzed the secretion of cytokines upon reactivation, although even the cytokine secretion can be heterogeneous within each subpopulation. In this *in vitro* approach the identification of each subpopulation was quite clear for T<sub>H</sub>1, T<sub>H</sub>2 and T<sub>H</sub>17 and to a lesser degree for T<sub>reg</sub> cells. TGF $\beta$  and IL-10 are proposed as T<sub>reg</sub> cell specific cytokines, but my results showed that TGF $\beta$  was expressed in all cell types and that IL-10 was mainly expressed in T<sub>H</sub>2 cells and not in T<sub>reg</sub> cells upon antigen-stimulation (Figure 18). Expression of IL-10 in T<sub>H</sub>2 cells is confirmed by other publications (Rasquinha et al., 2021). It is thought, that IL-10 also plays an important role in T<sub>reg</sub> cell suppression function (Asseman et al., 1999; McGeachy & Anderton, 2005), but I could

not detect any IL-10, in antigen-stimulated T<sub>reg</sub> cells. However, T<sub>reg</sub> cells are a heterogeneous population that can secrete different cytokines (Shevyrev & Tereshchenko, 2019). Furthermore, there is indication that FoxP3<sup>+</sup> T<sub>reg</sub> cells do not express IL-10 (Vieira et al., 2004). In addition, I showed that the stimulation method impacts cytokine secretion. T<sub>H1</sub>, T<sub>H2</sub> and T<sub>reg</sub> cells secreted IL-10 upon restimulation with PMA/Ionomycin (Figure 20). PMA/Ionomycin stimulation leads to a strong immune response and the expression of the suppressive cytokine IL-10 might be a mechanism for targeting over-stimulation in these cells. That would explain the low IFN $\gamma$  protein secretion in T<sub>H1</sub> cells, although IFN $\gamma$  was highly upregulated on mRNA level in these cells. This assumption is further supported by other publications (Jankovic et al., 2010; Trinchieri, 2007). Altogether, my *in vitro* model allowed for the distinct characterization of each subpopulation by the expression of master transcription factors and lead cytokine secretion upon restimulation.

## **5.2 Commonly used activation marker**

As previously mentioned, there are many conflicting reports about T cell reactivation in the tissue, many of which are due to the lack of distinction between primary T cell activation and secondary T cell reactivation. My transcriptome analysis showed a minor upregulation of CD69, one of the commonly accepted activation markers, in reactivated T<sub>H1</sub> cells compared to resting T<sub>H1</sub> cells (Log<sub>2</sub>Foldchange of 0.44, Table 1), demonstrating that this marker is not suitable as a marker for effector T cell reactivation. Another commonly used T cell activation marker is Ki67. Upon T cell priming, naïve T cells proliferate and upregulate Ki67, but there is no evidence that effector T cells also proliferate upon reactivation in the tissue. Normally, Ki67 is a marker for active and recent cell divisions and can be detected up to 3 to 4 days after the last mitosis (Di Rosa et al., 2021; Gossel et al., 2017). Therefore, the expression of Ki67 in effector T cells in tissues still might derive from recent cell division occurred during priming and clonal expansion in the lymph nodes. In addition, studies indicate that memory T cells have less proliferative capacity compared to naïve T cells (MacLeod et al., 2008), which makes proliferation markers rather useless as specific markers for reactivation. Supporting this assumption, my transcriptome data showed no upregulation of Ki67 during T<sub>H1</sub> cell reactivation (Log<sub>2</sub>Foldchange of -0.25, Table

1). Another commonly used activation marker is the lymphocyte function-associated antigen-1 (LFA-1), a leukocyte specific integrin, which plays an important role in regulating T cell activation and migration. Adhesion of LFA-1 to the intracellular adhesion receptor 1 (ICAM-1) facilitates robust endothelium adhesion, prolonged contact with APCs as part of the immune synapse, and binding to target cells for killing (Walling & Kim, 2018). LFA-1 seems to be upregulated upon antigen encounter, thereby has been proposed as a marker for T cell activation (Li, Molldrem, & Ma, 2009). However, LFA-1 plays a role in both naïve and effector T cell extravasation into the lymph node and tissue. Moreover, its expression is usually upregulated during recruitment, a process that by definition occurs prior to reactivation in the tissue, by tissue specific APCs (Gérard et al., 2021; Ley et al., 2007). It is worth noting that conformational changes lead to increased affinity and thereby activation of LFA-1 (Stanley et al., 2008). Nonetheless, LFA-1 upregulation is not a suitable marker for T cell reactivation in the tissue. My transcriptome analysis supports this statement showing nearly no upregulation of LFA-1, specifically during reactivation (Log<sub>2</sub>Foldchange of 0.11, Table 1). Other commonly known activation markers are CD25 and Ox40 (Flügel et al., 2001). CD25 is part of the IL-2 receptor and it is predominantly expressed on T<sub>reg</sub> cells and memory T cells (Bajnok et al., 2017). Therefore, it is more of a marker for primary activation and differentiation status. Indeed, my transcriptome data confirms no significant changes in CD25 expression but slight downregulation upon reactivation (Log<sub>2</sub>Foldchange of -1.3, Table 1). Ox40 is a member of the tumor-necrosis factor (TNF) receptor superfamily and was previously identified as a co-stimulatory receptor (Sugamura et al., 2004). This gene is rather a marker for primary T cell activation than a specific reactivation marker, also confirmed by my data showing a minor Ox40 upregulation (Log<sub>2</sub>Foldchange of 1.08, Table 1). Finally, IFN $\gamma$  was also upregulated in reactivated T<sub>H</sub>1 cells compared to resting T<sub>H</sub>1 cells (Log<sub>2</sub>Foldchange of 5.97, Table 1). As mentioned before, it is common practice to examine T cell reactivation by a cytokine assay. Here T cells recovered from the site of inflammation are stimulated *ex vivo* to elicit effector cytokine production. However, the observed response does not mean that these T cells were previously reactivated *in vivo*, especially when the cells were reactivated unspecifically with PMA/ Ionomycin and not with the unique antigen. The difference in cytokine secretion of antigen-

stimulated versus PMA/Ionomycin stimulated T cells was also shown in this thesis (Figure 18 and 21).

Furthermore, I analyzed the expression of PD-1, which was upregulated in the transcriptome analysis in reactivated T<sub>H</sub>1 cells compared to resting T<sub>H</sub>1 cells indicating T cell anergy (Log<sub>2</sub>Foldchange of 3.81, Table 1). PD-1 is often seen as an inhibitory receptor and exhaustion marker (Y. Dong et al., 2019; Wherry et al., 2007). However, there are publications confirming the functional upregulation of PD-1 during T cell activation and its' function as a negative regulator to prevent autoimmunity (Agata et al., 1996; Elliot et al., 2021; Nishimura et al., 1999). In addition, single-cell transcriptome analysis in SARS-Cov-2-reactive human T cells confirms my assumption that the upregulation of inhibitory receptors reflects T cell activation rather than T cell exhaustion (Fischer et al., 2021). Furthermore, *Nfatc2* expression was upregulated (Log<sub>2</sub>Foldchange of 2,01), while *Jun* and *Fos* were downregulated (Log<sub>2</sub>Foldchange of -1,52 and -1,03). However, for functional T<sub>H</sub>1 cell activation and especially IFN $\gamma$  expression both NFAT and AP1, as well as T-Bet, are needed (Hermann-Kleiter & Baier, 2010). The downregulation of AP1 in the transcriptome data might be due to the late time point chosen for sorting: First, T cells were activated and then the expression of inhibitory receptors was induced to prevent autoimmunity.

In summary, I showed that commonly used activation markers are not suitable for the identification of reactivated effector T cells and there is currently no proper measurement of the physiological functionality of reactivated effector T cells *in vivo*, at least not without the use of mouse reporter models or viral reporters.

### **5.3 Reactivation-specific genes identified in transcriptome analysis**

For the first time, the transcriptome analysis in this thesis revealed genes specific for effector T cell reactivation besides T cell priming and differentiation. In summary, the expression of selected genes from this transcriptome analysis showed similar tendencies in expression in all CD4<sup>+</sup> T cell subpopulations, although expression strength differed. These results might indicate that reactivation could be a process independent of the subpopulation type. Furthermore, the method chosen for restimulation (antigen- or PMA/Ionomycin stimulation) had effects on Nur77<sup>GFP</sup> and

leading cytokine expression, but not a significant impact on the expression of the selected genes. It is particularly interesting that most of these genes were not described and characterized in T cell populations elsewhere. Clec4e is the only one of the chosen genes, which was not only significantly upregulated *in vitro* in all CD4<sup>+</sup> T cell subpopulations, but was also significantly upregulated in sorted CD4<sup>+</sup> T cells from inflamed kidneys (NTN model) and significantly upregulated in human T<sub>H</sub>1 cells upon reactivation. To my knowledge, Clec4e was mainly characterized in innate immune cells and there is no study available, which describes the expression of Clec4e on T cells. Furthermore, my results showed that Clec7a was significantly upregulated *in vitro* in all CD4<sup>+</sup> T cell subpopulations, except T<sub>H</sub>17 cells - although there is a trend towards upregulation. Furthermore, it was significantly upregulated on protein level on sorted CD4<sup>+</sup> T cells from inflamed kidneys (NTN) and on Nur77<sup>GFP+</sup> CD4<sup>+</sup> T cells from inflamed CNS (EAE), although it was not significantly upregulated on human T<sub>H</sub>1 cells, but results showed a trend towards upregulation. Clec7a is mainly described on innate immune cells, but a recent publication showed that Clec7a expression in CAR T cells leads to significantly higher cytokine secretion and may increase their clinical potential (Liang et al., 2021). This study and my findings make Clec7a a possible candidate for immunotherapy. Like Clec7a, Siglec5 was significantly upregulated *in vitro* in all CD4<sup>+</sup> T cell subpopulations. Siglecs are sialic-acid-binding immunoglobulin-like lectins which are mainly expressed on cells of the innate immune system and play a role in cell expansion and activation (Crocker et al., 2007). Furthermore, both genes were not regulated on mRNA level, but they were significantly upregulated on protein level in CD4<sup>+</sup> T cells from inflamed kidneys and inflamed CNS. This indicates that these genes were upregulated on mRNA level before and that timing of T cell isolation from the tissue is an important factor for the analysis of the reactivation state of effector T cells in the tissue. Unfortunately, neither SIGLEC5 nor SIGLEC8 were detected in human T<sub>H</sub>1 cells. Siglec5 is a gene which function was predominantly analyzed in eosinophils and macrophages (Feng & Mao, 2012; M. Zhang et al., 2007). Zhang *et al.* did not only analyze Siglec5 expression on eosinophils, but also found that Siglec5 (also named Siglec-F) was expressed on activated CD8<sup>+</sup> and CD4<sup>+</sup> T cells from the spleen and peripheral blood. They also found Siglec5 expression in reactivated CD4<sup>+</sup> T cells after an allergic response in the lung (M. Zhang et al., 2007). Furthermore, Pdzk1ip1, like Edn1, was significantly upregulated *in vitro* in all CD4<sup>+</sup> T cell subpopulations, but it was

significantly downregulated in sorted CD4<sup>+</sup> T cells from inflamed kidneys and not regulated in sorted Nur77<sup>GFP+</sup> CD4<sup>+</sup> T cells from inflamed CNS. However, it was upregulated on human T<sub>H</sub>1 cells upon reactivation. Pdzk1ip1 is a gene overexpressed in some tumor entities and inflamed tissues, but it was not described in T cells yet (García-Heredia & Carnero, 2017). Since Pdzk1ip1 is downregulated or not regulated at all *in vivo*, it is likely a factor in the microenvironment that leads to this downregulation. Most of the selected genes from the transcriptome analysis were not described in T cells yet, except Ccr4, Socs2 and Lyz2. However, many genes involved in adhesion or actin-binding were identified as reactivation-specific genes. This observation was also found in other studies indicating that these genes play a role in effector functions (Fischer et al., 2021). Furthermore, another study showed that a dynamic actin filament network created upon TCR activation is necessary for effector functions (Tsopoulidis et al., 2019). In addition to actin binding processes, metabolic changes are also involved in activation, differentiation and reactivation processes. Pathway analysis with the transcriptome as well as proteome data showed that metabolic pathways play a role in effector T cell reactivation. It is commonly known, that there are metabolic changes upon T cell activation and differentiation (Almeida et al., 2016; Gubser et al., 2013; Rangel Rivera et al., 2021; Shyer et al., 2020). Naïve T cells rely mostly on oxidative phosphorylation while memory T cells most efficiently engage glycolysis (Rangel Rivera et al., 2021). It is therefore worthwhile to analyze metabolic differences between these T cell states more closely and analyze which metabolic changes are specific for reactivated effector T cells

The transcriptome analysis as well as the proteome analysis were first attempts to identify genes, which might be specific and crucial for CD4<sup>+</sup> T cell reactivation. However, the performed experiments are insufficient to identify one of the selected genes as a suitable marker for reactivated CD4<sup>+</sup> T cells or a potential target for immunotherapy. Follow-up experiments have to be performed to investigate if selected genes are expressed on protein level. The question whether these genes might be suitable reactivation markers or have a functional role in reactivation processes, has to be addressed by using knock-down/knock-out or overexpression experiments.

#### **5.4 *In vitro* vs *in vivo***

Some of the selected genes were differentially expressed *in vitro* but not *in vivo*, which indicates that the microenvironment as well as the time point chosen have an impact on the expression of selected genes in effector CD4<sup>+</sup> T cells (Figure 24 and 25). This discrepancy might be attributed to different reasons. The immune microenvironment is a very complex system, consisting of many different cell types interacting with each other, and cytokines secreted by these cells, which have a substantial influence on surrounding cells. The disadvantage of *in vitro* systems is that they lack this microenvironment. For example, T cells, predominantly memory T cells, cannot only be activated by TCR signaling, they can also be activated by a process called bystander activation (Boyman, 2010; H. G. Lee et al., 2020). Bystander activation is best described for CD8<sup>+</sup> T cells and IL-15 is the most important cytokine secreted by APC, which is able to induce unspecific activation of unrelated CD8<sup>+</sup> T cells (T. S. Kim & Shin, 2019; X. Zhang et al., 1998). Compared to bystander activation in CD8<sup>+</sup> T cells, this process is less well understood and less efficient in CD4<sup>+</sup> T cells. In CD4<sup>+</sup> T cells, IL-15, IL-2 and IL-7 may play a role in bystander activation (Di Genova et al., 2010). Furthermore, different cytokines might induce bystander effects in different subpopulations (H. G. Lee et al., 2020). However, cytokines are not only activating molecules; they can also be immunosuppressive (Accogli et al., 2021). To my knowledge, there is no study available that analyzed differences in the signaling pathways of bystander, or TCR activated T cells. In my thesis, I focused on the TCR/antigen-specific activation of T cells and did not take bystander effects into account. Furthermore, differences in the expression of selected genes in both *in vivo* models, the NTN and EAE model, could be explained by differential cytokine expression in distinct tissues.

Additionally, the composition of different cell types plays a role in the tissue environment. In contrast to T<sub>H1</sub>, T<sub>H2</sub> and T<sub>H17</sub> cells, T<sub>reg</sub> cells have suppressive functions. They need TCR activation, and direct contact with other T cells for suppressive functions and they cluster around DC so it is more difficult for other T cell subpopulations to get activated (Onishi et al., 2008; Sakaguchi et al., 2009; Schmidt et al., 2012; Shevryev & Tereshchenko, 2019). T<sub>reg</sub> cells play a major role in inflamed tissues, mainly to prevent autoimmunity. In the NTN as well as in the EAE model, T<sub>reg</sub> cells suppress partially excessive T<sub>H1</sub> and T<sub>H17</sub> cell immune responses, especially in

the later stages, to minimize tissue damage (Koutrolos et al., 2014; Paust et al., 2011). That could be another reason why some of the selected genes, like *Pdzk1ip1*, *Edn1*, *Ccr4* or *Dach2*, were not differentially regulated in CD4<sup>+</sup> T cells *in vivo*. Furthermore, other cells can have immune-modulatory functions, like macrophages. Macrophages can have either a pro-inflammatory M1 phenotype or an immune-suppressive M2 phenotype and modulate the immune-microenvironment (Duan & Luo, 2021; Pan et al., 2020; Qiu et al., 2021; Seifert et al., 2016). Besides macrophages, there are other APC, which are able to functionally present antigen and lead to TCR activation or inhibition of effector T cell functions in the tissue. For example, the presence of co-regulatory receptors or immune checkpoint inhibitory receptors like programmed death ligand-1 (PD-L1) on APCs or tumor cells can inhibit functional T cell activation (Grywalska et al., 2018; Juneja et al., 2017; Simon & Labarriere, 2017). However, my results also indicate that tissue-specific mechanisms might play a role (inflamed kidney vs inflamed CNS). The discrepancy in the expression of selected genes between different *in vivo* models can be explained in part by the presence of tissue-specific cells, such as podocytes in the kidneys, microglia in the brain, Langerhans cells in the skin, or tissue-resident alveolar macrophages in the lungs. Furthermore, the selected point in time for the isolation of reactivated CD4<sup>+</sup> T cells could also play a role (day 10 in the NTN vs day 14 in the EAE model). The microenvironment, the composition of APCs and the cytokine milieu are complex systems, which have a huge impact on T cell functions. Therefore, antigen-reactive T cells can show broad inter- and intra-clonal heterogeneity (Fischer et al., 2021). However, it is unclear how the selected genes pan out in this scenario. More comprehensive experiments with more time points in different disease models should be performed in future experiments to characterize reactivated effector CD4<sup>+</sup> T cells in different tissues in detail.

### **5.6 Mouse vs human**

In 2014, the Mouse ENCODE Consortium mapped the mouse genome in diverse cell and tissue types and compared it to the human genome (Yue et al., 2014). They found that gene expression was more similar between different tissues than the same tissue between mice and humans (Lin et al., 2014). Furthermore, they found that 95% of the overall transcription factor regulatory network architecture was identical between

humans and mice (Stergachis et al., 2014). In addition, transcription factor binding sites are highly conservative between mice and humans (Cheng et al., 2014). Humans and mice share almost the same set of genes and show 70-85% identical sequences in the protein-coding region, which is around 1.5% of the whole genome. Overall, half of the human genome can be aligned to the mouse genome. Despite this similarity, major differences between the murine and human immune system are observed. For example, one difference is that human blood is neutrophil rich (50–70% neutrophils, 30–50% lymphocytes), while mouse blood is lymphocyte rich (75–90% lymphocytes, 10–25% neutrophils). Furthermore, immune cells of human and mouse show some differences in FcR expression and Ig isotypes and class switching. Mestas *et al.* summarized overall immunological differences between mice and humans (Mestas and Hughes 2004). Therefore, it is important to carefully analyze the results generated with mouse models, especially transgenic mouse models, and cautiously translate these results into the human setting.

For translational purposes, it is essential to analyze the genes identified in my transcriptome analysis also in human T cells. It is rather difficult to get samples from inflamed human tissues, so I used T cells from peripheral blood of healthy donors for my analysis. Almost all of the murine genes have a human orthologue. However, there are distinct differences between murine and human Siglec genes. Murine Siglec5 is the orthologue for human SIGLEC5, but there is also a functionally convergent paralogue that is human SIGLEC-8 (Angata et al., 2001; Tateno et al., 2005). Therefore, I analyzed both human SIGLEC5 and SIGLEC8, but I could not detect any expression on mRNA level. However, one publication showed that SIGLEC5 is not expressed on human lymphocytes, but transfection of SIGLEC5 on human T cells and Jurkats inhibits TCR responses and anti-CD3-induced intracellular calcium mobilization indicating a link between SIGLEC5 expression and TCR signaling (Nguyen et al., 2006). A recently published study found that SIGLEC5 indeed is expressed on activated human T cells 2-4 days after stimulation and might be a previously unrecognized inhibitory T cell immune checkpoint molecule (Vuchkovska et al., 2022). Therefore, SIGLEC5 might still be another interesting target for immunotherapy. Furthermore, CLEC4e, PDZK1ip1, EDN1 and probably CLEC7a might be exciting targets in human T cells, because these genes showed similar expression patterns in murine T cells. Further experiments would include analysis of

protein expression on isolated T cells from peripheral blood of sick and healthy donors and mRNA or protein expression on isolated tissue-infiltrated human T cells in inflamed tissues.

In addition, I analyzed publicly available single-cell data from human samples to identify overlaps or differences between murine and human data sets. There is a publication available in which isolated T cells from lungs, lymph nodes, bone marrow and blood were isolated and stimulated with anti-CD3/CD28, but just already known T cell subset and activation markers were analyzed (Szabo et al., 2019). However, it was found that activated T cells were more similar across different tissues than resting counterparts, which supports the hypothesis that reactivation mechanisms might be similar in different tissues. One of the genes described in this study, *Mx1*, which is a known IFN $\gamma$ -inducible gene, I also detected in my transcriptome analysis. However, the aim of this analysis was not to identify already known IFN $\gamma$ -inducible genes, but rather new genes, targets and pathways, which are reactivation-specific. Another study analyzed reactive SARS-CoV2 T cells from blood and lung tissue samples and they found that they could perform reverse phenotyping to identify antigen-specific and reactive T cells by *ex vivo* stimulation and identification of IFN $\gamma$  secretion (Fischer et al., 2021). Furthermore, they found that *ex vivo* stimulated T cells from the blood are similar to T cells found in the infected respiratory tract. However, they also focused on known activation markers as in another publication analyzing single-cell data from CMV reactivated CD4<sup>+</sup> T cells (Lyu et al., 2021). Another publication analyzed the influence of the cytokine milieu on T cell activation in naïve and memory T cells (Cano-Gamez et al., 2020). However, they also focused on the known activation and differentiation markers and they did not analyze differences between naïve and memory T cell activation.

Overall, most published single-cell data analyzing (re)activated T cells focus on already established markers, predominantly cytokines like IFN $\gamma$ , *Gzmb*, *Ccl3*, *Ccl4* or inhibitory receptors like PD-1 and CTLA4, but they do not look into other genes, which might be reactivation-specific. Therefore, it would be interesting to reanalyze the raw data again and compare all differentially expressed genes to the genes found in my transcriptome analysis.

### **5.7 Transcriptome and Proteome analysis**

I investigated the transcriptional and proteomic profile of reactivated effector T cells, focusing mainly on T<sub>H</sub>1 cells. Since there are limitations/challenges of current techniques to obtain sufficient numbers of CD4<sup>+</sup> T cells from tissues for extensive transcriptome analysis, I performed bulk transcriptome analysis in resting and activated naïve T cells as well as in resting and reactivated T<sub>H</sub>1 cells *in vitro* (Figure 1). The advantage of this experimental setup is that characterization and sorting of resting and (re)activated naïve and effector T cells were based on clearly defined conditions as illustrated by the gating strategy (Figure 10), thereby eliminating possible variability caused by population heterogeneity in tissues. The disadvantage of bulk transcriptomics is that a sufficient number of cells is required to perform high-quality analysis and that different cell types and gradients in this bulk cannot be identified. In addition to bulk transcriptomics, novel techniques such as single cell transcriptomics could solve these disadvantages. However, even though single cell transcriptomics is getting more sensitive and common, higher cost and relatively limited accessibility make bulk transcriptome analysis preferable (Kuksin et al., 2021). Nevertheless, the *in vitro* model of T cell priming, differentiation and reactivation with established conditions provides high level specificity of naïve, activated naïve, T<sub>H</sub>1 and reactivated T<sub>H</sub>1 cells for differential bulk transcriptome analysis. Analyzing the bulk transcriptome from different T cell stages, I showed that priming, differentiation and reactivation are transcriptionally distinct processes (Figure 14). To my knowledge, this is the first study, which specifically shows these differences as well as defines reactivation as a distinct transcriptional process from naïve T cell activation – in addition to differentiation specific differences. I defined a "reactivated T<sub>H</sub>1 cell" state through the clearly defined conditions via bulk analysis, which cannot be performed by single cell transcriptomics since there would be a wide variety of expression patterns to be found. With the clearly defined "standard" and the reactivation-specific genes identified, one can analyze the reactivation status of heterogeneous effector T cell subsets in different tissues via single-cell transcriptomics in future experiments.

In addition to transcriptome analysis, I also performed proteome analysis in reactivated T<sub>H</sub>1 cells and compared it with the transcriptome data. I detected differential protein expression between resting and reactivated T<sub>H</sub>1 cells. Interestingly, I identified 35 genes, which showed up in transcriptome as well as in proteome analysis

(Figure 33, D). There could be different reasons explaining the discrepancy between transcriptome and proteome data. First, protein synthesis is controlled by post-transcriptional modifications and upregulation at protein level takes place sometime later after upregulation on mRNA level. Second, the poor correlation could be due to the different reactivation approaches (peptide-pulsed macrophages vs anti-CD3/CD28 stimulation). For proper proteome analysis, a high amount of initial sample material was required and the former approach with reactivated T<sub>H</sub>1 cells by peptide-pulsed macrophages had limitations in this case. Therefore, T<sub>H</sub>1 cells were reactivated with anti-CD3 and anti-CD28 for six hours and protein from all cells was isolated. Another technical limitation of this experiment was that naïve T cells have very few protein and I could not isolate enough protein of naïve and activated naïve T cells to perform similar experiments to those in the transcriptome analysis. However, there are different studies available analyzing proteomics of activated and differentiated T cells. One publication analyzed data of naïve, activated naïve (24 hours) and differentiated murine CD8<sup>+</sup> T cells and T<sub>H</sub>1 cells (Howden et al., 2019). Another study analyzed proteomics and phosphoproteomics at different time points (2, 8 and 16 hours) of murine naïve T cell activation (Tan et al., 2017). However, these studies did not analyze specifically the protein expression of reactivated effector T cells. A thorough analysis comparing naïve T cell activation-specific proteins from other studies and differentially expressed proteins from my analysis could lead to the identification of proteins specific for reactivated effector T cells. In addition, there is a study analyzing proteomics of resting and activated CD4<sup>+</sup> T cells from human blood. However, the disadvantage of this experimental setup is that blood contains a mixed population of naïve and effector T cells. Therefore, it is difficult to analyze which proteins are specific for naïve or specific for effector T cells (Subbannayya et al., 2020). Furthermore, there is a study analyzing proteomics of CD4<sup>+</sup> and CD8<sup>+</sup> T cells from whole blood of Multiple Sclerosis patients (Berge et al., 2019). However, going through some genes of their list of top differentially expressed proteins in CD4<sup>+</sup> T cells, I could not see any overlaps with differentially expressed genes from my analysis.

### **5.7 Outlook**

This thesis revealed a unique signature to T<sub>H</sub>1 cell reactivation and it is a gate-opener for many follow-up projects. First, the identified genes should be analyzed not only in autoimmune models like NTN and EAE, but also in other diseases and tissues. For example, it would be interesting to analyze these genes in the tumor setting and hopefully identify targets, which might be interesting for immunotherapy. Furthermore, these genes can be analyzed via overexpression or knock-down experiments *in vitro* and *in vivo* in the already mentioned disease models to identify the molecular function and impact on the reactivation potential of effector T cells in the tissue. Furthermore, these genes can be analyzed in more detail in human T cells in blood and inflamed tissue. In addition, there are already many single-cell data of human cells available, which might be interesting to reanalyze and check for the genes I found in my transcriptome analysis. In addition, the analysis of proteome and phosphoproteome data needs more detailed bioinformatical methods and tests together with thorough comparison with published data. Targets identified by these experiments might lead to the identification of new reactivation markers and molecular pathways, which could be translated into clinical studies.

## 6. Materials and Methods

### 6.1 Materials

#### 6.1.1 Devices

Equipment	Company
BD FACS Aria	BD
Cell Culture Centrifuge	HERMLE Labortechnik GmbH
CTX Connect Real-Time System	Bio-Rad
Cytoflex S	Beckman Coulter
Gel chamber	Bio-Rad
GentleMACS	Miltenyi
Incubator	Axon Labortechnik GmbH
Laminar airflow cabinet (Biowizard Golden Line)	LMS
Light microscope CKX41SF	Olympus
Magnetic holder	Miltenyi
Microplate reader	HIDEX Sense
NanoDrop	Thermo Scientific
PowerPac Universal Power Supply	Bio-Rad
Sonifier	EpiShear, Active Motif
T100 Thermal Cycler	Bio-Rad
Table Top Centrifuge	LMS
Thermomixer	Eppendorf
UVP GelSolo	Analytika
Vortex	LMS

#### 6.1.2 Laboratory and cell culture material

Material	Company
1, 2, 5 and 10 ml syringes	BD
1.5, 2 ml microcentrifuge tubes	VWR
15 and 50 ml polypropylene tubes	Corning

5, 10, 25 ml serological pipettes	Sarstedt
6, 12, 24 and 96 well cell culture plates	Corning
70 µm cell strainer	VWR
C-tubes	Miltenyi
LS columns	Miltenyi
Neubauer chamber	Glaswarenfabrik Karl Hecht
Pipette 0.2-2 µl	Gilson
Pipette 0.5-10 µl	Gilson
Pipette 100-1000 µl	Gilson
Pipette 10-100 µl	Gilson
Pipette tips	VWR
Pipette tips	Sarstedt
Sterile filter pipette tips	Sarstedt

### 6.1.3 Buffers

Solutions	Ingredients	Volume/Concentration
cDMEM	DMEM	417 ml
	FBS	10%
	L-glutamine	6 ml
	NEAA	6 ml
	Sodium pyruvate	6 ml
	Sodium bicarbonate	6 ml
	Penicillin/Streptomycin	1%
	β-Mercaptoethanol	0.00168%
MACS Buffer	PBS (w/o Ca, Mg)	500 ml
	BSA	0.5%
	EDTA	2 mM

### 6.1.4 Solutions and materials

Solution	Company
Acetic Acid	Carl Roth

ACK LYSING BUFFER	LONZA or Gibco
Ammonium Persulfate	Sigma
BLASTICIDIN S HCL	Life Technologies
Bordetella pertussis toxin	Sigma
Bovine serum albumin	VWR
Brefeldin A	Biologend
CD4 (L3T4) MicroBeads, mouse	Miltenyi
CD4 Microbeads	Miltenyi
CFA	Thermo Fisher
Chloroform	Carl Roth
Collagenase type I	Life Technologies
Collagenase type IV	Life Technologies
Collagenase type XI	Sigma
Colloidal commasie blue	Sigma
DMEM	Life Technologies
DMSO	ITW
DNase I from bovine pancreas	AppliChem
D-PBS, Dulbecco's Phosphate Buffered Saline	Life Technologies
EDTA	Sigma
Ethanol	Carl Roth
FBS (fetal bovine serum)	Life Technologies
GelRed nucleic acid gel stain 10 000x in water	Sigma
GeneRuler 100bp Plus	Thermo Scientific
Geneticin (G418 Sulfate)10 mg	Bertin Pharma
IMJECT OVALBUMIN, HEN EGG, 5 X 20 MG	Life Technologies
Ionomycin	Life Technologies
Isoflurane	Piramel
Isopropanol	Carl Roth
L- Glutamine solution	Lonza
LymphoSep, lymphocyte separation medium	MPBio
M. Tuberculosis Des. H37 R $\alpha$	BD

MOG <sub>35-55</sub> peptide	from AG Sorokin (Münster) or Sigma
OVA <sub>323-339</sub> peptide	Invivogen
PBS, DULB (1X)+CA,+MG (CE) 500ML	Life Technologies
Penicillin/Streptomycin	Life Technologies
Pierce™ 660nm Protein Assay Reagent	ThermoFisher
PMA	Sigma
Polyacrylamide	Carl Roth
Protease inhibitor	Roche
Purified anti-mouse CD28	BioLegend
Purified anti-mouse CD3e	BioLegend
Purified anti-mouse IL-4	BioLegend
Puromycin Dihydrochlorid ≥98%, ultrapure	VWR Chemicals
Recombinant Human TGF-β1 (carrier-free)	Biolegend
Recombinant Mouse GM-CSF (carrier-free)	BioLegend
Recombinant Mouse IL-12 (p70) (carrier-free)	BioLegend
Recombinant Mouse IL-2 (carrier-free)	BioLegend
Recombinant Mouse IL-23 (carrier-free)	Biolegend
Recombinant Mouse IL-6 (carrier-free)	Biolegend
Recombinant Mouse M-CSF (carrier-free)	BioLegend
RPMI	Life Technologies
SDS	Carl Roth
Sodium Bicarbonate	Lonza
Sodium Pyruvate	Lonza
TAE Buffer (50x)	VWR
TEMED	Thermo Scientific
TRIzol	Ambion (Life Technologies)
Trypan Blue	Sigma
Trypsin-EDTA (10X)	Life Technologies
β-Mercaptoethanol	Sigma

## 6.1.5 Antibodies- murine

Target	Clone	Fluorophore	Company
7AAD		PerCP-Cy5.5	Biolegend
CD11b	M1/70	PE/Cy7	Biolegend
CD11c	N418	APC/Cy7	Biolegend
CD19	6D5	BV510	Biolegend
CD25	PC61	BV510	Biolegend
CD3	17A2	Alexa700	Biolegend
CD4	GK1.5	PE/Cy7	Biolegend
CD4	RM4-5	BV650	Biolegend
CD44	IM7	APC/Cy7	Biolegend
CD44	IM7	APC	Biolegend
CD45	30-F11	PerCP-Cy5.5	Biolegend
CD45	30-F11	FITC	Biolegend
CD62L	MEL-14	PE/Cy7	Biolegend
CD62L	MEL-14	APC/Cy7	Biolegend
CD69	H1.2F3	PE	Biolegend
CD8	53-6.7	BV510	Biolegend
CD8	53-6.7	FITC	Biolegend
CD8	53-6.7	PE/Cy7	Biolegend
F4/80	BM8	APC	Biolegend
FoxP3	150D	PE	Biolegend
Gata3	16E10A23	AlexaFluor488	Biolegend
Gr1	RB6-8C5	PE	Biolegend
IFNy	XMG1.2	PE	Biolegend
IFNy	XMG1.2	APC	Biolegend
IL-17a	TC11-18H10.1	PE	Biolegend
IL-2	JES6-5H4	PE	Biolegend
IL-4	11B11	PE	Biolegend
MHC-II	M5/114.15.2	APC/Cy7	Biolegend
Nur77	12-5965-82	PE	Biolegend

RORyt	Q31-378	AlexaFluor647	BD Biosciences
T-bet	4B10	PE	Biolegend
Zombie green		FITC	Biolegend
Zombie NIR		APC/Cy7	Biolegend
Zombie violet		BV421	Biolegend

### 6.1.6 Antibodies- human

Target	Clone	Fluorophore	Company
FOXP3	150D	PE	Biolegend
GATA3	16E10A23	AlexaFluor488	Biolegend
IFN $\gamma$	B27	PE	Biolegend
IL-17a	BL168	APC	Biolegend
IL-4	MP4-25D2	FITC	Biolegend
RORyt	Q121-559	AlexaFluor647	BD Biosciences
T-Bet	4B10	PE	Biolegend

### 6.1.7 Oligonucleotides- murine

Gene	Forward primer	Reverse primer
B-Actin	AGAGGGAAATCGTGCGTGAC	CAATAGTGATGACCTGGCCGT
Ccr4	AGATAAGGGTGTGGGACAAT CC	AACATACCAGAAAGCCAAACTG C
Clec4e	ACCAAATCGCCTGCATCC	CACTTGGGAGTTTTTGAAGCAT C
Clec7a	CATCGTCTCACCGTATTAATGC AT	CCCAGAACCATGGCCCTT
Coro6	TTCTAGCCATTATTGTGGAGGC TG	CAGTGACCAGTGGGTAGTTCTT AT
Dach2	ACTGAAAGTGGCTTTGGATAA	TTCAGACGCTTTTGCATTGTA

Edn1	AAGACTCCAAGAAAGGAAAAC CCT	CAACACGAAAAGATGCCTTGAT G
Enah	TGCCATGATGCATGCCTTAGAA	ACATCGCAAATTAGTGCTGTCC T
FoxP3	GCCTACAGTGCCCCTAGTCA	TTGAGGGAGAAGACCCCAGT
Gata3	GCAACCTCTACCCCCTGTG	CCCATTAGCGTTCCTCCTCC
Gipr	CCAAACTGGCCTTTGAAATCTT CC	CTGCACCTCTTTGTTGATGAAG C
IFN $\gamma$	TCAAGTGGCATAGATGTGGAA GAA	TGGCTCTGCAGGATTTTCATG
Il-17a	AACATGAGTCCAGGGAGAGC	GAGGTAGTCTGAGGGCCTTC
Il-2	CCTGAGCAGGATGGAGAATTA CA	TCCAGAACATGCCGCAGAG
Il-4	AGATGGATGTGCCAAACGTCC TCA	AATATGCGAAGCACCTTGAAG CC
Lyz2	GTCACCATGAAGACTCTCCTGA CT	AGTTCTGGCAAACCTCACACGT TCA
Nur77	GCACAGCTTGGGTGTTGATG	CAGACGTGACAGGCAGCTG
Pdzk1ip1	GTTCTTGGTCCTTGTTGCAATC G	CATTGAGGAGTATCTGCCATCC A
Roryt	TAGCACTGACGGCCAACCTTA	TCGGAAGGACTTGACAGACAT
Siglec5	TCATCCAACATTGCGTTGGGAT A	GTGGAGTTCAGGCTCATCCTTT T
Socs2	GCTCAGTCAAACAGGATGGTA CTGGGGAAGTATG	TCTGAATTTCCCATCTTGGTAC TCAATCCGCAGG
T-bet	CTGGAGCCCACAAGCCATTA	CCCCTTGTTGTTGGTGAGCT
TGF $\beta$ 1t	CGTCAGACATTCCGGGAAGCA	TGCCGTACAACCTCCAGTGAC

### 6.1.8 Oligonucleotides- human

Gene	Forward primer	Reverse primer
ActB	CTGGAACGGTGAAGGTGACA	AAGGGACTTCTGTAACAATG CA

CCR4	ATTGCCTCACAGACCTTCCTC	GGTGTCTGCTATATCCGTGGG
CLEC4e	TGGA CTGTCAGACCAGGTTGT C	CTCTCATGGTGGCACAGTCCT C
CLEC7a	GATTTAGAAAATTTGGATGAAG ATGG	TATCACCAGTATTACCAAGCAT A
CORO6	TGCTCATTTTCGCTGAGGGAC	AGGGTGTGCTGCGACAA
DACH2	GTGATCTCTGCAACTTCCAGC	GTCCATCAGGAACGAAGCCA
EDN1	CTACTTCTGCCACCTGGACAT C	TCACGGTCTGTTGCCTTTGTG G
ENAH	TCAAGGGTAAGGGAAACTGG	TGGCTCACAAGTGGTCCTCC
FOXP3	CACCTGGCTGGGAAAATGG	GGAGCCCTTGTCGGATGA
GATA3	TCATTAAGCCCAAGCGAAGG	GTCCCCATTGGCATTCT
GIPR	AACGGGTCCTTCGATATGTAC G	ATGGTCTCTCCAAAGTCCCC
IFN $\gamma$	TGGCTTTTCAGCTCTGCATC	CCGCTACATCTGAATGACCTG
IL-17a	CAACCGATCCACCTCACCTT	GGCACTTTGCCTCCCAGAT
IL-4	CCGAGTTGACCGTAACAGACA T	GTCCTTCTCATGGTGGCTGTA G
LYZ2	TGGGAATGGATGGCTACAGG	TGCTTCTGTCTCCAGCATTGT
PDZK1ip1	CGTCGGAAACAAGGCAGATG	TCACTGGACCTGAAACTGGC
ROR $\gamma$ t	GCAGCGCTCCAACATCTTCT	ACGTA CTGAATGGCCTCGGT
SIGLEC5	ACCGGGATCTTGGAGCTTCG	GCAACTGTGGGAGGGAGTAAA CTG
SIGLEC8	AGACGCCAGGAAGAGGGATAA	AGTTCCAAGGAGGGTCTGTCA
SOCS2	GAGCTCGGTCAGACAGGATG	AGTTGGTCCAGCTGATGTTTT
T-Bet	CCCCTTGGTGTGGACTGAGA	ACGCGCCTCCTCTTAGAGTC

### 6.1.9 Kits

Product	Company
CD4 <sup>+</sup> naïve T cell isolation kit, human II	Miltenyi
CD4 <sup>+</sup> T cell isolation Kit, murine	Miltenyi

CD45 <sup>+</sup> T cell isolation Kit, murine	Miltenyi
iScript cDNA Synthesis Kit	Bio-Rad
iTaq Universal SYBR Green Supermix	Bio-Rad
OneTaq Quick-Load 2X Master Mix	NEB
RNeasy MinElute Kit	Qiagen
True Nuclear Transcription Factor Buffer Set	Biolegend

### 6.1.10 Software

BD FACS Diva
Biorad CFX Manager
Cytexpert
Graph Pad Prism 6
GSEA/Cytoscape
Illustrator
Image J
Microsoft Office
PANTHER
R studio

## 6.2 Mice

**6.2.1 Nur77<sup>GFP</sup> mouse: C57BL/6-Tg(Nr4a1-EGFP/cre)820Khog/J (Jackson/Charles River 016617)**

In 2011, Moran *et. al* published the Nur77<sup>GFP</sup> mouse model, which were used in this thesis. They constructed a 170 kb C57BL/6J mouse artificial bacterial chromosome (BAC) RP24-366J14 containing the entire Nr4a1 locus (Nur77). They inserted an eGFP-hCre fusion protein cDNA sequence (enhanced green fluorescent protein, fused with a codon-optimized "humanized" Cre to improve the translation efficiency in eukaryotic cells), a frt-flanked neocassette and a TGA-STOP Codons into the ATG start site of the Nr4a1 gene on the RP24-366J14-BAC by homologous recombination/BAC recombination. The frt-flanked neo was removed during the recombination of BAC by arabinose treatment. A ~ 135 kb fragment from the modified

BAC targeting the Nr4a1 locus and 60 kb sequence flanking each side of the Nr4a1 locus was purified and then microinjected into the resulting C57BL/6J embryos. Only 77GFP-BAC transgenic founder mice were bred with C57BL/6NCr mice (Moran et al., 2011). Nur77<sup>GFP</sup> mice were used as a reporter system for the identification of TCR activated T cells. Nur77 is a gene early upregulated during TCR activation and correlates with the activation strength of the TCR (Au-Yeung et al., 2014; Moran et al., 2011).

#### 6.2.2 OT-II mouse: *B6.Cg-Tg(TcraTcrb)425Cbn/J* (Jackson/Charles River 004194)

OT-II mice were initially generated and published by Barnden *et. al* in 1998. They generated a transgene by co-injection of two constructs obtained by separate cloning of PCR amplified cDNAs. The mouse alpha chain and beta chain T cell receptor subunits, which were expressed by a CD4<sup>+</sup> T cell hybridoma, were generated in a T cell receptor expression vector. The reconstituted receptor pairs with the CD4 co-receptor and is specific for chicken ovalbumin residues 323-339 associated with H2-Ab1 (I-Ab) (Barnden, Allison, Heath, & Carbone, 1998). Therefore, OT-II mice generate ovalbumin-specific (Ova<sub>323-339</sub> peptide-specific) CD4<sup>+</sup> T cells. This antigen-specific model was used as a standard transgenic antigen-specific mouse models, because antigen-specific model are able to generate enough T cells, which can be activated with a specific antigen.

Nur77<sup>GFP</sup> mice were crossed with OT-II mice (OT-II/Nur77<sup>GFP</sup>). Both mouse strains were purchased from Charles River. They were bred and maintained at Weyertal and Nuclear Medicine animal facilities at the University Hospital Cologne. All animal experiments were approved by the local animal care committee. Female and male mice between 8 and 16 weeks were used for experiments.

### 6.3 Genotyping

To ensure the desired transmittance of transgenes after crossbreeding, genotyping was performed using PCR amplification. Ear biopsies were taken from each mouse to be genotyped to extract genomic DNA. The biopsies were digested overnight in 200 µl SDS-Lysis buffer with Proteinase K (0.5 mg/ml) at 800 rpm, 55 °C. After centrifugation (15min, max. speed), 200 µl supernatant were transferred and mixed with Isopropanol

(v/v), inverted multiple times and centrifuged for 1 minute at max. speed at room temperature (RT). The supernatant was discarded and the pellet was washed in 600  $\mu$ l 70% Ethanol, inverted multiple times and centrifuged again for 1 minute at max. speed at RT. The supernatant was discarded and the pellet was dried at 37 °C for 30 minutes before it was resuspended in 60  $\mu$ l ddH<sub>2</sub>O. The DNA content was measured photometrically with the NanoDrop. The genotyping PCR assays for IFN $\gamma$ <sup>YFP</sup>, Nur77<sup>GFP</sup> and OT-II mouse strains were performed using a common forward and reverse primers (Sigma) to obtain PCR products of different sizes depending on the genotype. Primer sequences and genotyping PCR protocols were obtained and adapted from The Jackson Laboratories (Nur77<sup>GFP</sup>: <https://www.jax.org/strain/016617>; OT-II: <https://www.jax.org/strain/004194>).

<b>Nur77</b>	Nur77-tg-FW	GAC ACC CGC TTC CTT GTC T
	Nur77-tg-RV	CTG AAC TTG TGG CCG TTT AC
	Nur77-ctrl-FW	AGT GGC CTC TTC CAG AAA TG TG
		AGT GGC CTC TTC CAG AAA TG
		AGT GGC CTC TTC CAG AAA TG
Nur77-ctrl-RV	TGC GAC TGT GTC TGA TTT CC	
<b>OT-II</b>	OT-II-tg-FW	AAA GGG AGA AAA AGC TCT CC
	OT-II-tg-RV	ACA CAG CAG GTT CTG GGT TC
	OT-II-ctrl-FW	CTA GGC CAC AGA ATT GAA AGA TCT
	OT-II-ctrl-RV	GTA GGT GGA AAT TCT AGC ATC ATC C

PCR were performed with OneTaq Quick-Load 2X Master Mix (NEB) according to manufactures' recommendation:

<b>Component</b>	<b>25 <math>\mu</math>l reaction</b>
10 $\mu$ M Forward Primer	0.5 $\mu$ l
10 $\mu$ M Reverse Primer	0.5 $\mu$ l
Template DNA	1 $\mu$ l
OneTaq Quick-Load 2x Master Mix	12.5 $\mu$ l
Nuclease-free water	to 25 $\mu$ l

Cycling conditions:

1	94 °C	30 sec
2	94 °C	20 sec
3	65 °C	15 sec
4	68 °C	10 sec
		go to 2 and repeat 10x
5	94 °C	15 sec
6	60°C	15 sec
7	72 °C	10 sec
		go to 5 and repeat 28x
8	72 °C	5 min
9	10 °C	∞

1.5% Agarose gel in TEA buffer was prepared and mixed with 1:10.000 with GelRed nucleic acid gel stain. Samples were run for ~30 minutes at 100-120 V.

## 6.4 Cell culture

### 6.4.1 Murine CD4<sup>+</sup> T cell isolation and T<sub>H</sub>1 differentiation

OT-II/Nur77<sup>GFP</sup> mice were terminated by cervical dislocation and spleens were dissected. Spleens were homogenized into single cell suspensions by mashing through a 70 µm cell strainer and washed with magnetic activated cell sorting (MACS) buffer. Before T cell preparation, each well of a 24-well plate was pre-coated with 1mg/ml anti-CD3e in 250 µl PBS and incubated for 2 hours at 37°C. CD4<sup>+</sup> T cell isolation was performed according to the CD4<sup>+</sup> T cell isolation kit from Miltenyi. Briefly, the single cell suspension was centrifuged at 500 g for 5 minutes, the pellet was resuspended in 500 µl MACS buffer and cells were magnetically labeled with 20 µl CD4 microbeads. After 20 minutes incubation at 4°C, the cell suspension was washed with 20 ml MACS buffer and centrifuged at 500 g for 5 minutes at 4°C. During centrifugation a LS column was placed into a magnetic field and moisturized with 5ml MACS buffer. The cells were filtered through a 70 µm cell strainer to remove residual

tissue, applied onto the column and washed with 8 ml MACS buffer to remove unlabeled cells. The column was removed from the magnetic field and the CD4<sup>+</sup> labeled cells were collected by pressing two times 5 ml MACS buffer through the LS column. Cells were counted with a Neubauer chamber using trypan blue.  $1 \times 10^6$  cells were resuspended in 1 ml cDMEM with 10  $\mu\text{g/ml}$  anti-CD28, 0.5  $\mu\text{g/ml}$  anti-IL4, 2 ng/ml IL-12 and 10 ng/ml IL2. Before adding the cell suspension into the wells, anti-CD3e solution was removed from the plate and rinsed three times with PBS. After 3 days the cells were split into two new wells in cDMEM with 10 ng/ml IL2. The cells were ready for downstream applications after 5 days of culture.

#### 6.4.2 Murine T<sub>H2</sub>, T<sub>H17</sub> and T<sub>reg</sub> differentiation

T cells were isolated as mentioned above.  $1 \times 10^6$  cells were resuspended in 1 ml cDMEM with 10  $\mu\text{g/ml}$  anti-CD28, 50 ng/ml IL4 and 20 ng/ml IL2 for T<sub>H2</sub> differentiation.  $1 \times 10^6$  cells were resuspended in 1 ml cDMEM with 5  $\mu\text{g/ml}$  anti-CD28, 10  $\mu\text{g/ml}$  anti-IL4, 10  $\mu\text{g/ml}$  anti-IFN $\gamma$ , 50 ng/ml IL6, 5 ng/ml IL23 and 1 ng/ml human TGF- $\beta$ 1 for T<sub>H17</sub> differentiation.  $1 \times 10^6$  cells were resuspended in 1 ml cDMEM with 3  $\mu\text{g/ml}$  anti-CD28, 20 ng/ml IL2 and 5 ng/ml hTGF $\beta$ 1. Before adding the cell suspension into the wells, anti-CD3e solution was removed from the plate and rinsed three times with PBS. After 3 days the cells were split into two new wells in cDMEM with according cytokines. The cells were ready for downstream applications at day 5.

#### 6.4.3 Murine bone marrow derived macrophage isolation and differentiation

Macrophages are professional APCs, beside DCs, B cells and epithelial cells, which were used for effector T cell reactivation in this thesis (Roche & Furuta, 2015). They take up and present antigen and are able to efficiently reactivate effector T cells. Therefore, this *in vitro* assay was chosen as a model for *in vivo* reactivation of CD4<sup>+</sup> effector T cells. In detail, OT-II/Nur77<sup>GFP</sup> mice were sacrificed by cervical dislocation and both femur and tibia were dissected. Connective and muscle tissue were removed and the bones were transferred into a 60 mm dish containing 70% ethanol for 30 seconds to dehydrate remaining tissue. Femur and tibia were flushed with DMEM + 10% FBS + 1% P/S (Penicillin/Streptomycin) by a 5 ml syringe with a 23-gauge needle. The cells were resuspended and centrifuged in 10 ml DMEM + 10% FBS + 1% P/S for 10 minutes at 400 g at 4°C. For erythrocyte lysis the pellet was resuspended in 1 ml

ACK buffer and incubated for 5 min at RT. The cells were washed in 10 ml DMEM + 10% FBS + 1% P/S and centrifuged again for 5 min at 400 g.  $3 \times 10^6$  cells were seeded in 1 ml DMEM + 10% FBS + 1% P/S with 20 ng/ml Macrophage Colony-Stimulating Factor (M-CSF) into a well of a 24 well plate. On day 3 and day 5 the medium was replaced and the macrophages were ready for downstream applications at day 7. The generated bone marrow derived macrophages are CD11b<sup>+</sup> and F4/80<sup>+</sup> (Toda, Yamauchi, Kadowaki, & Ueki, 2021).

#### *6.4.4 Co-culture: T cell stimulation by macrophages*

After macrophage and T cell differentiation, a co-culture assay was performed to reactivate T<sub>H</sub>1 cells and the other helper T cell subpopulations. First macrophages were pulsed in 500 µl cDMEM with 10 µg/ml Ova<sub>323-339</sub> peptide and incubated for 30-60 minutes at 37°C. In the meantime, differentiated T<sub>H</sub> cells were counted and resuspended at  $2 \times 10^6$ /ml in cDMEM. 500 µl T cell suspension was added to the pre-pulsed macrophages and incubated for 6 hours at 37°C in the 5% CO<sub>2</sub> incubator.

#### *6.4.5 T cell stimulation by PMA/Ionomycin*

T cells were counted with a Neubauer chamber and  $1 \times 10^6$  cells were mixed with 1 ml cDMEM + 50 ng/ml PMA + 1 µg/ml Ionomycin and incubated for 4 hours in the 5% CO<sub>2</sub> incubator.

#### *6.4.6 Human naïve CD4<sup>+</sup> T cell isolation and T<sub>H</sub>1 differentiation*

PBMCs were isolated from healthy human blood samples with LymphoSep (lymphocyte separation medium, MPbio), which has a density of 1.077 g/ml, according to manufacturer's instruction. Briefly, around 15 ml heparinized blood was mixed 1:1 with PBS and carefully layered over 20 ml of Lymphosep cell separation medium (RT) in a 50 ml centrifuge tube, creating a sharp blood-Lymphosep interphase. The tube was centrifuged at 800 g for 30-40 minutes at RT. Centrifugation sediments erythrocytes and polynuclear leukocytes and band mononuclear lymphocytes above the Lymphosep. The top layer of clear plasma to within 1 cm above the lymphocyte layer was removed. The lymphocyte layer was aspirated and transferred to a 50 ml centrifuge tube. An equal volume of PBS was added to the lymphocyte layer and centrifuged for 10 minutes at 400 g at RT. The pellet was washed and the cells were

further processed to CD4<sup>+</sup> T cell isolation using naïve T cell isolation kit, human IL (Miltenyi). Subsequently, 1x10<sup>6</sup> cells were resuspended in 1 ml cDMEM and differentiated with 10 µg/ml anti-CD3, 10 µg/ml anti-CD28, 1 µg/ml anti-IL4, 10 ng/ml IL-12 and 10 ng/ml IL2 for T<sub>H</sub>1 differentiation. Before adding the cell suspension into the wells, anti-CD3e solution was incubated for 2 hours at 37°C, removed from the plate and rinsed three times with PBS. After 4 days the medium was changed with according cytokines. The cells were ready for downstream applications after 7 days. Human T cells were stimulated with PMA/Ionomycin.

### **6.5 Flow cytometry**

Flow cytometry is the standard method to analyze physical properties of a large number of cells on a single cell level. Antibodies conjugated to specific fluorophores can be used to detect surface antigens or intracellular structures. Furthermore, the expression of intracellular fluorescent reporter proteins, such as GFP, can be measured. During flow cytometric analysis the cells are separated in a capillary by a fluidic stream. Single cells separately pass the light path of an excitation laser beam and the emitted light of the coupled fluorophores and scattered incident light are detected in photomultiplier tubes (PMTs) amplifying the signal. The scattered incident light provides information about the cell size (axial light scattering, forward scatter) and granularity (perpendicular light scattering, side scatter).

#### *6.5.1 Surface and intracellular staining*

Live cells were determined by Zombie violet (1:500, Biolegend) and surface staining was performed in a 1:200 dilution in a total volume of 100 µl PBS with 1:1000 Brefeldin incubated for 20 min at 4°C in the dark. The cells were washed twice and for intracellular staining the True Nuclear Transcription Factor Buffer Set (Biolegend) was used. Briefly cells were fixed in 200 µl in True Nuclear Fix Buffer over night at 4°C or at least 1-2h in the dark at RT. Fixed cells were washed with 500 µl 1x Perm Buffer twice and the cells were intracellularly stained 1:50 in 1x Perm Buffer for at least 45 min at RT. Samples were measured at the Cytoflex S (Beckman Coulter). Files from flow cytometry measurements were analyzed with CytExpert (Version 2.3, Beckman Coulter).

### *6.5.2 Fluorescence activated cell sorting (FACS)*

FACS allows to simultaneously collect data and sort a biological sample, which can be performed in specific cell sorter systems. The principle is similar to flow cytometry, just that the analyzed cells can be sorted into different tubes. A vibrating mechanism causes the stream of cells to break into individual droplets so that there is just one cell per droplet. As in flow cytometry, just before the stream breaks into droplets, the cells pass the light path of an excitation laser beam and the emitted light of the coupled fluorophores and scattered incident light are detected. An electrical charging ring is placed at the point where the stream breaks into droplets and the charged droplet containing the cell of interest is directed through an electrostatic deflection system into the designated collection tube.

Cell sorting was performed with BD FACS Aria and Sony MA900 using a 100  $\mu\text{m}$  nozzle at the Laboratory of Experimental Immunology, Institute of Virology (Kleins Lab, Cologne) and the Department of Pathology (Hillmers Lab, Cologne). To exclude dead cells, cellular debris, and doublets from the sorted population, a pre-gating strategy of the scattered light (FSC and SSC) was performed as a pre-requisite to every sort. Live cells were determined by 7AAD (1:50, Biolegend) and surface staining was performed in a 1:200 dilution in a total volume of 100  $\mu\text{l}$  PBS incubated for 20 min at 4°C in the dark. After staining cells were washed twice and resuspended a  $1 \times 10^7$  cells/ml in PBS and sorted into a 1.5 ml tube containing PBS. After sorting, the cells were centrifuged at 500 g for 5 minutes, up to  $5 \times 10^6$  cells were resuspended in 1 ml TRIzol, a monophasic solution of phenol, guanidine isothiocyanate and other components permitting the isolation of total RNA, and stored at -80°C. We sorted around  $1 \times 10^6$  naïve/activated naïve T cells and around  $1 \times 10^5$  effector/reactivated effector T cells to isolate enough RNA for bulk sequencing.

## **6.6 Molecular biological methods**

### *6.6.1 RNA isolation for qRT-PCR*

Total RNA was extracted using TRIzol Reagent. Up to  $5 \times 10^6$  cells were resuspended in 1 ml TRIzol and 200  $\mu\text{l}$  Chloroform per ml TRIzol was added. After centrifugation for 12 min at 12000 g at 4°C, the homogenate was separated into a clear aqueous upper

phase (containing the RNA), an interphase and an organic lower layer containing DNA and protein. The aqueous phase was transferred into a new tube, RNA was precipitated with 5 µg glycogen and 110% isopropanol and centrifuged at full speed for 12 min at 4 °C. The supernatant was discarded and the pellet was washed with 1 ml 80% ethanol. After centrifugation (30 sec, full speed, RT), the ethanol was discarded, the pellet was air-dried, and resuspended in 25 µl of RNase free ddH<sub>2</sub>O. The RNA content was measured at the NanoDrop.

### 6.6.2 cDNA Synthesis (reverse transcription)

For the reverse transcription (RT) to enzymatically generate cDNA (complementary DNA) from RNA the iScript cDNA Synthesis Kit (Biorad) was used according to the manufacturer's instructions. Briefly, reverse transcription was performed using 200 ng RNA in 20 µl reaction mix containing 4 µl 5x iScript Reaction Mix, 1 µl iScript Reverse Transcriptase and RNase free ddH<sub>2</sub>O. The iScript Reaction Mix contains a pre-mixed blend of Oligo-dT- and random primers allowing high cDNA yields from all regions of the RNA transcript. Cycling conditions were as follows: Priming for 5 minutes at 25°C, reverse transcription for 20 minutes at 46°C, inactivation for 1 minute at 95°C.

### 6.6.3 qRT-PCR

Quantitative RT PCR (qRT-PCR) was performed to determine the relative copy number of a specific amplicon in cDNA. This method was used for the verification of RNAseq results. Briefly, a SYBR Green based assay (iTaQ Universal SYBR Green Supermix, Bio-Rad) was performed in triplicates on a CFX Connect Real Time System (Bio-Rad) in a 20 µl reaction volume (10 µl of 2x iTaq Universal SYBR Green Supermix, 0.5 µM forward primer, 0.5 µM reverse primer and 1 µl (=10ng) cDNA in ddH<sub>2</sub>O. SYBR green fluoresces upon intercalation into double-stranded DNA. The fluorescence intensity was measured after each PCR amplification cycle and was used to quantitate the amount of template DNA. Cycling conditions were as follows:

1	95 °C	30 sec
2	95 °C	5 sec
3	60 °C	30 sec
4		go to 2 and repeat 40x
5	10 °C	∞

### **6.7 Next-generation sequencing/RNA sequencing**

Next-generation sequencing (NGS) is a massively parallel sequencing technology that offers ultra-high throughput, scalability, and speed. NGS-based RNA sequencing (RNAseq) allows measuring gene expression patterns across the whole transcriptome. First, the mRNA is converted into cDNA fragments, to a so-called cDNA library. Adapters are added to each end of the fragments, like the amplification element and the primary sequencing site, which permit sequencing. The cDNA library is analyzed by NGS, producing short sequences, which correspond to either one or both ends of the fragment. The depth to which the library is sequenced varies depending on techniques, which the output data will be used for. The sequencing often follows either single-read which is faster and cheaper or paired-end sequencing methods which sequences from both ends, and are therefore more accurate, but also more expensive and time-consuming.

#### *6.7.1 RNA isolation for RNA sequencing*

TRizol-sorted cells were thawed on ice. 200  $\mu$ L Chloroform per ml TRizol were added to the suspension and mixed vigorously for 15 seconds. Further, the suspension was centrifuged for 12 minutes at 12000g at 4°C. After centrifugation for 12 min at 12000 g at 4°C, the homogenate was separated into a clear aqueous upper phase (containing the RNA), an interphase and an organic lower layer containing DNA and protein. The aqueous phase was carefully transferred to a new, clean tube. The same volume of RNA quality 70% ethanol was added to the aqueous phase and the suspension was mixed thoroughly. The suspension was transferred to an RNeasy MinElute spin column and centrifuged for 30 seconds at 8000 g at RT. After discarding the flow-through the column was transferred to a new clean tube. 500 $\mu$ L RPE Buffer (provided by MiniElute Kit) was added and again the tube was centrifuged for 30 seconds at 8000 g at RT. The flow-through was discarded and 500  $\mu$ L of RNA quality 80% ethanol was added to the column. The tube was centrifuged for 2 minutes at 8000 g at RT, the flow-through was discarded and the column transferred to a new tube. The tube was centrifuged with an open lid for 5 minutes at maximum speed to dry the column completely. Afterwards the column was transferred to a 1.5ml collection tube, 14  $\mu$ l RNase-free water was added directly to the column membrane and centrifuged for 1 minute at full speed at RT. Afterwards the RNA was stored at -80°C for further downstream analysis.

### 6.7.2 QC and RNA sequencing

RNA quality measurements, library preparation and sequencing was performed at the Cologne Center for Genomics (CCG) NGS platform (Cologne). RNA quality was measured with the TapeStation System (Agilent) and the RNA integrity number (RIN) was around 9 for each sample indicating good quality. At least 10 ng of total RNA was needed for robust RNA sequencing. RNA preparation was performed with the TruSeq Stranded RNA Kit (Illumina). During that procedure cytoplasmic ribosomal RNA (rRNA) is depleted by magnetically capturing rRNA species, leaving p. the desired rRNA-depleted, mRNA enriched RNA in solution. During library preparation, which was performed on a poly-A based method, adapter sequences are added to the cDNA fragments. Paired-end sequencing was performed with the NovaSeq Illumina System.

### 6.7.3 RNAseq analysis

FASTQ files were analyzed. The sequences were aligned with STAR to the mm10 (mus musculus assembly 10) genome. Further reads were count with HTSeq and differential gene expression analysis was performed with DESeq2 via RStudio. Gene ontology analysis was performed with GSEA/Cytoscape and PANTHER. In addition, RNAseq analysis was also performed via Kallisto/Sleuth pipeline.

## **6.8 Proteome- and Phosphoproteome analysis**

Proteome analysis is a quantitative mass spectrometry (MS) analysis of proteins and peptides of a cell or an organism. Sample processing starts with cell lysis, fractionation, and digestion of the proteins. The resulting peptide mixture is separated by reversed phase chromatography using nano-UHPLC system. As the peptides elute from the column they are ionized and detected by a Quadrupole Orbitrap hybrid mass spectrometer. In data-dependent acquisition mode masses of intact peptides are detected by MS scans which are followed by peptide fragmentation to determine the sequence and post-translational modifications of the peptides.

For proteome and phosphoproteome analysis around  $25 \times 10^6$  *in vitro* differentiated T<sub>H</sub>1 cells were either directly used for protein isolation or reactivated with 10 µg/ml plate-bound anti-CD3/ and 10 µg/ml soluble anti-CD28 for 6 hours and then used for protein isolation.

### 6.8.1 Protein isolation

Protein isolation was performed according to a standard protocol provided by the proteomics facility, CECAD, cologne. In addition, chemicals were provided by the proteomics facility, CECAD, cologne. Cells were centrifuged for 5 minutes, 500 g, 4 °C and the pellet was lysed in 500 µl Urea buffer (8 M Urea in 50 mM Triethylammoniumbicarbonate (TEAB)). Chromatin was degraded using a sonifier (EpiShear, Active Motif) 3-6 x 30 seconds, amplitude 35 %, with 30 second break in between sonication steps. Mixture was then centrifuged for 15 minutes at ~20000 g to remove cell debris. Protein concentration was measured by a Bradford assay at 660nm with a microplate reader (HIDEX sense). 1 mg protein was transferred to a new tube, dithiothreitol (DTT) was added to a final concentration of 5mM, vortexed and incubated for 1 hour at 25 °C. Then chloroacetamide (CAA) was added to a final concentration of 40mM and incubated at RT in the dark for 30 minutes. Lysyl Endopeptidase (Lys-C, 0.5 µg/µl) was added at an enzyme: substrate ratio of 1/75 and incubated at 25 °C for 4 hours. The sample was further diluted with 50 mM TEAB to achieve a final Urea concentration less than 2 M. Finally trypsin (1 µg/µl) was added at an enzyme: substrate ratio of 1/75 and incubated at 25 °C overnight.

### 6.8.2 Proteome analysis

Isolated protein samples were further analyzed by the proteomics facility, CECAD, cologne. Data analysis was performed with Perseus software 1.6.1.1.

## 6.9 *In vivo* experiments: Nephrotoxic nephritis (NTN)

The so-called "passive nephrotoxic nephritis model" is a model of a rapid progressive GN (RPGN) with crescent formation. Nur77<sup>GFP</sup> mice were used for these experiments. This model involves *i.p./i.v.* (*intraperitoneal/intravenous*) injection of a heterologous serum or antibody obtained from sheep that have been immunized against rabbit glomeruli. A maximum of 0.1 ml serum/10 g body weight was administered *i.p.* or 0.05 ml serum/10 g body weight was administered *i.v.* once (the concentration of the serum varies from batch to batch). The effectiveness of the serum is analyzed using the albumin-creatinine quotient in the urine. Antibodies are deposited on the glomerular basement membrane and passive damage to the podocytes occurs. After 3 days a

nephritic disease develops with the formation of glomerular crescents in 20–34% of the glomeruli as well as podocyte loss and segmental parietal and mesangial cell proliferation. The course of the disease was assessed by collecting spontaneous urine at day 5 and day 10 and determining the albumin/creatinine ratio. Mice were terminated at day 10 after serum injection.

#### 6.9.1 Colloidal coomassie blue staining

	Stacking 2 GELS		Resolving 2 GELS
Gel Percentage (%)	4	Gel Percentage (%)	10
30% Polyacrylamide/Bis(mL)	1.36	30% Polyacrylamide/Bis(mL)	3.33
1 M Tris (pH6.8) (mL)	1	1.5 M Tris (pH6.8) (mL)	2.5
10% SDS (mL)	0.08	10% SDS (mL)	0.1
10% APS Ammonium Persulfate (mL)	0.08	10% APS Ammonium Persulfate (mL)	0.1
TEMED (mL)	0.008	TEMED (mL)	0.004
H <sub>2</sub> O (mL)	5.44	H <sub>2</sub> O (mL)	3.966
Total volume (mL)	8	Total volume (mL)	10

SDS Gel was prepared according to the table above. 1  $\mu$ l urine was mixed with 9  $\mu$ l ddH<sub>2</sub>O and 10  $\mu$ l 2x loading dye. The mixture was incubated for 5 minutes at 95°C and loaded onto an SDS Gel. The gel was run for around 30 minutes to 1 hour at 60-80 V for stacking and then for another 1-2 hours at 100-120 V for separation of the proteins. The gel was fixed afterwards in fixing solution (250 ml isopropanol and 100 ml acetic acid filled up to 1 l with ddH<sub>2</sub>O) at RT for 30 minutes. Afterwards the gel was washed 2 times with VE water. 30 ml colloidal coomassie blue solution was mixed with 6 ml Methanol and shook over night at RT. Finally, the gel was washed for 6-8 hours with VE water and picture was taken.

#### 6.9.2 CD45 cell isolation from healthy and NTN kidneys

NTN mice were terminated 10 days after NTN induction and perfusion was performed (flush heart with 10 ml PBS). Both kidneys were isolated and stored on ice in PBS. Kidneys were cut into small pieces and transferred to C-tubes (Miltenyi) with 3 ml

cDMEM. 2 ml digest medium (cDMEM + 5  $\mu$ l DNase I + 25  $\mu$ l Collagenase IV) were added to the mix and incubated for 45 minutes at 37°C in water bath. Afterwards C-tubes were put on gentleMACS and program “mSpleen 02.01. C Tube” and program “mLung 02.01. C Tube” were used to dissociate the kidneys further. The mixture was filtered through a 70  $\mu$ m cell strainer and washed with MACS buffer. Cells were centrifuged for 5 minutes at 500 g. The pellet was resuspended in 500  $\mu$ l MACS buffer and 20  $\mu$ l CD45 beads (Miltenyi) was added. Cells were incubated for 20 minutes on ice, washed with 20 ml MACS buffer and centrifuged for 5 minutes at 500 g. During centrifugation a LS column was placed into a magnetic field and moisturized with 5 ml MACS buffer. The cells were filtered through a 70  $\mu$ m cell strainer to remove residual tissue, applied onto the column and washed with 8 ml MACS buffer to remove unlabeled cells. The column was removed from the magnetic field and the CD45<sup>+</sup> labeled cells were collected by pressing two times 5 ml MACS buffer through the LS column. Cells were ready for downstream analysis (flow cytometry or sorting).

### **6.10 *In vivo* experiments: Experimental autoimmune encephalomyelitis (EAE)**

Furthermore, an autoimmune model, that corresponds to human multiple sclerosis (EAE), was used to analyze reactivated CD4<sup>+</sup>T cells more precisely *in vivo*. 100 mg M. Tuberculosis was mixed with 1 ml CFA. On day 0, Nur77<sup>GFP</sup> mice were treated s.c. in the hip area with 200  $\mu$ g MOG<sub>35-55</sub> peptide emulsified with the CFA/M. Tuberculosis mix at a 1:1 ratio. In total 100  $\mu$ l of the CFA/peptide mix was injected on the left and right side of the spine, thus 100  $\mu$ g MOG<sub>35-55</sub> peptide was injected per mouse. In addition, mice were administered 200 ng of PTX i.p. in 50  $\mu$ l PBS on day 0 and 2. Between day 9 and 14 mice develop signs of paralysis. Mice were terminated at day 14, when tail paralysis occurred and first signs of hind limb paresis were visible.

#### **6.10.1 *Single cell isolation from spinal cord of EAE induced mice***

Mice were terminated and perfusion was performed. The heart was flushed with 10 ml PBS. Afterwards brain and spinal cord were isolated. The spinal cord was isolated by flushing the spine with a 23 G needle and 10 ml PBS into a 60 mm dish. 9 ml percoll was mixed with 1ml 10x PBS or HBSS to generate isotonic percoll (SIP) and 70% SIP solution was prepared. Spinal cord was mashed with 3 ml PBS in a 5 ml pistil tube.

The pistil tube was filled up to 7 ml with PBS. To the 7 ml spinal cord mix 3 ml SIP was added to generate 30% SIP. Slowly the 30% SIP/spinal cord mix was layered on top of 2 ml 70% SIP in a 15 ml falcon tube. The mix was centrifuged at 500 g for 30 min at RT without break. Around 2ml of the interphase was collected and washed with 10 ml PBS. Cells were centrifuged at 500 g for 5 minutes and were ready for downstream analysis (flow cytometry or sorting). I sorted at least 20.000 Nur77<sup>GFP-</sup> and 1000-3000 Nur77<sup>GFP+</sup> CD4<sup>+</sup> T cells from the brain and spinal cord of EAE induced mice and performed qRT-PCR.

### **6.11 Statistical analysis**

T-test analysis was performed using GraphPad Prims 6 Software. Results were given as mean +/- SD. \* p<0.05; \*\* p<0.01, \*\*\* p<0.001

## 7. References

- 't Hart, B. A., Gran, B., & Weissert, R. (2011). EAE: imperfect but useful models of multiple sclerosis. *Trends Mol Med*, 17(3), 119-125. doi:10.1016/j.molmed.2010.11.006
- Accogli, T., Bruchard, M., & Végran, F. (2021). Modulation of CD4 T Cell Response According to Tumor Cytokine Microenvironment. *Cancers (Basel)*, 13(3). doi:10.3390/cancers13030373
- Agata, Y., Kawasaki, A., Nishimura, H., Ishida, Y., Tsubata, T., Yagita, H., & Honjo, T. (1996). Expression of the PD-1 antigen on the surface of stimulated mouse T and B lymphocytes. *Int Immunol*, 8(5), 765-772. doi:10.1093/intimm/8.5.765
- Almeida, L., Lochner, M., Berod, L., & Sparwasser, T. (2016). Metabolic pathways in T cell activation and lineage differentiation. *Semin Immunol*, 28(5), 514-524. doi:10.1016/j.smim.2016.10.009
- Angata, T., Hingorani, R., Varki, N. M., & Varki, A. (2001). Cloning and characterization of a novel mouse Siglec, mSiglec-F: differential evolution of the mouse and human (CD33) Siglec-3-related gene clusters. *J Biol Chem*, 276(48), 45128-45136. doi:10.1074/jbc.M108573200
- Ashouri, J. F., & Weiss, A. (2017). Endogenous Nur77 Is a Specific Indicator of Antigen Receptor Signaling in Human T and B Cells. *J Immunol*, 198(2), 657-668. doi:10.4049/jimmunol.1601301
- Asseman, C., Mauze, S., Leach, M. W., Coffman, R. L., & Powrie, F. (1999). An essential role for interleukin 10 in the function of regulatory T cells that inhibit intestinal inflammation. *J Exp Med*, 190(7), 995-1004. doi:10.1084/jem.190.7.995
- Au-Yeung, B. B., Zikherman, J., Mueller, J. L., Ashouri, J. F., Matloubian, M., Cheng, D. A., . . . Weiss, A. (2014). A sharp T-cell antigen receptor signaling threshold for T-cell proliferation. *Proc Natl Acad Sci U S A*, 111(35), E3679-3688. doi:10.1073/pnas.1413726111
- Azcutia, V., Bassil, R., Herter, J. M., Engelbertsen, D., Newton, G., Autio, A., . . . Luscinskas, F. W. (2017). Defects in CD4+ T cell LFA-1 integrin-dependent adhesion and proliferation protect Cd47-/- mice from EAE. *J Leukoc Biol*, 101(2), 493-505. doi:10.1189/jlb.3A1215-546RR

- Baatar, D., Olkhanud, P., Sumitomo, K., Taub, D., Gress, R., & Biragyn, A. (2007). Human peripheral blood T regulatory cells (Tregs), functionally primed CCR4+ Tregs and unprimed CCR4- Tregs, regulate effector T cells using FasL. *J Immunol*, *178*(8), 4891-4900. doi:10.4049/jimmunol.178.8.4891
- Bajnok, A., Ivanova, M., Rigó, J., & Toldi, G. (2017). The Distribution of Activation Markers and Selectins on Peripheral T Lymphocytes in Preeclampsia. *Mediators Inflamm*, *2017*, 8045161. doi:10.1155/2017/8045161
- Barnden, M. J., Allison, J., Heath, W. R., & Carbone, F. R. (1998). Defective TCR expression in transgenic mice constructed using cDNA-based alpha- and beta-chain genes under the control of heterologous regulatory elements. *Immunol Cell Biol*, *76*(1), 34-40. doi:10.1046/j.1440-1711.1998.00709.x
- Becattini, S., Latorre, D., Mele, F., Foglierini, M., De Gregorio, C., Cassotta, A., . . . Sallusto, F. (2015). T cell immunity. Functional heterogeneity of human memory CD4<sup>+</sup> T cell clones primed by pathogens or vaccines. *Science*, *347*(6220), 400-406. doi:10.1126/science.1260668
- Bending, D., Prieto Martín, P., Paduraru, A., Ducker, C., Marzaganov, E., Laviron, M., . . . Ono, M. (2018). A timer for analyzing temporally dynamic changes in transcription during differentiation in vivo. *J Cell Biol*, *217*(8), 2931-2950. doi:10.1083/jcb.201711048
- Berge, T., Eriksson, A., Brorson, I. S., Høgestøl, E. A., Berg-Hansen, P., Døskeland, A., . . . Berven, F. (2019). Quantitative proteomic analyses of CD4. *Clin Proteomics*, *16*, 19. doi:10.1186/s12014-019-9241-5
- Bettelli, E., Sullivan, B., Szabo, S. J., Sobel, R. A., Glimcher, L. H., & Kuchroo, V. K. (2004). Loss of T-bet, but not STAT1, prevents the development of experimental autoimmune encephalomyelitis. *J Exp Med*, *200*(1), 79-87. doi:10.1084/jem.20031819
- Bhattacharyya, N. D., & Feng, C. G. (2020). Regulation of T Helper Cell Fate by TCR Signal Strength. *Front Immunol*, *11*, 624. doi:10.3389/fimmu.2020.00624
- Blériot, C., Chakarov, S., & Ginhoux, F. (2020). Determinants of Resident Tissue Macrophage Identity and Function. *Immunity*, *52*(6), 957-970. doi:10.1016/j.immuni.2020.05.014
- Boccasavia, V. L., Bovolenta, E. R., Villanueva, A., Borroto, A., Oeste, C. L., van Santen, H. M., . . . Alarcón, B. (2021). Antigen presentation between T cells

- drives Th17 polarization under conditions of limiting antigen. *Cell Rep*, 34(11), 108861. doi:10.1016/j.celrep.2021.108861
- Bonecchi, R., Bianchi, G., Bordignon, P. P., D'Ambrosio, D., Lang, R., Borsatti, A., . . . Sinigaglia, F. (1998). Differential expression of chemokine receptors and chemotactic responsiveness of type 1 T helper cells (Th1s) and Th2s. *J Exp Med*, 187(1), 129-134. doi:10.1084/jem.187.1.129
- Boyman, O. (2010). Bystander activation of CD4+ T cells. *Eur J Immunol*, 40(4), 936-939. doi:10.1002/eji.201040466
- Breitfeld, D., Ohl, L., Kremmer, E., Ellwart, J., Sallusto, F., Lipp, M., & Förster, R. (2000). Follicular B helper T cells express CXC chemokine receptor 5, localize to B cell follicles, and support immunoglobulin production. *J Exp Med*, 192(11), 1545-1552. doi:10.1084/jem.192.11.1545
- Brähler, S., Zinselmeyer, B. H., Raju, S., Nitschke, M., Suleiman, H., Saunders, B. T., . . . Shaw, A. S. (2018). Opposing Roles of Dendritic Cell Subsets in Experimental GN. *J Am Soc Nephrol*, 29(1), 138-154. doi:10.1681/ASN.2017030270
- Buck, M. D., O'Sullivan, D., & Pearce, E. L. (2015). T cell metabolism drives immunity. *J Exp Med*, 212(9), 1345-1360. doi:10.1084/jem.20151159
- Cano-Gamez, E., Soskic, B., Roumeliotis, T. I., So, E., Smyth, D. J., Baldrighi, M., . . . Trynka, G. (2020). Single-cell transcriptomics identifies an effectorness gradient shaping the response of CD4. *Nat Commun*, 11(1), 1801. doi:10.1038/s41467-020-15543-y
- Casciano, F., Diani, M., Altomare, A., Granucci, F., Secchiero, P., Banfi, G., & Reali, E. (2020). CCR4. *Front Immunol*, 11, 529. doi:10.3389/fimmu.2020.00529
- Chang, J. T., Wherry, E. J., & Goldrath, A. W. (2014). Molecular regulation of effector and memory T cell differentiation. *Nat Immunol*, 15(12), 1104-1115. doi:10.1038/ni.3031
- Channathodiyil, P., & Houseley, J. (2021). Glyoxal fixation facilitates transcriptome analysis after antigen staining and cell sorting by flow cytometry. *PLoS One*, 16(1), e0240769. doi:10.1371/journal.pone.0240769
- Chen, D., Xu, L., Li, X., Chu, Y., Jiang, M., Xu, B., . . . Ren, G. (2018). Enah overexpression is correlated with poor survival and aggressive phenotype in gastric cancer. *Cell Death Dis*, 9(10), 998. doi:10.1038/s41419-018-1031-x

- Chen, L., & Flies, D. B. (2013). Molecular mechanisms of T cell co-stimulation and co-inhibition. *Nat Rev Immunol*, *13*(4), 227-242. doi:10.1038/nri3405
- Cheng, Y., Ma, Z., Kim, B. H., Wu, W., Cayting, P., Boyle, A. P., . . . Consortium, m. E. (2014). Principles of regulatory information conservation between mouse and human. *Nature*, *515*(7527), 371-375. doi:10.1038/nature13985
- Cibrián, D., & Sánchez-Madrid, F. (2017). CD69: from activation marker to metabolic gatekeeper. *Eur J Immunol*, *47*(6), 946-953. doi:10.1002/eji.201646837
- Constantinescu, C. S., Farooqi, N., O'Brien, K., & Gran, B. (2011). Experimental autoimmune encephalomyelitis (EAE) as a model for multiple sclerosis (MS). *Br J Pharmacol*, *164*(4), 1079-1106. doi:10.1111/j.1476-5381.2011.01302.x
- Crocker, P. R., Paulson, J. C., & Varki, A. (2007). Siglecs and their roles in the immune system. *Nat Rev Immunol*, *7*(4), 255-266. doi:10.1038/nri2056
- Daley, D., Mani, V. R., Mohan, N., Akkad, N., Ochi, A., Heindel, D. W., . . . Miller, G. (2017). Dectin 1 activation on macrophages by galectin 9 promotes pancreatic carcinoma and peritumoral immune tolerance. *Nat Med*, *23*(5), 556-567. doi:10.1038/nm.4314
- Dardalhon, V., Awasthi, A., Kwon, H., Galileos, G., Gao, W., Sobel, R. A., . . . Kuchroo, V. K. (2008). IL-4 inhibits TGF-beta-induced Foxp3+ T cells and, together with TGF-beta, generates IL-9+ IL-10+ Foxp3(-) effector T cells. *Nat Immunol*, *9*(12), 1347-1355. doi:10.1038/ni.1677
- David, R., Ma, L., Ivetic, A., Takesono, A., Ridley, A. J., Chai, J. G., . . . Marelli-Berg, F. M. (2009). T-cell receptor- and CD28-induced Vav1 activity is required for the accumulation of primed T cells into antigenic tissue. *Blood*, *113*(16), 3696-3705. doi:10.1182/blood-2008-09-176511
- Debes, G. F., Arnold, C. N., Young, A. J., Krautwald, S., Lipp, M., Hay, J. B., & Butcher, E. C. (2005). Chemokine receptor CCR7 required for T lymphocyte exit from peripheral tissues. *Nat Immunol*, *6*(9), 889-894. doi:10.1038/ni1238
- Delgoffe, G. M., Pollizzi, K. N., Waickman, A. T., Heikamp, E., Meyers, D. J., Horton, M. R., . . . Powell, J. D. (2011). The kinase mTOR regulates the differentiation of helper T cells through the selective activation of signaling by mTORC1 and mTORC2. *Nat Immunol*, *12*(4), 295-303. doi:10.1038/ni.2005

- Desalegn, G., & Pabst, O. (2019). Inflammation triggers immediate rather than progressive changes in monocyte differentiation in the small intestine. *Nat Commun*, *10*(1), 3229. doi:10.1038/s41467-019-11148-2
- Di Genova, G., Savelyeva, N., Suchacki, A., Thirdborough, S. M., & Stevenson, F. K. (2010). Bystander stimulation of activated CD4+ T cells of unrelated specificity following a booster vaccination with tetanus toxoid. *Eur J Immunol*, *40*(4), 976-985. doi:10.1002/eji.200940017
- Di Rosa, F., Cossarizza, A., & Hayday, A. C. (2021). Corrigendum: To Ki or Not to Ki: Re-Evaluating the Use and Potentials of Ki-67 for T Cell Analysis. *Front Immunol*, *12*, 756641. doi:10.3389/fimmu.2021.756641
- Disteldorf, E. M., Krebs, C. F., Paust, H. J., Turner, J. E., Nouailles, G., Tittel, A., . . . Panzer, U. (2015). CXCL5 drives neutrophil recruitment in TH17-mediated GN. *J Am Soc Nephrol*, *26*(1), 55-66. doi:10.1681/ASN.2013101061
- Dong, F., Li, R., Wang, J., Zhang, Y., Yao, J., Jiang, S. H., . . . Bao, Z. (2021). Hypoxia-dependent expression of MAP17 coordinates the Warburg effect to tumor growth in hepatocellular carcinoma. *J Exp Clin Cancer Res*, *40*(1), 121. doi:10.1186/s13046-021-01927-5
- Dong, Y., Li, X., Zhang, L., Zhu, Q., Chen, C., Bao, J., & Chen, Y. (2019). CD4. *BMC Immunol*, *20*(1), 27. doi:10.1186/s12865-019-0309-9
- Drummond, R. A., Dambuza, I. M., Vautier, S., Taylor, J. A., Reid, D. M., Bain, C. C., . . . Brown, G. D. (2016). CD4(+) T-cell survival in the GI tract requires dectin-1 during fungal infection. *Mucosal Immunol*, *9*(2), 492-502. doi:10.1038/mi.2015.79
- Duan, Z., & Luo, Y. (2021). Targeting macrophages in cancer immunotherapy. *Signal Transduct Target Ther*, *6*(1), 127. doi:10.1038/s41392-021-00506-6
- Duhen, T., Duhen, R., Lanzavecchia, A., Sallusto, F., & Campbell, D. J. (2012). Functionally distinct subsets of human FOXP3+ Treg cells that phenotypically mirror effector Th cells. *Blood*, *119*(19), 4430-4440. doi:10.1182/blood-2011-11-392324
- Duhen, T., Geiger, R., Jarrossay, D., Lanzavecchia, A., & Sallusto, F. (2009). Production of interleukin 22 but not interleukin 17 by a subset of human skin-homing memory T cells. *Nat Immunol*, *10*(8), 857-863. doi:10.1038/ni.1767

- Dusi, S., Angiari, S., Pietronigro, E. C., Lopez, N., Angelini, G., Zenaro, E., . . . Rossi, B. (2019). LFA-1 Controls Th1 and Th17 Motility Behavior in the Inflamed Central Nervous System. *Front Immunol*, *10*, 2436. doi:10.3389/fimmu.2019.02436
- Elliot, T. A. E., Jennings, E. K., Lecky, D. A. J., Thawait, N., Flores-Langarica, A., Copland, A., . . . Bending, D. (2021). Antigen and checkpoint receptor engagement recalibrates T cell receptor signal strength. *Immunity*, *54*(11), 2481-2496.e2486. doi:10.1016/j.immuni.2021.08.020
- Eyerich, S., Eyerich, K., Pennino, D., Carbone, T., Nasorri, F., Pallotta, S., . . . Cavani, A. (2009). Th22 cells represent a distinct human T cell subset involved in epidermal immunity and remodeling. *J Clin Invest*, *119*(12), 3573-3585. doi:10.1172/JCI40202
- Feng, Y. H., & Mao, H. (2012). Expression and preliminary functional analysis of Siglec-F on mouse macrophages. *J Zhejiang Univ Sci B*, *13*(5), 386-394. doi:10.1631/jzus.B1100218
- Fischer, D. S., Ansari, M., Wagner, K. I., Jarosch, S., Huang, Y., Mayr, C. H., . . . Schober, K. (2021). Single-cell RNA sequencing reveals ex vivo signatures of SARS-CoV-2-reactive T cells through 'reverse phenotyping'. *Nat Commun*, *12*(1), 4515. doi:10.1038/s41467-021-24730-4
- Fletcher, J. M., Lalor, S. J., Sweeney, C. M., Tubridy, N., & Mills, K. H. (2010). T cells in multiple sclerosis and experimental autoimmune encephalomyelitis. *Clin Exp Immunol*, *162*(1), 1-11. doi:10.1111/j.1365-2249.2010.04143.x
- Flügel, A., Berkowicz, T., Ritter, T., Labeur, M., Jenne, D. E., Li, Z., . . . Wekerle, H. (2001). Migratory activity and functional changes of green fluorescent effector cells before and during experimental autoimmune encephalomyelitis. *Immunity*, *14*(5), 547-560. doi:10.1016/s1074-7613(01)00143-1
- García-Heredia, J. M., & Carnero, A. (2017). The cargo protein MAP17 (PDZK1IP1) regulates the immune microenvironment. *Oncotarget*, *8*(58), 98580-98597. doi:10.18632/oncotarget.21651
- Gattinoni, L., Lugli, E., Ji, Y., Pos, Z., Paulos, C. M., Quigley, M. F., . . . Restifo, N. P. (2011). A human memory T cell subset with stem cell-like properties. *Nat Med*, *17*(10), 1290-1297. doi:10.1038/nm.2446

- Gerberick, G. F., Cruse, L. W., Miller, C. M., Sikorski, E. E., & Ridder, G. M. (1997). Selective modulation of T cell memory markers CD62L and CD44 on murine draining lymph node cells following allergen and irritant treatment. *Toxicol Appl Pharmacol*, *146*(1), 1-10. doi:10.1006/taap.1997.8218
- Germain, R. N. (2002). T-cell development and the CD4-CD8 lineage decision. *Nat Rev Immunol*, *2*(5), 309-322. doi:10.1038/nri798
- Gerwien, H., Hermann, S., Zhang, X., Korpos, E., Song, J., Kopka, K., . . . Sorokin, L. (2016). Imaging matrix metalloproteinase activity in multiple sclerosis as a specific marker of leukocyte penetration of the blood-brain barrier. *Sci Transl Med*, *8*(364), 364ra152. doi:10.1126/scitranslmed.aaf8020
- Goldwich, A., Burkard, M., Olke, M., Daniel, C., Amann, K., Hugo, C., . . . Gessner, A. (2013). Podocytes are nonhematopoietic professional antigen-presenting cells. *J Am Soc Nephrol*, *24*(6), 906-916. doi:10.1681/ASN.2012020133
- Gonzalez-Gil, A., & Schnaar, R. L. (2021). Siglec Ligands. *Cells*, *10*(5). doi:10.3390/cells10051260
- Gossel, G., Hogan, T., Cownden, D., Seddon, B., & Yates, A. J. (2017). Memory CD4 T cell subsets are kinetically heterogeneous and replenished from naive T cells at high levels. *Elife*, *6*. doi:10.7554/eLife.23013
- Goverman, J. (2009). Autoimmune T cell responses in the central nervous system. *Nat Rev Immunol*, *9*(6), 393-407. doi:10.1038/nri2550
- Grywalska, E., Pasiarski, M., Gózdź, S., & Roliński, J. (2018). Immune-checkpoint inhibitors for combating T-cell dysfunction in cancer. *Onco Targets Ther*, *11*, 6505-6524. doi:10.2147/OTT.S150817
- Gubser, P. M., Bantug, G. R., Razik, L., Fischer, M., Dimeloe, S., Hoenger, G., . . . Hess, C. (2013). Rapid effector function of memory CD8+ T cells requires an immediate-early glycolytic switch. *Nat Immunol*, *14*(10), 1064-1072. doi:10.1038/ni.2687
- Guerriero, J. L. (2019). Macrophages: Their Untold Story in T Cell Activation and Function. *Int Rev Cell Mol Biol*, *342*, 73-93. doi:10.1016/bs.ircmb.2018.07.001
- Gérard, A., Cope, A. P., Kemper, C., Alon, R., & Köchl, R. (2021). LFA-1 in T cell priming, differentiation, and effector functions. *Trends Immunol*, *42*(8), 706-722. doi:10.1016/j.it.2021.06.004

- Harari, A., Dutoit, V., Cellerai, C., Bart, P. A., Du Pasquier, R. A., & Pantaleo, G. (2006). Functional signatures of protective antiviral T-cell immunity in human virus infections. *Immunol Rev*, *211*, 236-254. doi:10.1111/j.0105-2896.2006.00395.x
- Harrington, L. E., Hatton, R. D., Mangan, P. R., Turner, H., Murphy, T. L., Murphy, K. M., & Weaver, C. T. (2005). Interleukin 17-producing CD4<sup>+</sup> effector T cells develop via a lineage distinct from the T helper type 1 and 2 lineages. *Nat Immunol*, *6*(11), 1123-1132. doi:10.1038/ni1254
- Hasselmann, J. P. C., Karim, H., Khalaj, A. J., Ghosh, S., & Tiwari-Woodruff, S. K. (2017). Consistent induction of chronic experimental autoimmune encephalomyelitis in C57BL/6 mice for the longitudinal study of pathology and repair. *J Neurosci Methods*, *284*, 71-84. doi:10.1016/j.jneumeth.2017.04.003
- He, Y. D., Luo, Z. H., Yang, M., Ruan, X. X., Liu, S. Y., Wu, Z. Q., . . . Li, L. Y. (2015). Prospective validation of DACH2 as a novel biomarker for prediction of metastasis and prognosis in muscle-invasive urothelial carcinoma of the bladder. *Biochem Biophys Res Commun*, *459*(3), 416-423. doi:10.1016/j.bbrc.2015.02.119
- Hengel, R. L., Thaker, V., Pavlick, M. V., Metcalf, J. A., Dennis, G., Yang, J., . . . Lane, H. C. (2003). Cutting edge: L-selectin (CD62L) expression distinguishes small resting memory CD4<sup>+</sup> T cells that preferentially respond to recall antigen. *J Immunol*, *170*(1), 28-32. doi:10.4049/jimmunol.170.1.28
- Hermann-Kleiter, N., & Baier, G. (2010). NFAT pulls the strings during CD4<sup>+</sup> T helper cell effector functions. *Blood*, *115*(15), 2989-2997. doi:10.1182/blood-2009-10-233585
- Herter, J. M., Grabie, N., Cullere, X., Azcutia, V., Rosetti, F., Bennett, P., . . . Mayadas, T. N. (2015). AKAP9 regulates activation-induced retention of T lymphocytes at sites of inflammation. *Nat Commun*, *6*, 10182. doi:10.1038/ncomms10182
- Hoepli, R. E., Wu, D., Cook, L., & Levings, M. K. (2015). The environment of regulatory T cell biology: cytokines, metabolites, and the microbiome. *Front Immunol*, *6*, 61. doi:10.3389/fimmu.2015.00061
- Hoppe, J. M., & Vielhauer, V. (2014). Induction and analysis of nephrotoxic serum nephritis in mice. *Methods Mol Biol*, *1169*, 159-174. doi:10.1007/978-1-4939-0882-0\_15

- Howden, A. J. M., Hukelmann, J. L., Brenes, A., Spinelli, L., Sinclair, L. V., Lamond, A. I., & Cantrell, D. A. (2019). Quantitative analysis of T cell proteomes and environmental sensors during T cell differentiation. *Nat Immunol*, *20*(11), 1542-1554. doi:10.1038/s41590-019-0495-x
- Huang, C., & Fu, Z. X. (2011). Localization of IL-17+Foxp3+ T cells in esophageal cancer. *Immunol Invest*, *40*(4), 400-412. doi:10.3109/08820139.2011.555489
- Huntemann, N., Vogelsang, A., Groeneweg, L., Willison, A., Herrmann, A. M., Meuth, S. G., & Eichler, S. (2022). An optimized and validated protocol for inducing chronic experimental autoimmune encephalomyelitis in C57BL/6J mice. *J Neurosci Methods*, *367*, 109443. doi:10.1016/j.jneumeth.2021.109443
- Hutton, H. L., Levin, A., Gill, J., Djurdjev, O., Tang, M., & Barbour, S. J. (2017). Cardiovascular risk is similar in patients with glomerulonephritis compared to other types of chronic kidney disease: a matched cohort study. *BMC Nephrol*, *18*(1), 95. doi:10.1186/s12882-017-0511-z
- Hwang, E. S., Hong, J. H., & Glimcher, L. H. (2005). IL-2 production in developing Th1 cells is regulated by heterodimerization of RelA and T-bet and requires T-bet serine residue 508. *J Exp Med*, *202*(9), 1289-1300. doi:10.1084/jem.20051044
- Iellem, A., Mariani, M., Lang, R., Recalde, H., Panina-Bordignon, P., Sinigaglia, F., & D'Ambrosio, D. (2001). Unique chemotactic response profile and specific expression of chemokine receptors CCR4 and CCR8 by CD4(+)CD25(+) regulatory T cells. *J Exp Med*, *194*(6), 847-853. doi:10.1084/jem.194.6.847
- Jankovic, D., Kugler, D. G., & Sher, A. (2010). IL-10 production by CD4+ effector T cells: a mechanism for self-regulation. *Mucosal Immunol*, *3*(3), 239-246. doi:10.1038/mi.2010.8
- Jennings, E., Elliot, T. A. E., Thawait, N., Kanabar, S., Yam-Puc, J. C., Ono, M., . . . Bending, D. (2020). Nr4a1 and Nr4a3 Reporter Mice Are Differentially Sensitive to T Cell Receptor Signal Strength and Duration. *Cell Rep*, *33*(5), 108328. doi:10.1016/j.celrep.2020.108328
- Jennings, E. K., Lecky, D. A. J., Ono, M., & Bending, D. (2021). Application of dual. *STAR Protoc*, *2*(1), 100284. doi:10.1016/j.xpro.2020.100284
- Jiang, S., & Dong, C. (2013). A complex issue on CD4(+) T-cell subsets. *Immunol Rev*, *252*(1), 5-11. doi:10.1111/imr.12041

- Juedes, A. E., & Ruddle, N. H. (2001). Resident and infiltrating central nervous system APCs regulate the emergence and resolution of experimental autoimmune encephalomyelitis. *J Immunol*, *166*(8), 5168-5175. doi:10.4049/jimmunol.166.8.5168
- Juneja, V. R., McGuire, K. A., Manguso, R. T., LaFleur, M. W., Collins, N., Haining, W. N., . . . Sharpe, A. H. (2017). PD-L1 on tumor cells is sufficient for immune evasion in immunogenic tumors and inhibits CD8 T cell cytotoxicity. *J Exp Med*, *214*(4), 895-904. doi:10.1084/jem.20160801
- Jutz, S., Leitner, J., Schmetterer, K., Doel-Perez, I., Majdic, O., Grabmeier-Pfistershammer, K., . . . Steinberger, P. (2016). Assessment of costimulation and coinhibition in a triple parameter T cell reporter line: Simultaneous measurement of NF- $\kappa$ B, NFAT and AP-1. *J Immunol Methods*, *430*, 10-20. doi:10.1016/j.jim.2016.01.007
- Kalia, N., Singh, J., & Kaur, M. (2021). The role of dectin-1 in health and disease. *Immunobiology*, *226*(2), 152071. doi:10.1016/j.imbio.2021.152071
- Kawakami, N., Nägerl, U. V., Odoardi, F., Bonhoeffer, T., Wekerle, H., & Flügel, A. (2005). Live imaging of effector cell trafficking and autoantigen recognition within the unfolding autoimmune encephalomyelitis lesion. *J Exp Med*, *201*(11), 1805-1814. doi:10.1084/jem.20050011
- Kim, T. S., & Shin, E. C. (2019). The activation of bystander CD8. *Exp Mol Med*, *51*(12), 1-9. doi:10.1038/s12276-019-0316-1
- Kim, W. S., Kim, M. J., Kim, D. O., Byun, J. E., Huy, H., Song, H. Y., . . . Choi, I. (2017). Suppressor of Cytokine Signaling 2 Negatively Regulates NK Cell Differentiation by Inhibiting JAK2 Activity. *Sci Rep*, *7*, 46153. doi:10.1038/srep46153
- Knosp, C. A., Carroll, H. P., Elliott, J., Saunders, S. P., Nel, H. J., Amu, S., . . . Johnston, J. A. (2011). SOCS2 regulates T helper type 2 differentiation and the generation of type 2 allergic responses. *J Exp Med*, *208*(7), 1523-1531. doi:10.1084/jem.20101167
- Komiyama, Y., Nakae, S., Matsuki, T., Nambu, A., Ishigame, H., Kakuta, S., . . . Iwakura, Y. (2006). IL-17 plays an important role in the development of experimental autoimmune encephalomyelitis. *J Immunol*, *177*(1), 566-573. doi:10.4049/jimmunol.177.1.566

- Koutouros, M., Berer, K., Kawakami, N., Wekerle, H., & Krishnamoorthy, G. (2014). Treg cells mediate recovery from EAE by controlling effector T cell proliferation and motility in the CNS. *Acta Neuropathol Commun*, 2, 163. doi:10.1186/s40478-014-0163-1
- Kryczek, I., Wu, K., Zhao, E., Wei, S., Vatan, L., Szeliga, W., . . . Zou, W. (2011). IL-17+ regulatory T cells in the microenvironments of chronic inflammation and cancer. *J Immunol*, 186(7), 4388-4395. doi:10.4049/jimmunol.1003251
- Kuksin, M., Morel, D., Aglave, M., Danlos, F. X., Marabelle, A., Zinovyev, A., . . . Verlingue, L. (2021). Applications of single-cell and bulk RNA sequencing in onco-immunology. *Eur J Cancer*, 149, 193-210. doi:10.1016/j.ejca.2021.03.005
- Kurts, C., Ginhoux, F., & Panzer, U. (2020). Kidney dendritic cells: fundamental biology and functional roles in health and disease. *Nat Rev Nephrol*, 16(7), 391-407. doi:10.1038/s41581-020-0272-y
- Kurts, C., Panzer, U., Anders, H. J., & Rees, A. J. (2013). The immune system and kidney disease: basic concepts and clinical implications. *Nat Rev Immunol*, 13(10), 738-753. doi:10.1038/nri3523
- Lee, H. G., Cho, M. Z., & Choi, J. M. (2020). Bystander CD4. *Exp Mol Med*, 52(8), 1255-1263. doi:10.1038/s12276-020-00486-7
- Lee, Y. K., Turner, H., Maynard, C. L., Oliver, J. R., Chen, D., Elson, C. O., & Weaver, C. T. (2009). Late developmental plasticity in the T helper 17 lineage. *Immunity*, 30(1), 92-107. doi:10.1016/j.immuni.2008.11.005
- Leuenberger, T., Paterka, M., Reuter, E., Herz, J., Niesner, R. A., Radbruch, H., . . . Siffrin, V. (2013). The role of CD8+ T cells and their local interaction with CD4+ T cells in myelin oligodendrocyte glycoprotein35-55-induced experimental autoimmune encephalomyelitis. *J Immunol*, 191(10), 4960-4968. doi:10.4049/jimmunol.1300822
- Ley, K., Laudanna, C., Cybulsky, M. I., & Nourshargh, S. (2007). Getting to the site of inflammation: the leukocyte adhesion cascade updated. *Nat Rev Immunol*, 7(9), 678-689. doi:10.1038/nri2156
- Li, D., Molldrem, J. J., & Ma, Q. (2009). LFA-1 regulates CD8+ T cell activation via T cell receptor-mediated and LFA-1-mediated Erk1/2 signal pathways. *J Biol Chem*, 284(31), 21001-21010. doi:10.1074/jbc.M109.002865

- Liang, X., Huang, Y., Li, D., Yang, X., Jiang, L., Zhou, W., . . . Wang, W. (2021). Distinct functions of CAR-T cells possessing a dectin-1 intracellular signaling domain. *Gene Ther.* doi:10.1038/s41434-021-00257-7
- Lim, H. W., Lee, J., Hillsamer, P., & Kim, C. H. (2008). Human Th17 cells share major trafficking receptors with both polarized effector T cells and FOXP3+ regulatory T cells. *J Immunol*, *180*(1), 122-129. doi:10.4049/jimmunol.180.1.122
- Lin, S., Lin, Y., Nery, J. R., Urich, M. A., Breschi, A., Davis, C. A., . . . Snyder, M. P. (2014). Comparison of the transcriptional landscapes between human and mouse tissues. *Proc Natl Acad Sci U S A*, *111*(48), 17224-17229. doi:10.1073/pnas.1413624111
- Liu, H. P., Cao, A. T., Feng, T., Li, Q., Zhang, W., Yao, S., . . . Cong, Y. (2015). TGF- $\beta$  converts Th1 cells into Th17 cells through stimulation of Runx1 expression. *Eur J Immunol*, *45*(4), 1010-1018. doi:10.1002/eji.201444726
- Liu, L., Nielsen, F. M., Riis, S. E., Emmersen, J., Fink, T., Hjortdal, J., . . . Zachar, V. (2017). Maintaining RNA Integrity for Transcriptomic Profiling of Ex Vivo Cultured Limbal Epithelial Stem Cells after Fluorescence-Activated Cell Sorting (FACS). *Biol Proced Online*, *19*, 15. doi:10.1186/s12575-017-0065-2
- Lodygin, D., Odoardi, F., Schläger, C., Körner, H., Kitz, A., Nosov, M., . . . Flügel, A. (2013). A combination of fluorescent NFAT and H2B sensors uncovers dynamics of T cell activation in real time during CNS autoimmunity. *Nat Med*, *19*(6), 784-790. doi:10.1038/nm.3182
- Low, J. S., Farsakoglu, Y., Amezcua Vesely, M. C., Sefik, E., Kelly, J. B., Harman, C. C. D., . . . Kaech, S. M. (2020). Tissue-resident memory T cell reactivation by diverse antigen-presenting cells imparts distinct functional responses. *J Exp Med*, *217*(8). doi:10.1084/jem.20192291
- Lyu, M., Wang, S., Gao, K., Wang, L., Zhu, X., Liu, Y., . . . Tian, L. (2021). Dissecting the Landscape of Activated CMV-Stimulated CD4+ T Cells in Humans by Linking Single-Cell RNA-Seq With T-Cell Receptor Sequencing. *Front Immunol*, *12*, 779961. doi:10.3389/fimmu.2021.779961
- Macian, F. (2005). NFAT proteins: key regulators of T-cell development and function. *Nat Rev Immunol*, *5*(6), 472-484. doi:10.1038/nri1632

- MacLeod, M. K., David, A., McKee, A. S., Crawford, F., Kappler, J. W., & Marrack, P. (2011). Memory CD4 T cells that express CXCR5 provide accelerated help to B cells. *J Immunol*, *186*(5), 2889-2896. doi:10.4049/jimmunol.1002955
- MacLeod, M. K., McKee, A., Crawford, F., White, J., Kappler, J., & Marrack, P. (2008). CD4 memory T cells divide poorly in response to antigen because of their cytokine profile. *Proc Natl Acad Sci U S A*, *105*(38), 14521-14526. doi:10.1073/pnas.0807449105
- Macpherson, P. C., Farshi, P., & Goldman, D. (2015). Dach2-Hdac9 signaling regulates reinnervation of muscle endplates. *Development*, *142*(23), 4038-4048. doi:10.1242/dev.125674
- Marangoni, F., Murooka, T. T., Manzo, T., Kim, E. Y., Carrizosa, E., Elpek, N. M., & Mempel, T. R. (2013). The transcription factor NFAT exhibits signal memory during serial T cell interactions with antigen-presenting cells. *Immunity*, *38*(2), 237-249. doi:10.1016/j.immuni.2012.09.012
- Marshall, J. S., Warrington, R., Watson, W., & Kim, H. L. (2018). An introduction to immunology and immunopathology. *Allergy Asthma Clin Immunol*, *14*(Suppl 2), 49. doi:10.1186/s13223-018-0278-1
- Martinez, G. J., Pereira, R. M., Äijö, T., Kim, E. Y., Marangoni, F., Pipkin, M. E., . . . Rao, A. (2015). The transcription factor NFAT promotes exhaustion of activated CD8<sup>+</sup> T cells. *Immunity*, *42*(2), 265-278. doi:10.1016/j.immuni.2015.01.006
- McGeachy, M. J., & Anderson, S. M. (2005). Cytokines in the induction and resolution of experimental autoimmune encephalomyelitis. *Cytokine*, *32*(2), 81-84. doi:10.1016/j.cyto.2005.07.012
- McLachlan, J. B., Catron, D. M., Moon, J. J., & Jenkins, M. K. (2009). Dendritic cell antigen presentation drives simultaneous cytokine production by effector and regulatory T cells in inflamed skin. *Immunity*, *30*(2), 277-288. doi:10.1016/j.immuni.2008.11.013
- Mempel, T. R., Henrickson, S. E., & Von Andrian, U. H. (2004). T-cell priming by dendritic cells in lymph nodes occurs in three distinct phases. *Nature*, *427*(6970), 154-159. doi:10.1038/nature02238
- Mendel, I., Kerlero de Rosbo, N., & Ben-Nun, A. (1995). A myelin oligodendrocyte glycoprotein peptide induces typical chronic experimental autoimmune encephalomyelitis in H-2b mice: fine specificity and T cell receptor V beta

- expression of encephalitogenic T cells. *Eur J Immunol*, 25(7), 1951-1959. doi:10.1002/eji.1830250723
- Moran, A. E., Holzapfel, K. L., Xing, Y., Cunningham, N. R., Maltzman, J. S., Punt, J., & Hogquist, K. A. (2011). T cell receptor signal strength in Treg and iNKT cell development demonstrated by a novel fluorescent reporter mouse. *J Exp Med*, 208(6), 1279-1289. doi:10.1084/jem.20110308
- Mosmann, T. R., Cherwinski, H., Bond, M. W., Giedlin, M. A., & Coffman, R. L. (1986). Two types of murine helper T cell clone. I. Definition according to profiles of lymphokine activities and secreted proteins. *J Immunol*, 136(7), 2348-2357.
- Murphy, E., Shibuya, K., Hosken, N., Openshaw, P., Maino, V., Davis, K., . . . O'Garra, A. (1996). Reversibility of T helper 1 and 2 populations is lost after long-term stimulation. *J Exp Med*, 183(3), 901-913. doi:10.1084/jem.183.3.901
- Nelson, M. H., Knochelmann, H. M., Bailey, S. R., Huff, L. W., Bowers, J. S., Majchrzak-Kuligowska, K., . . . Paulos, C. M. (2020). Identification of human CD4. *Sci Adv*, 6(27). doi:10.1126/sciadv.aba7443
- Nguyen, D. H., Hurtado-Ziola, N., Gagneux, P., & Varki, A. (2006). Loss of Siglec expression on T lymphocytes during human evolution. *Proc Natl Acad Sci U S A*, 103(20), 7765-7770. doi:10.1073/pnas.0510484103
- Ni, L., Gayet, I., Zurawski, S., Duluc, D., Flamar, A. L., Li, X. H., . . . Oh, S. (2010). Concomitant activation and antigen uptake via human dectin-1 results in potent antigen-specific CD8+ T cell responses. *J Immunol*, 185(6), 3504-3513. doi:10.4049/jimmunol.1000999
- Nishi, H., Furuhashi, K., Cullere, X., Saggi, G., Miller, M. J., Chen, Y., . . . Mayadas, T. N. (2017). Neutrophil FcγRIIA promotes IgG-mediated glomerular neutrophil capture via Abl/Src kinases. *J Clin Invest*, 127(10), 3810-3826. doi:10.1172/JCI94039
- Nishimura, H., Nose, M., Hiai, H., Minato, N., & Honjo, T. (1999). Development of lupus-like autoimmune diseases by disruption of the PD-1 gene encoding an ITIM motif-carrying immunoreceptor. *Immunity*, 11(2), 141-151. doi:10.1016/s1074-7613(00)80089-8
- Nodin, B., Fridberg, M., Uhlén, M., & Jirstrom, K. (2012). Discovery of dachshund 2 protein as a novel biomarker of poor prognosis in epithelial ovarian cancer. *J Ovarian Res*, 5(1), 6. doi:10.1186/1757-2215-5-6

- Nosko, A., Kluger, M. A., Diefenhardt, P., Melderis, S., Wegscheid, C., Tiegs, G., . . . Steinmetz, O. M. (2017). T-Bet Enhances Regulatory T Cell Fitness and Directs Control of Th1 Responses in Crescentic GN. *J Am Soc Nephrol*, *28*(1), 185-196. doi:10.1681/ASN.2015070820
- Odoardi, F., Kawakami, N., Klinkert, W. E., Wekerle, H., & Flügel, A. (2007). Blood-borne soluble protein antigen intensifies T cell activation in autoimmune CNS lesions and exacerbates clinical disease. *Proc Natl Acad Sci U S A*, *104*(47), 18625-18630. doi:10.1073/pnas.0705033104
- Oh, D. Y., & Fong, L. (2021). Cytotoxic CD4. *Immunity*, *54*(12), 2701-2711. doi:10.1016/j.immuni.2021.11.015
- Oh, H., & Ghosh, S. (2013). NF- $\kappa$ B: roles and regulation in different CD4(+) T-cell subsets. *Immunol Rev*, *252*(1), 41-51. doi:10.1111/imr.12033
- Onishi, Y., Fehervari, Z., Yamaguchi, T., & Sakaguchi, S. (2008). Foxp3+ natural regulatory T cells preferentially form aggregates on dendritic cells in vitro and actively inhibit their maturation. *Proc Natl Acad Sci U S A*, *105*(29), 10113-10118. doi:10.1073/pnas.0711106105
- Pan, Y., Yu, Y., Wang, X., & Zhang, T. (2020). Tumor-Associated Macrophages in Tumor Immunity. *Front Immunol*, *11*, 583084. doi:10.3389/fimmu.2020.583084
- Papadopoulou, M., Sanchez Sanchez, G., & Vermijlen, D. (2020). Innate and adaptive  $\gamma\delta$  T cells: How, when, and why. *Immunol Rev*, *298*(1), 99-116. doi:10.1111/imr.12926
- Park, H., Li, Z., Yang, X. O., Chang, S. H., Nurieva, R., Wang, Y. H., . . . Dong, C. (2005). A distinct lineage of CD4 T cells regulates tissue inflammation by producing interleukin 17. *Nat Immunol*, *6*(11), 1133-1141. doi:10.1038/ni1261
- Parkin, J., & Cohen, B. (2001). An overview of the immune system. *Lancet*, *357*(9270), 1777-1789. doi:10.1016/S0140-6736(00)04904-7
- Patin, E. C., Orr, S. J., & Schaible, U. E. (2017). Macrophage Inducible C-Type Lectin As a Multifunctional Player in Immunity. *Front Immunol*, *8*, 861. doi:10.3389/fimmu.2017.00861
- Paust, H. J., Ostmann, A., Erhardt, A., Turner, J. E., Velden, J., Mittrücker, H. W., . . . Tiegs, G. (2011). Regulatory T cells control the Th1 immune response in murine crescentic glomerulonephritis. *Kidney Int*, *80*(2), 154-164. doi:10.1038/ki.2011.108

- Pavenstädt, H., Kriz, W., & Kretzler, M. (2003). Cell biology of the glomerular podocyte. *Physiol Rev*, 83(1), 253-307. doi:10.1152/physrev.00020.2002
- Pearce, E. L. (2010). Metabolism in T cell activation and differentiation. *Curr Opin Immunol*, 22(3), 314-320. doi:10.1016/j.coi.2010.01.018
- Phan, H. V., van Gent, M., Drayman, N., Basu, A., Gack, M. U., & Tay, S. (2021). High-throughput RNA sequencing of paraformaldehyde-fixed single cells. *Nat Commun*, 12(1), 5636. doi:10.1038/s41467-021-25871-2
- Pollizzi, K. N., Patel, C. H., Sun, I. H., Oh, M. H., Waickman, A. T., Wen, J., . . . Powell, J. D. (2015). mTORC1 and mTORC2 selectively regulate CD8<sup>+</sup> T cell differentiation. *J Clin Invest*, 125(5), 2090-2108. doi:10.1172/JCI77746
- Posselt, G., Schwarz, H., Duschl, A., & Horejs-Hoeck, J. (2011). Suppressor of cytokine signaling 2 is a feedback inhibitor of TLR-induced activation in human monocyte-derived dendritic cells. *J Immunol*, 187(6), 2875-2884. doi:10.4049/jimmunol.1003348
- Prizant, H., Patil, N., Negatu, S., Bala, N., McGurk, A., Leddon, S. A., . . . Fowell, D. J. (2021). CXCL10. *Cell Rep*, 36(6), 109523. doi:10.1016/j.celrep.2021.109523
- Qiao, B., Zhao, M., Wu, J., Wu, H., Zhao, Y., Meng, F., . . . Zhang, H. (2020). A Novel RNA-Seq-Based Model for Preoperative Prediction of Lymph Node Metastasis in Oral Squamous Cell Carcinoma. *Biomed Res Int*, 2020, 4252580. doi:10.1155/2020/4252580
- Qiu, Y., Chen, T., Hu, R., Zhu, R., Li, C., Ruan, Y., . . . Li, Y. (2021). Next frontier in tumor immunotherapy: macrophage-mediated immune evasion. *Biomark Res*, 9(1), 72. doi:10.1186/s40364-021-00327-3
- Ragland, S. A., & Criss, A. K. (2017). From bacterial killing to immune modulation: Recent insights into the functions of lysozyme. *PLoS Pathog*, 13(9), e1006512. doi:10.1371/journal.ppat.1006512
- Rangel Rivera, G. O., Knochermann, H. M., Dwyer, C. J., Smith, A. S., Wyatt, M. M., Rivera-Reyes, A. M., . . . Paulos, C. M. (2021). Fundamentals of T Cell Metabolism and Strategies to Enhance Cancer Immunotherapy. *Front Immunol*, 12, 645242. doi:10.3389/fimmu.2021.645242
- Raphael, I., Joern, R. R., & Forsthuber, T. G. (2020). Memory CD4. *Cells*, 9(3). doi:10.3390/cells9030531

- Rasquinha, M. T., Sur, M., Lasrado, N., & Reddy, J. (2021). IL-10 as a Th2 Cytokine: Differences Between Mice and Humans. *J Immunol*, *207*(9), 2205-2215. doi:10.4049/jimmunol.2100565
- Reinhardt, R. L., Liang, H. E., & Locksley, R. M. (2009). Cytokine-secreting follicular T cells shape the antibody repertoire. *Nat Immunol*, *10*(4), 385-393. doi:10.1038/ni.1715
- Riedel, J. H., Paust, H. J., Turner, J. E., Tittel, A. P., Krebs, C., Disteldorf, E., . . . Panzer, U. (2012). Immature renal dendritic cells recruit regulatory CXCR6(+) invariant natural killer T cells to attenuate crescentic GN. *J Am Soc Nephrol*, *23*(12), 1987-2000. doi:10.1681/ASN.2012040394
- Rivero, M., Peinado-Serrano, J., Muñoz-Galvan, S., Espinosa-Sánchez, A., Suarez-Martinez, E., Felipe-Abrio, B., . . . Carnero, A. (2018). MAP17 (PDZK1IP1) and pH2AX are potential predictive biomarkers for rectal cancer treatment efficacy. *Oncotarget*, *9*(68), 32958-32971. doi:10.18632/oncotarget.26010
- Roberts, C. A., Dickinson, A. K., & Taams, L. S. (2015). The Interplay Between Monocytes/Macrophages and CD4(+) T Cell Subsets in Rheumatoid Arthritis. *Front Immunol*, *6*, 571. doi:10.3389/fimmu.2015.00571
- Roche, P. A., & Furuta, K. (2015). The ins and outs of MHC class II-mediated antigen processing and presentation. *Nat Rev Immunol*, *15*(4), 203-216. doi:10.1038/nri3818
- Ronchi, F., Basso, C., Preite, S., Reboldi, A., Baumjohann, D., Perlini, L., . . . Sallusto, F. (2016). Experimental priming of encephalitogenic Th1/Th17 cells requires pertussis toxin-driven IL-1 $\beta$  production by myeloid cells. *Nat Commun*, *7*, 11541. doi:10.1038/ncomms11541
- Rothoefl, T., Balkow, S., Krummen, M., Beissert, S., Varga, G., Loser, K., . . . Grabbe, S. (2006). Structure and duration of contact between dendritic cells and T cells are controlled by T cell activation state. *Eur J Immunol*, *36*(12), 3105-3117. doi:10.1002/eji.200636145
- Rudensky, A. Y. (2011). Regulatory T cells and Foxp3. *Immunol Rev*, *241*(1), 260-268. doi:10.1111/j.1600-065X.2011.01018.x
- Sakaguchi, S., Sakaguchi, N., Asano, M., Itoh, M., & Toda, M. (1995). Immunologic self-tolerance maintained by activated T cells expressing IL-2 receptor alpha-

- chains (CD25). Breakdown of a single mechanism of self-tolerance causes various autoimmune diseases. *J Immunol*, 155(3), 1151-1164.
- Sakaguchi, S., Wing, K., Onishi, Y., Prieto-Martin, P., & Yamaguchi, T. (2009). Regulatory T cells: how do they suppress immune responses? *Int Immunol*, 21(10), 1105-1111. doi:10.1093/intimm/dxp095
- Sallusto, F., Lenig, D., Förster, R., Lipp, M., & Lanzavecchia, A. (1999). Two subsets of memory T lymphocytes with distinct homing potentials and effector functions. *Nature*, 401(6754), 708-712. doi:10.1038/44385
- Sallusto, F., Lenig, D., Förster, R., Lipp, M., & Lanzavecchia, A. (2014). Pillars article: two subsets of memory T lymphocytes with distinct homing potentials and effector functions. *Nature*. 1999. 401: 708-712. *J Immunol*, 192(3), 840-844.
- Schaerli, P., Willimann, K., Lang, A. B., Lipp, M., Loetscher, P., & Moser, B. (2000). CXC chemokine receptor 5 expression defines follicular homing T cells with B cell helper function. *J Exp Med*, 192(11), 1553-1562. doi:10.1084/jem.192.11.1553
- Schenkel, J. M., & Masopust, D. (2014). Tissue-resident memory T cells. *Immunity*, 41(6), 886-897. doi:10.1016/j.immuni.2014.12.007
- Schmidt, A., Oberle, N., & Krammer, P. H. (2012). Molecular mechanisms of treg-mediated T cell suppression. *Front Immunol*, 3, 51. doi:10.3389/fimmu.2012.00051
- Schreiner, D., & King, C. G. (2018). CD4+ Memory T Cells at Home in the Tissue: Mechanisms for Health and Disease. *Front Immunol*, 9, 2394. doi:10.3389/fimmu.2018.02394
- Seifert, L., Werba, G., Tiwari, S., Giau Ly, N. N., Nguy, S., Alothman, S., . . . Miller, G. (2016). Radiation Therapy Induces Macrophages to Suppress T-Cell Responses Against Pancreatic Tumors in Mice. *Gastroenterology*, 150(7), 1659-1672.e1655. doi:10.1053/j.gastro.2016.02.070
- Shaw, T. N., Houston, S. A., Wemyss, K., Bridgeman, H. M., Barbera, T. A., Zangerle-Murray, T., . . . Grainger, J. R. (2018). Tissue-resident macrophages in the intestine are long lived and defined by Tim-4 and CD4 expression. *J Exp Med*, 215(6), 1507-1518. doi:10.1084/jem.20180019
- Shevryev, D., & Tereshchenko, V. (2019). Treg Heterogeneity, Function, and Homeostasis. *Front Immunol*, 10, 3100. doi:10.3389/fimmu.2019.03100

- Shyer, J. A., Flavell, R. A., & Bailis, W. (2020). Metabolic signaling in T cells. *Cell Res*, 30(8), 649-659. doi:10.1038/s41422-020-0379-5
- Simon, S., & Labarriere, N. (2017). PD-1 expression on tumor-specific T cells: Friend or foe for immunotherapy? *Oncoimmunology*, 7(1), e1364828. doi:10.1080/2162402X.2017.1364828
- Sojka, D. K., Bruniquel, D., Schwartz, R. H., & Singh, N. J. (2004). IL-2 secretion by CD4+ T cells in vivo is rapid, transient, and influenced by TCR-specific competition. *J Immunol*, 172(10), 6136-6143. doi:10.4049/jimmunol.172.10.6136
- St Paul, M., & Ohashi, P. S. (2020). The Roles of CD8. *Trends Cell Biol*, 30(9), 695-704. doi:10.1016/j.tcb.2020.06.003
- Stanley, P., Smith, A., McDowall, A., Nicol, A., Zicha, D., & Hogg, N. (2008). Intermediate-affinity LFA-1 binds alpha-actinin-1 to control migration at the leading edge of the T cell. *EMBO J*, 27(1), 62-75. doi:10.1038/sj.emboj.7601959
- Stergachis, A. B., Neph, S., Sandstrom, R., Haugen, E., Reynolds, A. P., Zhang, M., . . . Stamatoyannopoulos, J. A. (2014). Conservation of trans-acting circuitry during mammalian regulatory evolution. *Nature*, 515(7527), 365-370. doi:10.1038/nature13972
- Subbannayya, Y., Haug, M., Pinto, S. M., Mohanty, V., Meås, H. Z., Flo, T. H., . . . Kandasamy, R. K. (2020). The Proteomic Landscape of Resting and Activated CD4+ T Cells Reveal Insights into Cell Differentiation and Function. *Int J Mol Sci*, 22(1). doi:10.3390/ijms22010275
- Sugamura, K., Ishii, N., & Weinberg, A. D. (2004). Therapeutic targeting of the effector T-cell co-stimulatory molecule OX40. *Nat Rev Immunol*, 4(6), 420-431. doi:10.1038/nri1371
- Sutton, G., Pugh, D., & Dhaun, N. (2019). Developments in the Role of Endothelin-1 in Atherosclerosis: A Potential Therapeutic Target? *Am J Hypertens*, 32(9), 813-815. doi:10.1093/ajh/hpz091
- Szabo, P. A., Levitin, H. M., Miron, M., Snyder, M. E., Senda, T., Yuan, J., . . . Sims, P. A. (2019). Single-cell transcriptomics of human T cells reveals tissue and activation signatures in health and disease. *Nat Commun*, 10(1), 4706. doi:10.1038/s41467-019-12464-3

- Tan, H., Yang, K., Li, Y., Shaw, T. I., Wang, Y., Blanco, D. B., . . . Chi, H. (2017). Integrative Proteomics and Phosphoproteomics Profiling Reveals Dynamic Signaling Networks and Bioenergetics Pathways Underlying T Cell Activation. *Immunity*, *46*(3), 488-503. doi:10.1016/j.immuni.2017.02.010
- Tang, H., & Goldman, D. (2006). Activity-dependent gene regulation in skeletal muscle is mediated by a histone deacetylase (HDAC)-Dach2-myogenin signal transduction cascade. *Proc Natl Acad Sci U S A*, *103*(45), 16977-16982. doi:10.1073/pnas.0601565103
- Tateno, H., Crocker, P. R., & Paulson, J. C. (2005). Mouse Siglec-F and human Siglec-8 are functionally convergent paralogs that are selectively expressed on eosinophils and recognize 6'-sulfo-sialyl Lewis X as a preferred glycan ligand. *Glycobiology*, *15*(11), 1125-1135. doi:10.1093/glycob/cwi097
- Toda, G., Yamauchi, T., Kadowaki, T., & Ueki, K. (2021). Preparation and culture of bone marrow-derived macrophages from mice for functional analysis. *STAR Protoc*, *2*(1), 100246. doi:10.1016/j.xpro.2020.100246
- Trifari, S., Kaplan, C. D., Tran, E. H., Crellin, N. K., & Spits, H. (2009). Identification of a human helper T cell population that has abundant production of interleukin 22 and is distinct from T(H)-17, T(H)1 and T(H)2 cells. *Nat Immunol*, *10*(8), 864-871. doi:10.1038/ni.1770
- Trinchieri, G. (2007). Interleukin-10 production by effector T cells: Th1 cells show self control. *J Exp Med*, *204*(2), 239-243. doi:10.1084/jem.20070104
- Tsopoulidis, N., Kaw, S., Laketa, V., Kutscheidt, S., Baarlink, C., Stolp, B., . . . Fackler, O. T. (2019). T cell receptor-triggered nuclear actin network formation drives CD4. *Sci Immunol*, *4*(31). doi:10.1126/sciimmunol.aav1987
- Turner, J. E., Krebs, C., Tittel, A. P., Paust, H. J., Meyer-Schwesinger, C., Bennis, S. B., . . . Panzer, U. (2012). IL-17A production by renal  $\gamma\delta$  T cells promotes kidney injury in crescentic GN. *J Am Soc Nephrol*, *23*(9), 1486-1495. doi:10.1681/ASN.2012010040
- Vahedi, G., C Poholek, A., Hand, T. W., Laurence, A., Kanno, Y., O'Shea, J. J., & Hirahara, K. (2013). Helper T-cell identity and evolution of differential transcriptomes and epigenomes. *Immunol Rev*, *252*(1), 24-40. doi:10.1111/imr.12037

- van Panhuys, N., Klauschen, F., & Germain, R. N. (2014). T-cell-receptor-dependent signal intensity dominantly controls CD4(+) T cell polarization In Vivo. *Immunity*, 41(1), 63-74. doi:10.1016/j.immuni.2014.06.003
- Veldhoen, M., Uyttenhove, C., van Snick, J., Helmby, H., Westendorf, A., Buer, J., . . . Stockinger, B. (2008). Transforming growth factor-beta 'reprograms' the differentiation of T helper 2 cells and promotes an interleukin 9-producing subset. *Nat Immunol*, 9(12), 1341-1346. doi:10.1038/ni.1659
- Vieira, P. L., Christensen, J. R., Minaee, S., O'Neill, E. J., Barrat, F. J., Boonstra, A., . . . O'Garra, A. (2004). IL-10-secreting regulatory T cells do not express Foxp3 but have comparable regulatory function to naturally occurring CD4+CD25+ regulatory T cells. *J Immunol*, 172(10), 5986-5993. doi:10.4049/jimmunol.172.10.5986
- Vuchkovska, A., Glanville, D. G., Scurti, G. M., Nishimura, M. I., White, P., Ulijasz, A. T., & Iwashima, M. (2022). Siglec-5 is an inhibitory immune checkpoint molecule for human T cells. *Immunology*. doi:10.1111/imm.13470
- Walling, B. L., & Kim, M. (2018). LFA-1 in T Cell Migration and Differentiation. *Front Immunol*, 9, 952. doi:10.3389/fimmu.2018.00952
- Wang, D. D., Jin, Q., Wang, L. L., Han, S. F., Chen, Y. B., Sun, G. D., . . . Shi, B. (2017). The significance of ENAH in carcinogenesis and prognosis in gastric cancer. *Oncotarget*, 8(42), 72466-72479. doi:10.18632/oncotarget.19801
- Wang, X., Xiao, Y., Li, S., Yan, Z., & Luo, G. (2021). CORO6 Promotes Cell Growth and Invasion of Clear Cell Renal Cell Carcinoma via Activation of WNT Signaling. *Front Cell Dev Biol*, 9, 647301. doi:10.3389/fcell.2021.647301
- Wang, Y., Su, M. A., & Wan, Y. Y. (2011). An essential role of the transcription factor GATA-3 for the function of regulatory T cells. *Immunity*, 35(3), 337-348. doi:10.1016/j.immuni.2011.08.012
- Wang, Y., Tian, Q., Hao, Y., Yao, W., Lu, J., Chen, C., . . . Ye, L. (2021). The kinase complex mTORC2 promotes the longevity of virus-specific memory CD4. *Nat Immunol*. doi:10.1038/s41590-021-01090-1
- Weinreich, M. A., & Hogquist, K. A. (2008). Thymic emigration: when and how T cells leave home. *J Immunol*, 181(4), 2265-2270. doi:10.4049/jimmunol.181.4.2265

- Westhorpe, C. L. V., Norman, M. U., Hall, P., Snelgrove, S. L., Finsterbusch, M., Li, A., . . . Hickey, M. J. (2018). Effector CD4. *Nat Commun*, 9(1), 747. doi:10.1038/s41467-018-03181-4
- Wherry, E. J., Ha, S. J., Kaech, S. M., Haining, W. N., Sarkar, S., Kalia, V., . . . Ahmed, R. (2007). Molecular signature of CD8+ T cell exhaustion during chronic viral infection. *Immunity*, 27(4), 670-684. doi:10.1016/j.immuni.2007.09.006
- Wlodarczyk, A., Løbner, M., Cédile, O., & Owens, T. (2014). Comparison of microglia and infiltrating CD11c<sup>+</sup> cells as antigen presenting cells for T cell proliferation and cytokine response. *J Neuroinflammation*, 11, 57. doi:10.1186/1742-2094-11-57
- Wohlfert, E. A., Grainger, J. R., Bouladoux, N., Konkell, J. E., Oldenhove, G., Ribeiro, C. H., . . . Belkaid, Y. (2011). GATA3 controls Foxp3<sup>+</sup> regulatory T cell fate during inflammation in mice. *J Clin Invest*, 121(11), 4503-4515. doi:10.1172/JCI57456
- Wu, C., Ivars, F., Anderson, P., Hallmann, R., Vestweber, D., Nilsson, P., . . . Sorokin, L. M. (2009). Endothelial basement membrane laminin alpha5 selectively inhibits T lymphocyte extravasation into the brain. *Nat Med*, 15(5), 519-527. doi:10.1038/nm.1957
- Wu, Y., Zhang, X., Wei, X., Feng, H., Hu, B., Deng, Z., . . . Wang, T. (2021). Development of an Individualized Ubiquitin Prognostic Signature for Clear Cell Renal Cell Carcinoma. *Front Cell Dev Biol*, 9, 684643. doi:10.3389/fcell.2021.684643
- Yamamoto, J., Adachi, Y., Onoue, Y., Adachi, Y. S., Okabe, Y., Itazawa, T., . . . Miyawaki, T. (2000). Differential expression of the chemokine receptors by the Th1- and Th2-type effector populations within circulating CD4<sup>+</sup> T cells. *J Leukoc Biol*, 68(4), 568-574.
- Yamane, H., & Paul, W. E. (2013). Early signaling events that underlie fate decisions of naive CD4(+) T cells toward distinct T-helper cell subsets. *Immunol Rev*, 252(1), 12-23. doi:10.1111/imr.12032
- Yang, S., Wang, B., Guan, C., Wu, B., Cai, C., Wang, M., . . . Yang, P. (2011). Foxp3+IL-17+ T cells promote development of cancer-initiating cells in colorectal cancer. *J Leukoc Biol*, 89(1), 85-91. doi:10.1189/jlb.0910506

- Yu, F., Sharma, S., Edwards, J., Feigenbaum, L., & Zhu, J. (2015). Dynamic expression of transcription factors T-bet and GATA-3 by regulatory T cells maintains immunotolerance. *Nat Immunol*, *16*(2), 197-206. doi:10.1038/ni.3053
- Yue, F., Cheng, Y., Breschi, A., Vierstra, J., Wu, W., Ryba, T., . . . Consortium, M. E. (2014). A comparative encyclopedia of DNA elements in the mouse genome. *Nature*, *515*(7527), 355-364. doi:10.1038/nature13992
- Zhang, M., Angata, T., Cho, J. Y., Miller, M., Broide, D. H., & Varki, A. (2007). Defining the in vivo function of Siglec-F, a CD33-related Siglec expressed on mouse eosinophils. *Blood*, *109*(10), 4280-4287. doi:10.1182/blood-2006-08-039255
- Zhang, X., Sun, S., Hwang, I., Tough, D. F., & Sprent, J. (1998). Potent and selective stimulation of memory-phenotype CD8+ T cells in vivo by IL-15. *Immunity*, *8*(5), 591-599. doi:10.1016/s1074-7613(00)80564-6
- Zhang, X., Wang, Y., Song, J., Gerwien, H., Chuquisana, O., Chashchina, A., . . . Sorokin, L. (2020). The endothelial basement membrane acts as a checkpoint for entry of pathogenic T cells into the brain. *J Exp Med*, *217*(7). doi:10.1084/jem.20191339
- Zhou, L., Chong, M. M., & Littman, D. R. (2009). Plasticity of CD4+ T cell lineage differentiation. *Immunity*, *30*(5), 646-655. doi:10.1016/j.immuni.2009.05.001
- Zhu, J., Yamane, H., & Paul, W. E. (2010). Differentiation of effector CD4 T cell populations (\*). *Annu Rev Immunol*, *28*, 445-489. doi:10.1146/annurev-immunol-030409-101212

## 8. List of Abbreviation

AKT	Protein Kinase B
AP-1	Adaptor-related Protein complex 1
APC	Antigen Presenting Cell
BSA	Bovine Serum Albumin
CAA	Chloroacetamide
CD	Cluster of Differentiation
CFA	Complete Freund's Adjuvant
CNS	Central Nervous System
DAG	Diacylglycerol
DC	Dendritic Cell
DTT	Dithiothreitol
EAE	Experimental Autoimmune Encephalomyelitis
ER	Endoplasmic reticulum
ERK	Extracellular signal Regulated Kinase
FACS	Fluorescence Activated Cell Sorting
FoxP3	Forkhead Box P3
Gata3	GATA Binding Protein 3
GC	Germinal Center
GFP	Green Fluorescent Protein
GM-CSF	Granulocyte-Macrophage Colony-Stimulating Factor
GRP1	Ras Guanyl-Releasing Protein 1
GZM	Granzymes
i.p.	intraperitoneal
i.v.	intravenous
IFN $\gamma$	Interferon gamma
IL	Interleukin
IP3	Inositol-1,4,5-triphosphate
IRES	Internal Ribosomal Entry Side
ITAM	Immunoreceptor Tyrosine based Activation Motifs
ITK	Inducible T cell Kinase

LAT	Linker for Activated T cells
LCK	Lymphocyte-specific protein tyrosine Kinase
Lys-C	Lysyl Endopeptidase
MACS	Magnetic activated cell sorting
MAPK	Mitogen Activated Protein Kinase
M-CSF	Macrophage Colony-Stimulating Factor
MHC	Major Histocompatibility Complex
mTOR	Mechanistic Target Of Rapamycin
NEAA	Non-Essential Amino Acids
NFAT	Nuclear Factor of Activated T cells
NFkB	Nuclear Factor Kappa-light-chain-enhancer of activated B cells
NK cell	Natural Killer cell
NKT cell	Natural Killer T cell
NTN	Nephrotoxic Nephritis
NTS	Nephrotoxic Serum
Nur77	Nr4a1; Nuclear Receptor Subfamily 4 Group A Member 1
PCR	Polymerase Chain Reaction
PI3K	Phosphatidylinositol 3-Kinase
PIP2	Phosphatidylinositol 4,5-bisphosphate
PKC	Protein Kinase C
PKC $\theta$	Protein Kinase C theta
PRF1	Perforin 1
PRR	Pattern Recognition Receptors
PTK	Protein Tyrosine Kinases
PTX	Pertussis Toxin
qRT-PCR	Quantitative Real Time PCR
ROR $\gamma$ t	RAR-related orphan receptor gamma
s.c.	subcutan
STAT	Signal transducer and activator of transcription
T-Bet	T-Box trancription factor
T <sub>CM</sub> cell	central memory T cell
TCR	T cell receptor

TEAB	Triethylammoniumbicarbonate
T <sub>EM</sub> cell	effector memory T cell
T <sub>fh</sub> cell	T follicular helper cells
TGF	Transforming growth factor
T <sub>H</sub> cell	T helper cell
TNF	Tumor Necrosis Factor
T <sub>reg</sub> cell	regulatory T cell
T <sub>RM</sub> cell	tissue-resident T cell
T <sub>SCM</sub> cell	stem cell like memory T cells
UTR	Untranslated region
YFP	Yellow Fluorescent Protein
Zap70	Zeta chain of T cell receptor Associated Protein kinase 70

## 9. List of Figures

Figure 1: The cancer-immunity cycle (Chen et al., Immunity, 2013).....	4
Figure 2: TCR signaling cascade (Bhattacharyya, Front. Immunol., 2020) .....	6
Figure 3: CD4 <sup>+</sup> T cell subpopulations (Jiang, Immunol Rev, 2013).....	8
Figure 4: Suggested models for memory T cell development (Raphael et al., Cells, 2020) .....	11
Figure 5: Anatomy of the kidney .....	15
Figure 6: Course of nephrotoxic nephritis model. Illustration of the four stages of immune activation in NTN (Kurts, Ginhoux, & Panzer, 2020).....	16
Figure 7: Experimental setup and disease progression of EAE (Huntemann et al., 2022) .....	18
Figure 8: The role of CD4 <sup>+</sup> T cells in EAE (Goverman, 2009).....	19
Figure 9: Schematic experimental design.....	21
Figure 10: Kinetics of activated naïve T cells and reactivated T <sub>H</sub> 1 cells .....	22
Figure 11: Gating strategy .....	24
Figure 12: Expression of T-Bet and IFN $\gamma$ during naïve T cell activation and T <sub>H</sub> 1 reactivation .....	25
Figure 13: Transcriptome analysis.....	26
Figure 14: Volcano blots of pairwise comparisons between the four groups .....	28
Figure 15: Venn diagrams of upregulated, downregulated and exclusively regulated genes identified via transcriptome analysis of reactivated T <sub>H</sub> 1 cells.....	29
Figure 16: Gene ontology analysis via PANTHER of differentially expressed genes identified via transcriptome analysis specific for reactivated T <sub>H</sub> 1 cells.....	29
Figure 17: Transcription factor/master regulator expression of CD4 <sup>+</sup> T cell subpopulations .....	31
Figure 18: Lead cytokine expression in CD4 <sup>+</sup> T cell subpopulations .....	32
Figure 19: Upregulated genes identified via reactivated T <sub>H</sub> 1 transcriptome analysis in CD4 <sup>+</sup> T cell subpopulations stimulated with antigen-pulsed macrophages.....	34
Figure 20: Downregulated genes identified via reactivated T <sub>H</sub> 1 transcriptome analysis in CD4 <sup>+</sup> T cell subpopulations stimulated with antigen-pulsed macrophages; .....	35
Figure 21: Lead cytokine expression in CD4 <sup>+</sup> T cell subpopulations stimulated with PMA/Ionomycin .....	37

Figure 22: Upregulated genes identified via reactivated T <sub>H</sub> 1 transcriptome analysis in CD4 <sup>+</sup> T cell subpopulations stimulated with PMA/Ionomycin.....	38
Figure 23: Downregulated genes identified via reactivated T <sub>H</sub> 1 transcriptome analysis in CD4 <sup>+</sup> T cell subpopulations stimulated with PMA/Ionomycin.....	39
Figure 24: NTN model .....	41
Figure 25: Gene expression analysis of upregulated genes from transcriptome analysis in CD4 <sup>+</sup> T cells isolated from NTN induced kidneys .....	42
Figure 26: Gene expression analysis of downregulated genes from transcriptome analysis in CD4 <sup>+</sup> T cells isolated from NTN induced kidneys.....	43
Figure 27: Flow cytometric analysis of Siglec5 (A) and Clec7a (B) expression on CD4 <sup>+</sup> T cells in the kidney of ctrl and NTN induced mice .....	43
Figure 28: Gene expression analysis of upregulated genes from transcriptome analysis in CD4 <sup>+</sup> T cells isolated from EAE induced CNS .....	45
Figure 29: Gene expression analysis of downregulated genes from transcriptome analysis in CD4 <sup>+</sup> T cells isolated from EAE induced CNS .....	45
Figure 30: Flow cytometric analysis of Siglec5 and Clec7a expression on sorted Nur77 <sup>GFP-</sup> and Nur77 <sup>GFP+</sup> CD4 <sup>+</sup> T cells isolated from EAE induced CNS (n=6) .....	45
Figure 31: T <sub>H</sub> 1 differentiation of human CD4 <sup>+</sup> T cells isolated from peripheral blood	46
Figure 32: Gene expression analysis of upregulated genes from transcriptome analysis in human T <sub>H</sub> 1 cells restimulated with PMA/Ionomycin.....	47
Figure 33: Gene expression analysis of downregulated genes from transcriptome analysis in human T <sub>H</sub> 1 cells restimulated with PMA/Ionomycin.....	48
Figure 34: Proteome and phosphoproteome analysis of resting and reactivated T <sub>H</sub> 1 cells stimulated for six hours with anti-CD3 and anti-CD28 .....	51

## 10. List of Tables

Table 1: Commonly used activation marker.....	27
Table 2: Overview of each analyzed gene according to differential expression from transcriptome analysis, in vitro reactivated murine CD4 <sup>+</sup> T <sub>H</sub> 1 cells, NTN model, EAE model and human CD4 <sup>+</sup> T cells .....	50

## Lebenslauf

Name: Martha Kiljan  
Geburtsdatum/-ort: 26.04.1990 in Kamp-Lintfort  
Adresse: Elsenbornerstraße 26, 50933 Köln  
Staatsangehörigkeit: Deutsch  
Geschlecht: Weiblich

## Schulbildung/Studium

Seit 10/2017	<p>Promotionsstudium der Biologie an der Universität zu Köln und wissenschaftliche Mitarbeiterin an der Klinik und Poliklinik für Radioonkologie, Cyberknife- und Strahlentherapie an der Uniklinik Köln mit Möglichkeit zur Promotion</p> <p>Promotionsthema: "T<sub>H</sub>1 reactivation in peripheral tissues"</p>
02/2016 – 08/2017	<p>Promotionsstudium der Biologie an der Universität Duisburg-Essen und wissenschaftliche Mitarbeiterin am Institut für Transfusionsmedizin an der Uniklinik Essen</p> <p>Promotionsthema: „MYBL2 tumor suppressor function in Myelodysplastic Syndromes“</p> <p>(Aufhebungsvertrag im gegenseitigen Einverständnis)</p>
10/2012 – 02/2015	<p>Masterstudium der Biologie an der Heinrich-Heine-Universität Düsseldorf</p> <p>Masterarbeitsthema: „Einfluss der stabilen grün fluoreszierendes Protein (GFP) - Transfektion mittels Vektortechnologie auf das osteogene Differenzierungspotential multipotenter mesenchymaler Stromazellen“ im Forschungslabor der Hand- und Unfallchirurgie Düsseldorf</p> <p>Abschluss: Master of Science, Note 1,8</p>
10/2009 - 09/2012	<p>Bachelorstudium der Biologie an der Heinrich-Heine-Universität Düsseldorf</p>

	<p>Bachelorarbeitsthema: „Quantifizierung von EBV-positiven B-Zellen in Blut und Liquor von Patienten mit Multipler Sklerose durch Einzelzell-PCR und real-time PCR“ im Forschungslabor der Neurologischen Klinik Düsseldorf</p> <p>Abschluss: Bachelor of Science, Note: 2,2</p>
09/2000 - 09/2009	<p>Allgemeine Hochschulreife am städtischen Gymnasium Kamp-Lintfort</p> <p>Abschluss: Abitur, Note: 2,2</p>

### Liste der Wissenschaftlichen Publikationen

- **Martha Kiljan**, Sabrina Weil, Andres Vásquez-Torres, Meike Hettich, Marimel Mayer, Olta Ibrulib, Matthias Reinscheid, Isabelle Heßelmann, Jiali Cai, Li-na Niu, Yagmur Sahbaz, Christian Baues, Wolfgang W. Baus, Florian Kamp, Simone Marnitz, Grit S. Herter-Sprie, and Jan M. Herter

“CyberKnife radiation therapy as a platform for translational mouse studies”

International Journal of Radiation Biology 2021, Vol. 97, no. 9, 1261-1269

- **Jan Herter, Martha Kiljan**, Sabine Kunze, Matthias Reinscheid, Olta Ibruli, Jiali Cai, Li-Na Niu, Isabelle Hesselmann, Maike Trommer, Grit Sophie Herter-Sprie, Christhardt Köhler, Simone Marnitz

“Influence of chemoradiation on the immune microenvironment of cervical cancer patients”

Strahlentherapie und Onkologie, eingereicht am 16.03.2022

## **Erklärung zur Dissertation**

gemäß der Promotionsordnung vom 12. März 2020

Hiermit versichere ich an Eides statt, dass ich die vorliegende Dissertation selbstständig und ohne die Benutzung anderer als der angegebenen Hilfsmittel und Literatur angefertigt habe. Alle Stellen, die wörtlich oder sinngemäß aus veröffentlichten und nicht veröffentlichten Werken dem Wortlaut oder dem Sinn nach entnommen wurden, sind als solche kenntlich gemacht. Ich versichere an Eides statt, dass diese Dissertation noch keiner anderen Fakultät oder Universität zur Prüfung vorgelegen hat; dass sie - abgesehen von unten angegebenen Teilpublikationen und eingebundenen Artikeln und Manuskripten - noch nicht veröffentlicht worden ist sowie, dass ich eine Veröffentlichung der Dissertation vor Abschluss der Promotion nicht ohne Genehmigung des Promotionsausschusses vornehmen werde. Die Bestimmungen dieser Ordnung sind mir bekannt. Darüber hinaus erkläre ich hiermit, dass ich die Ordnung zur Sicherung guter wissenschaftlicher Praxis und zum Umgang mit wissenschaftlichem Fehlverhalten der Universität zu Köln gelesen und sie bei der Durchführung der Dissertation zugrundeliegenden Arbeiten und der schriftlich verfassten Dissertation beachtet habe und verpflichte mich hiermit, die dort genannten Vorgaben bei allen wissenschaftlichen Tätigkeiten zu beachten und umzusetzen. Ich versichere, dass die eingereichte elektronische Fassung der eingereichten Druckfassung vollständig entspricht.



Martha Kiljan

Köln, den 03.06.2022